

Kinetic Investigation and Modelling of Multi-Component Polymer Systems with
Depropagation

by

Michael Jeremiah Leamen

A thesis
presented to the University of Waterloo
in fulfilment of the
thesis requirement for the degree of
Doctor of Philosophy
in
Chemical Engineering

Waterloo, Ontario, Canada, 2005

©Michael Jeremiah Leamen 2005

AUTHOR'S DECLARATION FOR ELECTRONIC SUBMISSION OF A THESIS

I hereby declare that I am the sole author of this thesis. This is a true copy of the thesis, including any required final revisions, as accepted by my examiners.

I understand that my thesis may be made electronically available to the public.

Abstract

The phenomenon of depropagation or reverse polymerization for multicomponent polymerizations has been studied in detail. The monomer Alpha-Methyl Styrene (AMS) has been copolymerized with Methyl Methacrylate (MMA) and Butyl Acrylate (BA) at temperatures ranging from 60°C to 140°C and the kinetics have been studied in the form of propagation/cross propagation and depropagation parameters. There have been multiple attempts with varying amounts of success in the past to determine the kinetic parameters for depropagating systems including work by Lowry and Wittmer as well as other modelling methodologies that are not as mechanistic. The most recent development of the mechanistic terminal model is that of the Kruger model. The model is robust and can take into account all special cases as well as all reactions being reversible. The kinetic parameters have been estimated for each of the three binary systems using the Kruger model (MMA/AMS, MMA/BA, BA/AMS). The Alfrey-Goldfinger model is inadequate to describe depropagating terpolymer systems and in order to study them, a new model was developed based upon the binary Kruger model. This new model takes into account a fully depropagating terpolymer system leading to a total of 15 parameters to be estimated. These 15 parameters have the same definitions as those estimated from the binary Kruger model, thus making accurate analysis of the binary systems crucial since these will be used as first estimates for the terpolymer system. Extensive experimental data (composition, conversion and molecular weights) was collected and analysed for the MMA/AMS and BA/AMS systems. For the BA/AMS system both the bulk and solution copolymerizations were studied in detail with the results from the Kruger model not showing a significant difference in the reactivity ratios between the two types of polymerization. For the MMA/AMS system, a bulk study only was done which revealed an interesting phenomenon that points toward a break down of the long chain approximations used for all of the models being studied. For both of these systems, extensive ¹H NMR analysis was done to determine the copolymer composition. Data collected in previous research for the MMA/BA system was reanalysed using the Kruger model and it was found that the parameter estimates did not differ significantly from the published values. Extensive benchmarking was done with the newly developed terpolymer model on non-depropagating systems using data from the literature to ensure it worked for the simplest cases. It was found that the model matched the parameter estimates from the literature and in

some cases improving upon them to fit the data better. Along with the benchmarking a sensitivity analysis was done which revealed some interesting information. For the MMA/BA/AMS terpolymer system a set of experiments (based upon practical considerations) were performed and the composition of the polymer was determined using ^{13}C NMR instead of the usual ^1H NMR due to the difficulty of peak separation for the complex terpolymer. Using the depropagating terpolymer composition data in conjunction with the parameter estimates from the three binary systems allowed for estimation of the 15 kinetic parameters, which showed only minor variation from the binary estimates.

Acknowledgements

I gratefully acknowledge the Natural Sciences and Engineering Research Council (NSERC) of Canada, the Canada Research Chair (CRC) program, and ICI, Worldwide, for funding.

Matthew Scolah, William Ripmeester and Deborah Sarzotti for their support and help with the experimental aspects of this project

Dr. Neil McManus for his help with polymerizations, NMR analysis and the many discussions that have given me a better understanding of the many analytical aspects of this work.

Dr. Alexander Penlidis for being the best supervisor a graduate student could ask for. Our many conversations about the technical aspects of this work, about education, politics and life in general have allowed me to take a step back, refocus, and see the big picture on more than one occasion. This has been invaluable to me.

Dedication

I would like to dedicate this work to my family: Mom, Dad, Grandma, Grandpa and my sister Lisa. You have all been an enormous encouraging factor since as long as I can remember and that will never be forgotten. I hope this Doctorate can show the rest of the world what a country boy from the middle of nowhere can accomplish.

Table of Contents

1. Introduction	1
2. Background and Literature Review	4
2.1. Bulk vs. Solution Polymerization	4
2.2. Thermal Initiation	5
2.2.1. Thermal Initiation of Methyl Methacrylate.....	6
2.2.2. Thermal Initiation of Butyl Acrylate (BA)	7
2.2.3. Thermal Initiation of Styrene/AMS	7
2.3 Depropagation/Reverse Polymerization.....	8
3. Modeling	13
3.1. Reactivity Ratios	13
3.2. Binary Copolymer Composition Equations	13
3.2.1. The Mayo-Lewis Equation.....	13
3.2.2. Lowry's Models	16
3.2.3. Wittmer's Model	18
3.2.4. Kruger's Model	20
3.2.5. Model Comparisons	21
3.3. Ternary Copolymer Composition Models	25
3.3.1. Alfrey-Goldfinger Model	26
3.3.2. Expanded Kruger Model	27
4. Experimental Methods	32
4.1. Reagent Purification.....	32
4.1.1. Monomer Washing.....	32
4.1.2. Monomer Distillation.....	33
4.2. Solution Preparation.....	33
4.3. Polymerization Reaction	34
4.4. Copolymer Characterization	34
4.4.1. Gravimetry	34
4.4.2. Copolymer Composition: ¹ H Proton NMR.....	35
4.4.3. Copolymer Composition: ¹³ C Carbon NMR	37
4.4.4. Molecular Weight	38
5. Butyl Acrylate/ Alpha-Methyl Styrene Copolymerization in Bulk and Solution.....	40
5.1. Introduction.....	40
5.2. Results and Discussion.....	41
5.2.1. Low Conversion Studies	41
5.2.2. Full Conversion Range Studies.....	48
5.3. Concluding Remarks.....	53
6. Methyl Methacrylate/Alpha-Methyl Styrene Copolymerization in Bulk	55
6.1. Introduction.....	55
6.2. Results and Discussion.....	56
6.3. Concluding Remarks.....	65
7. Butyl Acrylate/Methyl Methacrylate Copolymerization in Bulk	66
7.1. Introduction.....	66
7.2. Results.....	66
8. MMA/BA/AMS Terpolymerization in Bulk	68

8.1. Introduction and Experimental Considerations.....	68
8.2. Experimental Results	69
8.3. Modeling	70
8.3.1. Sensitivity Analysis.....	71
8.3.2. Benchmarking	74
8.4. MMA/BA/AMS Parameter Estimation: Results and Discussion	76
8.5. Concluding Remarks.....	79
9. Conclusions and Recommendations	80
9.1. Concluding Remarks.....	80
9.2. Recommendations	81
9.3. Contributions.....	82
9.4. Publications	83
10. References	84
APPENDIX A: THERMAL POLYMERIZATION OF BUTYL ACRYLATE.....	91
APPENDIX B: TERPOLYMER MODEL DEVELOPMENT USING MAPLE.....	99
APPENDIX C: COPOLYMER REFRACTIVE INDEX	103
APPENDIX D: FULL CONVERSION MMA/AMS DATA	109
APPENDIX E: BENCHMARKING RESULTS	111
APPENDIX F: TERPOLYMER PROBABILITY VALUES	116
APPENDIX G: SENSITIVITY CONTOURS FOR THE BINARY KRUGER MODEL..	118

List of Tables

Table 1: Ceiling Temperatures for Common Monomers.....	12
Table 2: Bulk Parameter Estimates for the Kruger model (1 = AMS, 2 = BA).....	44
Table 3: Solution Parameter Estimates for the Kruger model (1 = AMS, 2 = BA).....	45
Table 4: 95% Joint Confidence Contour Areas	47
Table 5: Full Conversion Solution Polymerizations	49
Table 6: M_w Summary	53
Table 7: Bulk Parameter Estimates for the Kruger model (1 = AMS, 2 = MMA).....	58
Table 8: Bulk Parameter Estimates for the Kruger model (1 = MMA, 2 = BA)	67
Table 9: Expanded Kruger Fit vs. Alfrey-Goldfinger Fit	75
Table 10: Parameter Estimates for Binary and Ternary Systems	76
Table 11: dn/dc Values for AMS/MMA Copolymers	106
Table 12: Full Conversion MMA/AMS Data for 100, 115 and 140°C.....	110
Table 13: Hocking Parameter Estimates.....	112
Table 14: Hocking NMR Results/Kruger Results.....	112
Table 15: Braun and Cei Parameter Estimates.....	112
Table 16: Braun and Cei NMR Results/Kruger Results	113
Table 17: Valvassori and Sartori Parameter Estimates.....	114
Table 18: Valvasorri and Sartori NMR Results/Kruger Results.....	114
Table 19: Koenig Parameter Estimates.....	115
Table 20: Koenig NMR Results/Kruger Results.....	115
Table 21: Terpolymer Probability Values: A=BA, B = AMS, C = MMA	117

Table of Figures

Figure 1: Model Comparison at 60°C	22
Figure 2: Model Comparison at 100°C	22
Figure 3: Model Comparison at 140°C	23
Figure 4: Kruger Model Reduced to Lowry Model 140°C	24
Figure 5: NMR Spectra for Copolymer of BA and AMS	36
Figure 6: NMR Spectra for Copolymer of MMA and AMS.....	36
Figure 7: ¹³ C NMR Spectra for MMA/BA/AMS.....	38
Figure 8: Bulk Composition vs. Feed (60°C & 80°C).....	42
Figure 9: Bulk Composition vs. Feed (100°C, 120°C, 140°C).....	42
Figure 10: Solution Composition vs. Feed (60°C & 80°C).....	43
Figure 11: Solution Composition vs. Feed (100°C, 120°C, 140°C).....	44
Figure 12: Arrhenius Plot for Reactivity Ratios Obtained Using Kruger Model (Bulk and Solution).....	45
Figure 13: 95% Joint Confidence Contours for r_{AMS} and r_{BA} at 80°C and 140°C.....	47
Figure 14: 15% and 50% Toluene at 0% and 0.2% CTA	50
Figure 15: Effect of [BA].....	51
Figure 16: Copolymer Composition vs. Conversion	52
Figure 17: Copolymer Composition versus Feed Composition (60°C & 80°C)	57
Figure 18: Copolymer Composition versus Feed Composition (100°C, 120°C, 140°C)	57
Figure 19: Arrhenius Plot for Reactivity Ratios Obtained Using Kruger Model	59
Figure 20: Arrhenius Plots for Cross Propagation Ratios Obtained Using Kruger Model.....	59
Figure 21: 95% Joint Confidence Contours for r_{AMS} and r_{MMA}	60
Figure 22: Terpolymer NMR results.....	70
Figure 23: Terpolymer Model Gradient for r_{AB} (A = BA, B = AMS)	72
Figure 24: Terpolymer Model Gradient for r_{BC} (B = AMS, C = MMA)	72
Figure 25: Terpolymer Model Gradient for r_{AC} (A = BA, C = MMA).....	73
Figure 26: Terpolymer Composition Comparisons (Styrene).....	75
Figure 27: Terpolymer Composition Comparisons (Acrylonitrile)	76
Figure 28: Model Prediction vs. Experimental Data.....	78
Figure 29: BA Thermal Homopolymerization (Conversion vs. Time).....	95
Figure 30: BA Homopolymerizations at 90C	96
Figure 31: BA Thermal Homopolymerization Comparison at 100C.....	97
Figure 32: BA runs at 140C	98
Figure 33: dn/dc Model vs. Experimental Data	108
Figure 34: Copolymer Composition Gradient for r_{AMS} (r_1) @ 100°C, $r_2 = 0.3$	119
Figure 35: Copolymer Composition Gradient for r_2 @ 140°C, $R_b = 5$	120

1. Introduction

The area of high temperature copolymerizations is of great interest to both industry and academia. High temperature polymerizations allow for greater productivity (i.e. higher rates of conversion) and typically lead to lower molecular weight materials. Lower molecular weight materials are desirable in assisting coating manufacturers to comply with environmental standards[1]. Other factors besides elevated temperatures can be responsible for producing lower molecular weight material. Systems using monomers with low ceiling temperatures (e.g. α -Methylstyrene) are subject to depropagation of the monomer from the macro radical and at elevated temperatures this effect is amplified. The kinetics of these reactions is very important in predicting the copolymer microstructure and resulting properties. Knowledge of the governing kinetic parameters (e.g. reactivity ratios and reaction rate or equilibrium constants) will allow industry to predict what conditions to run reactions at in order to obtain a desirable end product.

Modeling of such behaviour is not an arbitrary task. The simple Mayo-Lewis and Alfrey-Goldfinger models are not applicable to these depropagating systems and subsequently more complex models are required. These more complex models take into account that there are no longer four (or nine) reactions to consider in a binary (or ternary) copolymerization with depropagation, but eight (or 18). This leads to upwards of 6 (or 15) unknown parameters for a binary (ternary) copolymerization. Due to the complexity of the models these parameters need to be estimated by using non-linear techniques.

The systems explored in this project primarily involve α -Methylstyrene (AMS) copolymerized with an acrylate (Methyl Methacrylate (MMA) and/or Butyl Acrylate (BA)). The interest in AMS is that it has a high glass transition temperature ($\approx 170^\circ\text{C}$) that increases the hardness and loading properties of the resulting copolymer [2]. Interest in the copolymers is found in the area of architectural and automotive coatings. The objective of this work is to explore the kinetics of AMS copolymers (under bulk and solution polymerization conditions) and to use rigorous techniques in order to properly determine unknown kinetic parameters so

that we can predict the composition and microstructure of the polymers under given reaction conditions.

Chapter two outlines some background information about reaction rate kinetics, the differences between bulk and solution polymerizations and the thermal initiation phenomena seen with styrenics and acrylate monomers. It also provides the necessary background for understanding depropagation or reversible polymerizations.

Chapter three describes the kinetic parameters that need to be estimated along with the models being used to do so. It goes on to explain how the Mayo-Lewis and Lowry models are inadequate for describing depropagating copolymerization systems and how Wittmer's model, while complete, is cumbersome and impractical for parameter estimation. It goes on to explain the benefits of using the Kruger model as well as how the Kruger model can be expanded to a terpolymer model to replace the Alfrey-Goldfinger model since it too is inadequate for describing depropagating systems.

Chapter four outlines the experimental methods used to prepare the monomer solutions for polymerization. It also describes the techniques used to analyze the final products including proton and carbon NMR as well as using GPC to determine molecular weight.

Chapter five summarizes the work on the BA/AMS copolymerization system. This includes both the bulk and solution experiments as well as low and full conversion range studies. Included here is also the kinetic parameter estimates for the system.

Chapter six describes the MMA/AMS bulk copolymerization. Included are the parameter estimates for the system as well as the description of an anomaly in the low MMA feed range which has made parameter estimates in the past difficult to obtain.

Chapter seven briefly revisits the BA/MMA system and reanalyses the data with the Kruger model to confirm the results obtained in the past using the Mayo-Lewis model.

Chapter eight ties chapters five through seven together in a MMA/BA/AMS terpolymer analysis. Here experimental considerations are discussed as well as sensitivity issues with the newly developed terpolymer model, benchmarking results as well as the final parameter estimates from the terpolymer system.

Appendix A describes the thermal homopolymerization of BA and how it is thought to undergo a similar mechanism for initiation to that of MMA. It also outlines the challenges inherent with high temperature BA polymerizations namely high levels of cross-linking which makes analysis of the resulting polymer difficult. It also describes ways that attempt to overcome these issues by using chain transfer agents that reduce the overall molecular weight such that the level of gel formation can be reduced.

Appendix B is related to the development of the new terpolymer model in Maple code

Appendix C discusses work that has been done to determine the refractive index of copolymers, which are distinctly different from their homopolymer counterparts.

Appendix D revisits some work done for full conversion MMA/AMS polymerizations that show a linear trend in conversion versus time as well as very little composition drift over the conversion ranges being observed.

Appendix E summarizes the benchmarking results for the new terpolymer model that were done on multiple systems taken from the literature. This analysis is directly related to chapter 8.

Finally, appendix F is a table of the final probability values that correspond to the kinetic parameter estimates from the MMA/BA/AMS terpolymer system.

2. Background and Literature Review

For typical polymerization reactions, the rate of polymerization depends on many variables. These include three rate constants that are primarily temperature dependent.

$$R_p = k_p \left(\frac{2fk_d}{k_t} \right)^{1/2} [M][I]^{1/2} \quad (1)$$

Each of the three rate constants contained in equation (1) (k_p , k_d , k_t) is assumed to be an Arrhenius function and consequently increases with temperature. The magnitude of the increases will be system dependent [3].

2.1. Bulk vs. Solution Polymerization

The interest in elevated temperature polymerizations lies in the fact that increased temperatures result in an increased rate of polymerization. The increased temperature (in many cases above the glass transition temperature (T_g) of the reaction mixture) results in lower viscosities allowing for easier operation and temperature control. This reduces diffusion resistance to termination (i.e. k_t increases) while increasing the rate of initiator decomposition (i.e. k_d increases) resulting in an overall increased rate of monomer consumption. The advantage here is that one obtains a higher limiting conversion and overall productivity. The consequence of this is that since termination has increased (in conjunction with smaller macro radicals), the average molecular weight of the polymer decreases [4, 5]. A way around this high termination rate is by conducting these free radical polymerizations in solution. The idea with using a solvent is that, without raising the temperature of the reactor, one has already decreased the viscosity of the mixture while maintaining a lower termination rate. The kinetics for a bulk and solution copolymerization has been illustrated to be very similar in mechanism [6-11]. The choice of solvent is not a trivial matter. The solvent should interact enough with the monomers, initiator and the resulting polymer so that at all times there exists only one phase. However, the solvent should neither thermally degrade nor change properties during the reaction. The solvent should also be such that it does not

participate in, or interfere with, the polymerization reaction (specifically monomer selectivity in copolymerization). The solvent should also be volatile enough that it can be easily separated from the polymer. Although carrying out the polymerization in solution has its advantages, it also has significant consequences. While the viscosity is readily decreased, so is the concentration of all reacting species (monomer(s) and initiator(s)). This will ultimately decrease the rate of polymerization (equation (2.1)). Another consequence is a decrease in average molecular weight at higher conversions. It is known that while solution polymerizations reduce the viscosity, they also maintain a more or less constant molecular weight throughout the entire reaction. Typically, in bulk polymerizations, once conversion goes beyond 20% an increase in viscosity is seen which slows diffusion of the polymer radicals allowing only monomer to reach the radical sites, thus reducing k_t . This is known as autoacceleration or the gel effect [3]. In solution, it was shown that the gel effect is not as significant and ultimately a lower molecular weight is achieved [11]. A balance between ease of operation (i.e. amount of solvent used) and rate of production must be found if solution polymerization is to be feasible.

2.2. Thermal Initiation

Depending on the monomers being used, other phenomena can occur when dealing with increased reaction temperatures. Two such phenomena are thermal initiation via decomposition and depropagation (i.e. reverse polymerization).

Thermal initiation occurs at temperatures high enough to cause spontaneous decomposition of monomer or impurities in the feed to produce radicals. The source of the radicals is highly dependent upon the type of monomer being used and the type (if any) of impurities that exist. Two particular classes of monomers that exhibit thermal initiation are acrylates (e.g. MMA and BA) and styrenics (e.g. styrene, AMS). The advantage to using thermal initiation is that additional initiator is not needed, increasing safety, reducing costs as well as minimizing the possibility of further contamination of the system. However, the rate of thermal initiation has been shown to be slower than that from a standard initiator that would undergo thermal homolysis [12, 13].

2.2.1. Thermal Initiation of Methyl Methacrylate

The thermal initiation of Methyl Methacrylate (MMA) has been studied in detail [12-15]. Walling's group[15] had great difficulty reproducing results. After trying many different distillation and purification techniques, the only way the group could get some consistent results was to add hydroquinone to the mixture. The group could only explain this behaviour by insisting that some impurity was present and that it acted like a peroxide or oxygen. A hydroquinone was to be used to scavenge a significant number of the radicals produced by the impurity. Walling claims this allowed the reaction to continue as expected for thermally initiated MMA. However, the hydroquinone was only effective at high temperatures (above 130°C) indicating that the half-life of the impurity is significant at lower temperatures. These results coincide with the hypothesis of Fenouillot's[13] group that the impurity burns out quickly only at high temperatures. This was shown by increasing the temperature of reaction and observing the rate of polymerization level off sooner, compared to lower temperature reactions, as the impurity was consumed. The work of Clouet et al. [12] found that no matter what technique was used to purify the monomer, the level of conversion obtained during thermally initiated polymerization could not be explained simply by initiation via the MMA monomer molecule. Using a dilatometric reactor to measure conversion while the reaction is taking place at high temperatures (80°C – 180°C), Clouet's group also found that the levels of conversion achieved did not coincide with what was expected by a thermally initiated reaction of pure MMA. Once again it was concluded that an impurity was present that initially increased the rate of polymerization, but died off quickly under high temperature conditions. The group also did some modeling to show what the theoretical thermal polymerization conversion curve should look like. Clouet's group postulates the impurity to be peroxide, which is the result of MMA radicals reacting with oxygen. The group's attempts to isolate and analyze the impurity were not successful. Lingnau and Meyerhoff [14] have had seemingly more success in determining a mechanism for the self-initiation of MMA, while not denouncing the fact that impurities exist. They show a reaction scheme that relies on the formation of a biradical from two monomers that abstracts hydrogen from some other species to form a monoradical. The dependence upon two monomer molecules to initiate the reaction

leads to an entirely different rate of initiation equation that ultimately leads to a polymerization rate that is dependent upon [MMA] to the second power: $R_p \propto [\text{MMA}]^2$.

2.2.2. Thermal Initiation of Butyl Acrylate (BA)

At elevated temperatures the thermal polymerization of BA is evident from work done in our group (see Appendix A). Given the nature of BA it is also thought that some form of impurity is responsible for the high rates of reaction. Another feature of the homopolymerization of BA at elevated temperatures is gel formation which in turn leads to decreased levels of monomer conversion. The creation of gel leads to analysis issues since GPC cannot be used for molecular weight determination and a Soxhlet extraction must be used to determine the gel content. Due to the differences in equipment, it will not be possible to run the exact same types of experiments done by Clouet's [12] group in order to determine parameter values for such a model. However, since the reaction mechanism being proposed for BA is virtually identical to that of MMA, it may be possible that such elaborate experiments are unnecessary. In the case that a quantitative analysis of the reaction is not possible with our equipment, a qualitative study might be done in order to support the model/mechanisms being proposed. It may be possible to negate the effects of the impurity by using a radical scavenger like hydroquinone [15] (or 2,2'-diphenyl-1-picrylhydrazyl, 4-tert-butylcatechol) to consume the radicals produced by the impurity, hence delaying the reaction long enough that all impurity is consumed leaving only the BA to undergo its own pure thermal polymerization [16].

2.2.3. Thermal Initiation of Styrene/AMS

The thermal initiation of Styrene has been well documented [17, 18] and a mechanism for the initiation is well understood [19]. Starting with two monomers a Diels-Alder adduct is formed. This adduct then reacts with another monomer molecule creating a stable di-aromatic compound and a radical. This Diels-Alder adduct contributes to the molecular weight distribution of thermally initiated polystyrene since it acts as a chain transfer agent. Hui and Hamielec [17] explore the kinetics behind the thermal initiation of styrene and develop a model for the rate of initiation that has third order dependence on the concentration of styrene.

This is in contrast to the typical rate of initiation that has a first order dependence on the concentration of initiator. The thermal initiation of styrene is well behaved when compared to that of MMA. The work done would indicate that the styrene molecule is the only participant in radical production and no evidence of an active impurity can be found.

No findings of this type have been reported for AMS since very little work has been done with the homopolymerization of AMS at high temperatures. Theoretically though, AMS can undergo self-initiation via a very similar mechanism to that of styrene, but due to the methyl substitution, it is expected that the rate of initiation would be slower [3]. Modelling work that has been done for the full conversion range of an MMA/AMS copolymer system indicates that in order to properly explain the rate of polymerization (given the work done by Stickler and Meyerhoff) that some initiation due to AMS must be occurring. The homopolymerization of AMS is a slow reaction due to the very low ceiling temperature of the reaction [2].

2.3 Depropagation/Reverse Polymerization

Analysis of free radical polymerization typically deals with the concept of an irreversible propagation step. A radical of length r adds a monomer unit M with a rate constant k_p :



However, the direction of the reaction is governed by the Gibbs free energy expression, which relates the enthalpy H_p , entropy S_p , and reaction temperature T :

$$\Delta G_p = \Delta H_p - T\Delta S_p \quad (3)$$

For a spontaneous polymerization reaction to occur, ΔG_p must take a negative value. Typical polymerizations are highly exothermic reactions with values of ΔH_p being negative.

Since order is being restored to the system by creating polymer, ΔS_p is also a negative value. As T increases, the right side of the equation grows and moves ΔG_p closer to zero: the temperature at which $\Delta G_p = 0$ is known as the ceiling temperature [20].



Where k_p describes the forward propagation and k_{dp} the depolymerization, the overall rate expression for polymerization then becomes

$$R_p = k_p [M][R\cdot] - k_{dp} [R\cdot] \quad (5)$$

At equilibrium, the net rate of polymerization (R_p) is zero giving the following expression:

$$\frac{k_p}{k_{dp}} = K = \frac{1}{[M]_{eq}} \quad (6)$$

For AMS, the homopolymerization ceiling temperature, T_c , is 61°C; so significant depropagation is expected at elevated temperatures. AMS consequently exhibits natural tendencies for producing low-molecular-weight polymer at high temperatures [21]. Above 61°C, the result from an AMS *homopolymerization* is an abundance of dimers, a small fraction of trimers and negligible amounts of larger oligomers [22]. However, *copolymerization* can proceed, as ΔH_p and ΔS_p of the cross-propagation reactions are different because of changes in radical stability. The ceiling temperature of MMA has been estimated to be 220°C [5, 23]. However, the T_c of MMA has also been reported to take other possible values: 155.5°C, 135°C and 164°C [10, 24]. It should be noted that these lower values of T_c are obtained from experiments done in solution where the equilibrium concentration of MMA is significantly lower. This discrepancy is of the utmost importance when it comes to modeling copolymerizations at temperatures above 120°C. An application where the

importance of properly accounting for the depropagation of MMA is shown in O’Driscoll and Burczyk’s work with a starved feed reactor [25]. In another work by Villalobos and Debling [26] the importance of depropagating monomers in multicomponent systems with multiple depropagating monomers is emphasized in their modelling of a steady state CSTR system.

T_c is shown by Odian to be a function of monomer concentration:

$$\Delta G_p^o = -RT \ln K = RT \ln[M]_{eq} \quad (7)$$

$$\Delta G_p^o = \Delta H_p^o - T\Delta S_p^o = RT \ln[M]_{eq} \quad (8)$$

$$T_c = \frac{\Delta H_p^o}{\Delta S_p^o + R \ln[M]_{eq}} \quad (9)$$

According to this relationship, T_c for a *homopolymerization* reaction is dependent upon thermodynamics as well as the equilibrium concentration of monomer. However, the thermodynamic functions of entropy and enthalpy (and consequently the equilibrium concentrations) for binary/ternary polymerizations have the potential to be very different from the homopolymerization. It is the cross-propagation reactions that may or may not occur simultaneously with the homopolymerization reactions that greatly change the thermodynamic functions of entropy and enthalpy and hence the T_c for a given monomer. Hutchinson et al. show some interesting work with bulk depropagation kinetics for homopolymerizations [27]. Evidence of cross-depropagation complications is found via a bulk polymerization of BA/MMA at 140°C [28] that showed insignificant levels of depropagation where one would expect to see it, supporting the data provided by Palmer[5] and O’Driscoll[23]. However, it is apparent that since MMA is being copolymerized here, that using AMS instead of BA at elevated temperatures, the depropagation of MMA is distinctly possible.

It is not only the monomer concentrations that need to be considered either. It has been discussed in detail [19] for various systems including AMS that the extent of reaction

also determines the T_c . The interaction between polymer and the surrounding monomer solution changes the thermodynamics. As the level of conversion increases, the overall monomer concentration decreases, but with the increased amount of polymer in solution, localized concentrations of monomer can increase which would force the reaction further to the right, theoretically increasing T_c [29].

Pressure is also a consideration in thermodynamics and its effect on T_c can be quantified by the Clapeyron-Clausius equation:

$$\frac{d \ln T_c}{dP} = \frac{\Delta V}{\Delta H} \quad (10)$$

Here ΔV and ΔH are the volume and heat changes for the polymerization for given conditions. For AMS, $\log T_c$ is shown to be a linear function of P [29] and the slope of the line is consistent with the known values of ΔV and ΔH . ΔV can be calculated by the slope of $RT \ln[M]_{eq}$ against P . For AMS $\Delta V = -14.1 \text{ cm}^3/\text{mol}$ and $\Delta H = -33.9 \text{ kJ/mol}$. These values indicate that by increasing pressure, the T_c is effectively increased for AMS leading higher rates of net polymerization at temperatures higher than the standard calculated T_c of 61°C .

ΔG is also affected by the structure of the monomers being polymerized. Typically unsubstituted and monosubstituted ethylenes like ethylene and styrene have negligible depropagating behaviour unless polymerized at extremely low concentrations and high temperatures. 1,1-disubstituted monomers however can have significant depropagating behaviour which depends almost entirely on the nature of the substituents, especially their bulkiness. Even methyl groups close to the unsaturated centre of the monomer can create significant strain in the polymer leading to a slower rate of reaction [29]. This change in rate can be seen especially when comparing AMS and styrene as well as MMA and methyl acrylate where the values for ceiling temperature are located in Table 1 along with other common monomers. The introduction of bulkier groups tends to make the reaction less favourable still.

Table 1: Ceiling Temperatures for Common Monomers

Monomer	$[M]_{eq}$	T_c ($^{\circ}C$)	Pressure	Solvent
AMS ^[30]	Pure	61	1 bar	n/a
AMS ^[30]	Pure	170	6.57 kbar	n/a
AMS ^[29]	0.76	0	1 bar	THF
AMS ^[31]	2.2	25	1 bar	THF
MMA ^[31]	Pure	220	1 bar	n/a
MMA ^[31]	0.14	110	1 bar	o-dichlorobenzene
MMA ^[30]	0.611	135	1 bar	Ethyl Benzoate
MMA ^[31]	1×10^{-3}	25	1 bar	unknown
Styrene ^[29]	1.2×10^{-4}	110	1 bar	Benzene
Styrene ^[30]	9.1×10^{-4}	150	1 bar	Benzene
Styrene ^[31]	Pure	310	1 bar	n/a
Styrene ^[31]	1.0×10^{-6}	25	1 bar	unknown
Methyl Acrylate ^[31]	1.0×10^{-9}	25	1 bar	unknown
Methyl Acrylate ^[31]	Pure	--	1 bar	n/a
Butyl Acrylate ^[20, 32]	Pure	--	1 bar	n/a
Vinyl Acetate ^[31]	Pure	--	1 bar	n/a
Vinyl Acetate ^[31]	1.0×10^{-9}	25	1 bar	unknown

It becomes even more obvious that even though high bulk ceiling temperatures are reported, in copolymerizations, depropagation can occur at much lower temperatures and this issue needs to be addressed. It is apparent that depropagation is a major hurdle when using AMS. So why use AMS at all? The high glass-transition temperature of AMS ($T_g \approx 170^{\circ}C$) effectively hardens the copolymer it is added to. This greatly improves adhesion and loading properties and gives rise to copolymers suitable for higher temperature applications. AMS copolymerizes with other monomers like styrene, divinyl benzene, acrylates (e.g. Methyl Methacrylate, Butyl Acrylate), acrylonitrile, butadiene (and others), improving heat distortion properties of ABS plastics, polystyrene, etc. AMS finds application in other various end products like perfumery chemicals, antioxidants, drying oils, lubricating oils, alkyd resins, modified phenolic resins, etc. Low molecular weight polymers of AMS are viscous liquids that are used as plasticizers in paints, waxes, adhesives and plastics in the automotive and architectural paint/coating industries [2, 20, 33, 34].

3. Modeling

3.1. Reactivity Ratios

Reactivity ratios (r_1 and r_2) are important parameters, revealing information about relative monomer reactivity allowing the determination of copolymer composition. This information combined with an appropriate model can help determine the reaction conditions to produce a desired product. With systems such as the one being studied, there are typically two different types of experiments to be done: low conversion and limiting (or high) conversion experiments. The information obtained from limiting conversion experiments can be useful in estimating conversion rates but also in determining the limiting molecular weight and the equilibrium concentration of monomers. Low conversion experiments (conversion below 5%) are used to estimate reactivity ratios and other kinetic parameters to be discussed. The idea behind using experiments with conversions below 5% is to assume that the concentration of monomers in solution is approximately constant [5]. This assumption allows one to use an instantaneous composition model to determine the reactivity ratios and other kinetic parameters. Limited amounts of the kinetic data required for use in copolymer composition equations for the systems being studied can be found in the literature [5, 11, 17, 24, 32, 35, 36] while the composition itself is determined using Nuclear Magnetic Resonance (NMR). By focusing magnetic pulses on the polymer in solution and collecting data from the resulting reflected signal, one can determine the number of each type of proton or carbon that exists on the polymer chain that corresponds to a given monomer [33, 34, 37, 38]

3.2. Binary Copolymer Composition Equations

3.2.1. The Mayo-Lewis Equation

A typical homopolymerization reaction consists of one reaction: a monomer unit reacting with a radical chain made entirely of that monomer. However, when dealing with a copolymerization, there are now four such reactions to consider [3]: two homopropagation reactions and two cross-propagation reactions (equations 11 – 14).



Here $R_{r,1}$ is a radical of length r ending in a unit of monomer 1 and M_1 is a monomer unit of type 1. These four reactions are assumed to be irreversible in many cases. Balances on monomers one and two (M_1 and M_2) along with the stationary state hypothesis for radicals (i.e. $R_{r,1}$ and $R_{r,2}$) leads to the following copolymer composition equation:

$$\frac{d[M_1]}{d[M_2]} = \frac{[M_1](r_1[M_1] + [M_2])}{[M_2]([M_1] + r_2[M_2])} \quad (15)$$

$$\text{where } r_1 = \frac{k_{11}}{k_{12}} \quad \text{and} \quad r_2 = \frac{k_{22}}{k_{21}} \quad (16)$$

This copolymerization equation can also be expressed in terms of mole fractions. If f_1 is the mole fraction of M_1 in solution and F_1 is the mole fraction of M_1 in the copolymer then:

$$f_1 = 1 - f_2 = \frac{[M_1]}{[M_1] + [M_2]} \quad \text{and} \quad F_1 = 1 - F_2 = \frac{d[M_1]}{d[M_1] + d[M_2]} \quad (17)$$

Combining equations (15) and (17), the following instantaneous composition equation, also known as the Mayo-Lewis equation, is obtained:

$$F_1 = \frac{r_1 f_1^2 + f_1 f_2}{r_1 f_1^2 + 2f_1 f_2 + r_2 f_2^2} \quad (18)$$

This equation works well for determining reactivity ratios for irreversible copolymerizations using data from low conversion experiments. However, the equation does not take into account depropagation of either monomer. In a system where depropagation can exist, there are no longer just four propagation reactions, but there is the addition of four possible depropagation reactions (equations 19 – 22):



Depropagation complicates modeling considerably, invalidating the Mayo-Lewis model. In conjunction with equations (19) – (22) the possibility exists that only one monomer in the system will depropagate (i.e. $k_{22}^{-} = k_{12}^{-} = 0$). The systems being studied have potential to have zero, one, or two depropagating monomer under the right temperature conditions. It is thus that the equations derived by Lowry are the first to be considered when dealing with depropagating monomers.

3.2.2. Lowry's Models

Three different specialized cases have been outlined in an attempt to describe a depropagating system [39]. Disregarding depropagation will lead to an over-estimation of the rate of polymerization, molecular weight and skew the expected instantaneous copolymer composition.

Lowry's first case (Case I) makes the following assumptions:

1. Monomer 1 (M_1) has negligible tendency to depolymerize
2. Monomer 2 (M_2) has negligible tendency to depolymerize if it is attached to an M_1 unit
3. M_2 has an appreciable tendency to depolymerize whenever it is attached to another M_2 unit
4. The rate of addition of a particular monomer to any given chain terminus, or the rate of removal of a particular monomer unit from any given chain terminus, is independent of the composition of the remainder of the chain

Based upon these assumptions, Lowry has constructed the following equations to describe the case where only one monomer (M_2) depropagates and will only depropagate if it is attached to another M_2 unit.

$$\alpha = \frac{\left([1 + \rho[M_2]] + (\rho/r_2)[M_1] \right) - \left\{ [1 + \rho[M_2]] + (\rho/r_2)[M_1] \right\}^2 - 4\rho[M_2] \right\}^{1/2}}{2} \quad (23)$$

$$\rho = \frac{k_{22}}{k_{-22}} \quad (24)$$

$$F_{AMS} = \frac{[M_2]}{r_1[M_1](1 - \alpha) + [M_2](2 - \alpha)} \quad (25)$$

Values of ρ (for AMS only) can be found in Lowry's paper between temperatures of 0°C and 100°C. Extrapolation can be made outside of this range if one were to assume that the equation for ρ would take the form of an Arrhenius expression. A plot of $\ln(\rho)$ versus

1/T(K) shows a linear trend. From here one can extract the necessary data in order to extrapolate values of ρ beyond 100°C. As with any extrapolation, the user must keep in mind that erroneous values may be obtained.

Lowry's Case II is based on the following assumptions:

1. M_1 has negligible tendency to depolymerize.
2. M_2 has negligible tendency to depolymerize if it is attached to an M_1 unit or to a *single* M_2 unit
3. M_2 has an appreciable tendency to depolymerize whenever it is attached to a sequence of two or more M_2 units
4. The rate of addition of a particular monomer to any given chain terminus, or the rate of removal of a particular monomer unit from any given chain terminus, is independent of the composition of the remainder of the chain

Similarly the following equations apply to Lowry's second case where M_2 will only appreciably depropagate if it is attached to two or more M_2 units in the polymer chain:

$$\beta = \frac{\left([1 + \rho[M_2] + (\rho/r_2)[M_1]] - \left\{ [1 + \rho[M_2] + (\rho/r_2)[M_1]]^2 - 4\rho[M_2] \right\}^{1/2} \right)}{2} \quad (26)$$

$$\gamma = \frac{\{ \rho[M_2] + (\rho/r_2)[M_1] - \beta \}}{\rho[M_2]} \quad (27)$$

$$F_{AMS} = \frac{\beta\gamma - 1 + [1/(1-\beta)^2]}{\left[\frac{r_1[M_1]}{[M_2]} + 1 \right] \left[\beta\gamma + \frac{\beta}{1-\beta} \right] + \beta\gamma - 1 + \frac{1}{(1-\beta)^2}} \quad (28)$$

Lowry's first two cases are simple enough and in combination with the proper Non-Linear Least Squares (NLLS) method and experimental data, one can solve for the reactivity ratios.

Finally, Lowry's Case III has the following assumptions:

1. M_1 has negligible tendency to depolymerize unless it is attached to a sequence of two or more M_2 units
2. M_2 has negligible tendency to depolymerize if it is attached to an M_1 unit or to a *single* M_2 unit
3. Either monomer has an appreciable tendency to depolymerize whenever it is attached to a sequence of two or more M_2 units
4. The rate of addition of a particular monomer to any given chain terminus, or the rate of removal of a particular monomer unit from any given chain terminus, is independent of the composition of the remainder of the chain with limits specified above.

Considering the very specialized nature of the Lowry models in conjunction with the restrictions of the second monomer depropagating, it was decided to look at more rigorous and generalized models. Such a model is Wittmer's general copolymer composition equation.

3.2.3. Wittmer's Model

In order to overcome the assumptions in Lowry's models, an effort is made to develop a model that takes into account all monomers in the system depropagating [40]. Wittmer assumes (as Lowry does) that the rate constants are independent of the chain and uses the radical steady-state hypothesis. Wittmer also assumes in his model a sequential distribution of the chain lengths of the reactive sequences to be equal to that of the unreactive sequences. This is done to account for the mole fractions of reactive chains ending in a single monomer unit of type 1 or type 2. Wittmer claims this to be a safe statistical assumption, how close to reality it comes is uncertain. His model is very general and few assumptions are made but the model is more complex than either Lowry's Case I or Case II, has more unknowns and can become unstable under certain conditions during NLLS calculations [11]. Wittmer's model relies heavily on special cases in order to properly converge. These cases typically involve at least one parameter to be zero (e.g. K_i or q_{ij} in equation (29)). Wittmer develops two such

cases, but ignores others. In many such cases the model requires reworking from the balance equations in order to eliminate indeterminate portions. As will be shown in the next sections, at high temperatures where all parameters are non-zero, convergence of Wittmer's model was not achievable. Similar problems with modeling at high concentrations of AMS (in an MMA/AMS system) were also seen by Martinet and Guillot (1997). Wittmer's general model is shown here:

$$\frac{d[M_1]}{d[M_2]} = \frac{1 + \frac{r_1 \frac{[M_1]}{[M_2]} - r_1 \frac{K_1}{[M_2]} (1 - x_1)}{1 - q_1 \frac{y_1}{[M_2]} \bullet \frac{[M_2] + q_2 x_1}{[M_1] + q_1 y_1}}}{1 + \frac{r_2 \frac{[M_2]}{[M_1]} - r_2 \frac{K_2}{[M_1]} (1 - y_1)}{1 - q_2 \frac{x_1}{[M_1]} \bullet \frac{[M_1] + q_1 y_1}{[M_2] + q_2 x_1}}} \quad (29)$$

where $K_i = \frac{k_{ii}}{k_{ii}}$; $q_1 = \frac{k_{12}}{k_{21}}$ and $q_2 = \frac{k_{21}}{k_{12}}$; r_1 and r_2 as before

where y_1 (and x_1) is the mole fraction of radical chains ending with monomer M_2 (and M_1) with a sequence length of 1. y_1 (and x_1) is found by calculating the distribution of the sequential lengths of the reactive chain ends. The reason these mole fractions are used is to correct for the fact that each step in the reaction does not lead to a chain end with a single unit of M_2 (or M_1), but only some do. Wittmer's general model can be simplified from its original form into an equation for one depropagating monomer (assuming that $AMS = M_2$):

$$\frac{d[M_1]}{d[M_2]} = \frac{1 + \frac{r_1 \frac{[M_1]}{[M_2]}}{q_1 y_1}}{1 + \frac{r_2 \frac{[M_2]}{[M_1]} - r_2 K_2 (1 - y_1)}{[M_1]}}; \text{ where } K_2 = \frac{k_{22}}{k_{22}}; \quad q_1 = \frac{k_{12}}{k_{21}} \quad (30)$$

3.2.4. Kruger's Model

Other work has been done to create another general terminal model copolymer composition equation also assuming that both monomers have the potential to depropagate [41]. In comparison with Wittmer's work, it would appear that Kruger has taken a simpler approach. Instead of using a sequential distribution, Kruger uses a probabilistic approach to determine which monomer will be added to a given radical chain. Other work in the past using probabilities has been done for prediction of composition and sequence lengths [42]. Kruger's definitions are simpler yet.

The terms P_{11} , P_{12} , P_{21} , and P_{22} represent probabilities (P_{ij}) that a radical of type i will react with a monomer of type j . The probability terms are derived from the steady state radical assumption for the two classes of radical types. The resulting equations depend only upon the six parameters defined in Equation 33 and the monomer concentrations. For example, P_{11} is the probability that an M_1 unit will be added to a radical chain ending with an M_1 unit. Substituting the corresponding probability into the radical balance equations, Kruger obtains the following equation:

$$\frac{d[M_1]}{d[M_2]} = \frac{[R_1] (k_{11}[M_1] - k_{11}^- P_{11} - k_{21}^- P_{12}) + [R_2] k_{21}[M_1]}{[R_2] (k_{22}[M_2] - k_{22}^- P_{22} - k_{12}^- P_{21}) + [R_1] k_{12}[M_2]} \quad (31)$$

Under the stationary state hypothesis for radicals, Kruger obtains the following equation:

$$[R_1] = [R_2] \frac{k_{21}[M_1] + k_{12}^- P_{21}}{k_{12}[M_2] + k_{21}^- P_{12}} \quad (32)$$

Substituting equation (32) into equation (31) along with the reactivity ratios and the cross-propagation ratios, the following is obtained:

$$\frac{d[M_1]}{d[M_2]} = \frac{[M_1]\{r_1([M_1] + R_1 P_{21}) + [M_2] - R_{11} P_{11}\} - R_1 P_{21}(R_{11} P_{11} + R_2 P_{12})}{[M_2]\{r_2([M_2] + R_2 P_{12}) + [M_1] - R_{22} P_{22}\} - R_2 P_{12}(R_{22} P_{22} + R_1 P_{21})} \quad (33)$$

$$\text{where } r_1 = \frac{k_{11}}{k_{12}}; \quad r_2 = \frac{k_{22}}{k_{21}}; \quad R_1 = \frac{k_{12}^-}{k_{21}}; \quad R_2 = \frac{k_{21}^-}{k_{12}}; \quad R_{11} = \frac{k_{11}^-}{k_{12}}; \quad R_{22} = \frac{k_{22}^-}{k_{21}}$$

Kruger's model can also be simplified for the case of a single depropagating monomer. However, because of the robustness of the model, such a simplification is unwarranted. No terms become indeterminate in the model if any of the parameters are set to zero. Since the Kruger model requires no special cases, and has shown no numerical instability, it is ideally suited for use in the estimation of kinetic parameters via non-linear regression.

3.2.5. Model Comparisons

In order to compare the models it was decided to use previously obtained parameters (e.g. reactivity ratios, cross propagation ratios etc.) from a bulk polymerization of MMA and AMS at elevated temperatures [5]. While these parameter estimates are not yet confirmed as being correct, they should be adequate to illustrate the differences between the models. Since the Mayo-Lewis equation does not take into account depropagation, one would expect it to overestimate the amount of AMS incorporated into the copolymer at increasing temperatures compared with the other models. Being that the Wittmer and Kruger models are more rigorous, one would also expect the predictions of AMS content from these two models to be lower (i.e. MMA content to be higher) than the Mayo-Lewis and the Lowry models. In order to see the effect of increasing temperature, the calculations were carried out at 60°C, 100°C, and 140°C. Calculations done at 140°C have shown that the Wittmer model is unstable so no results from the Wittmer model at 140°C are shown. The results can be seen in figures 1 – 3 below.

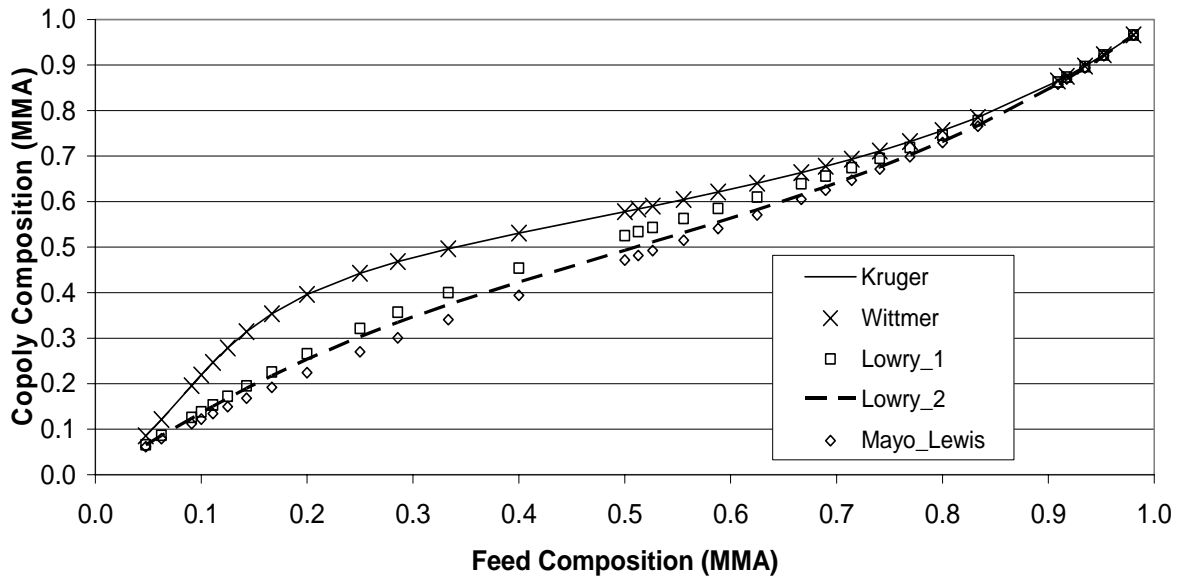


Figure 1: Model Comparison at 60°C

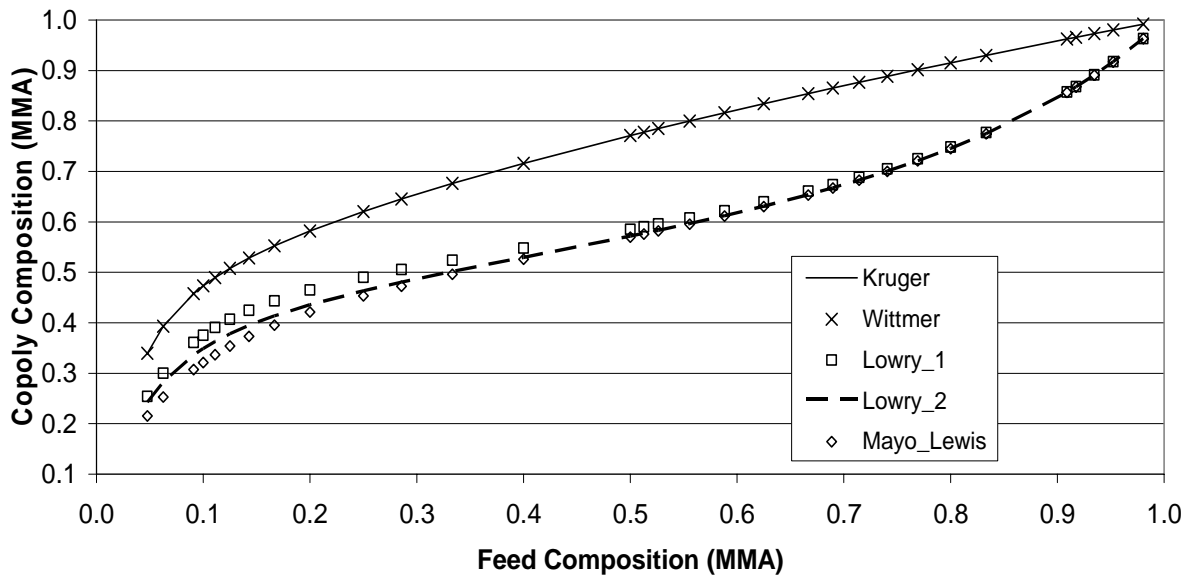


Figure 2: Model Comparison at 100°C

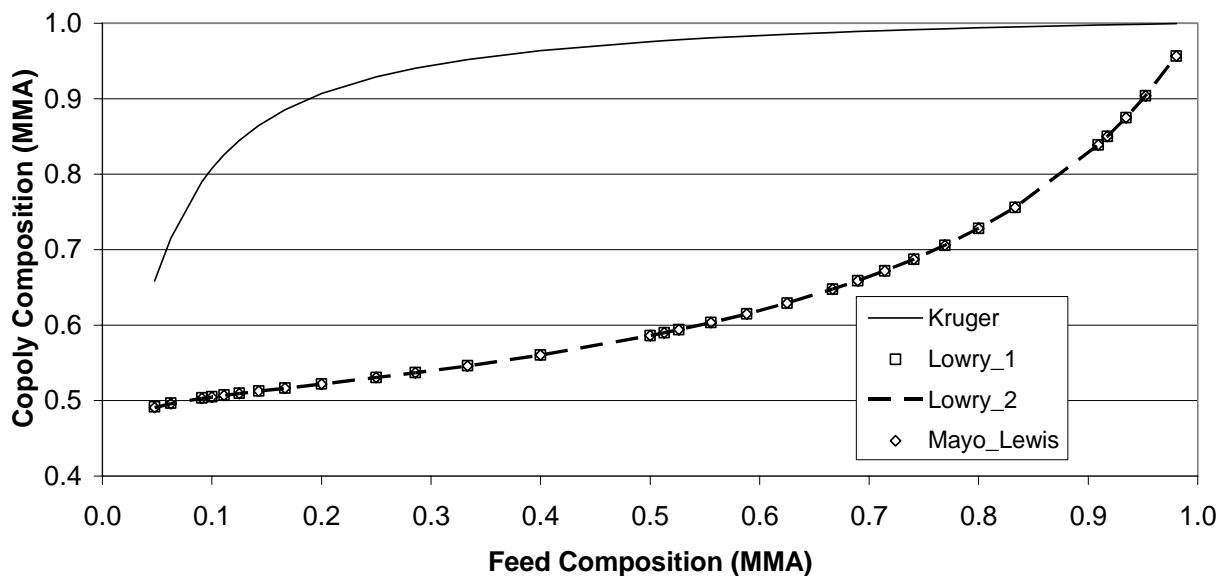


Figure 3: Model Comparison at 140°C

From the plots, it can be seen that all that was expected is seen, especially at 140°C where significant differences exist between the Lowry/Mayo-Lewis models and the Kruger model. What is also very interesting is that as one increases the temperature the Lowry models converge on the Mayo-Lewis model. This trend is expected at high feed ratios of MMA since Lowry assumes that MMA (e.g. M_2) is not going to depropagate as does Mayo-Lewis, but this does not take into account the convergence at high feed concentrations of AMS. A sensitivity analysis done on the Lowry models shows that at increasing temperatures the models become less sensitive to feed concentrations of AMS and more sensitive to the reactivity ratios, which is similarly found for the Mayo-Lewis equation. At increasing temperatures the data used shows r_{AMS} asymptotically approaching zero, and due to the dependency of the Lowry models on this parameter, it explains why the Lowry models and the Mayo-Lewis model converge at higher temperatures. Some other groups have used Lowry's kinetics as well [23, 42-46] but as we have seen, ignoring cross-depropagation is inadequate for modelling systems with depropagating monomers. As will be discussed later, this behaviour of r_{AMS} approaching zero at elevated temperatures is incorrect and misleading. It is expected that with a proper set of parameters, the Lowry and Mayo-Lewis models would not converge in this manner. Another note of value is that the Wittmer and Kruger model predictions are virtually identical at 60°C and 100°C. This is promising since difficulty in

convergence has been seen with Wittmer's model at high temperatures. This difficulty in convergence can be shown to stem from the same issue already mentioned. If the r_{AMS} parameter approaches zero, the Wittmer model becomes numerically unstable and this issue would be resolved using a proper set of parameter estimates at 140°C. However, this does not affect the model comparison up to this point. Wittmer's model is still not as robust as Kruger's model, and since Kruger's model requires no special cases (as can be seen here where one of the reactivity ratios approaches zero), it is the Kruger model which will be further explored.

In theory, if one were to use the Kruger model and set the appropriate parameters to zero, one should be able to use the Kruger model to simulate the Lowry model (and if desired the Mayo-Lewis model). To illustrate the reducibility of the Kruger model, a simulation was performed at 140°C using an updated set of parameters based on a set of experimental data (that will be shown in chapter 6) and the results are shown in Figure 4:

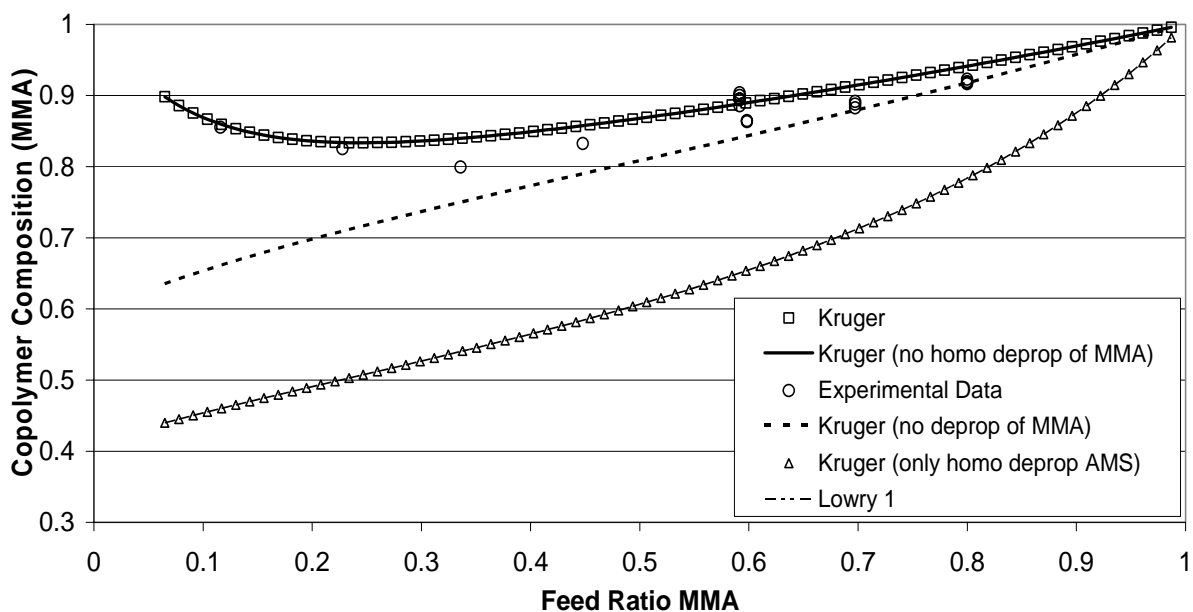


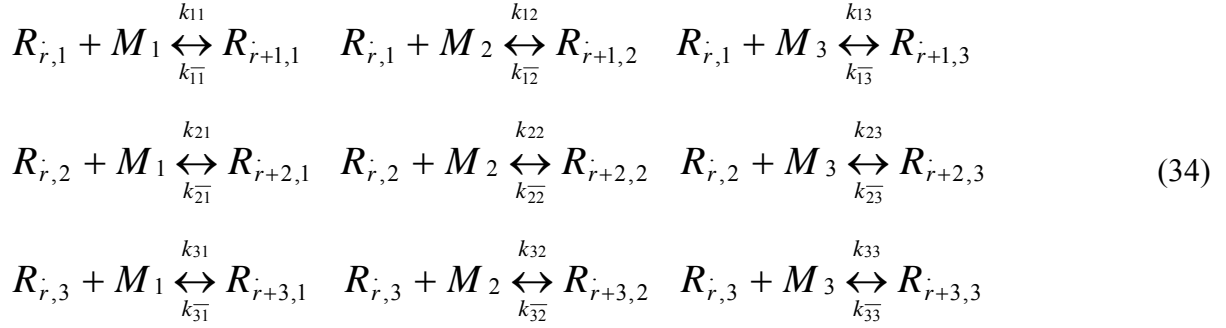
Figure 4: Kruger Model Reduced to Lowry Model 140°C

From Figure 4 it can be seen that using a given set of kinetic parameters and sequentially setting them to zero (to simulate a lack of depropagation in a given reaction) the Kruger model numerically matches the Lowry Case 1 Model. Sequentially what has been

done is to set R_{22} , R_1 and then R_2 to equal zero to reduce the Kruger model to Lowry 1. Setting R_{22} to zero eliminates any MMA homo depropagation which, as we can see here, has negligible effects on the composition. By setting R_1 as well as R_{22} equal to zero, one assumes that MMA will not depropagate from AMS. There is obviously a discrepancy here as indicated by the deviation at higher AMS feeds. If one assumes the parameter estimates are correct, then ignoring cross depropagation is erroneous. Setting all 3 parameters to zero leaves only the homo depropagation of AMS taken into account, which is the only reaction Lowry assumes reversible and here the Kruger model matches perfectly. In the second part of Meakin's paper [46] a different approach to modelling this depropagation behaviour is taken. In a similar set of reactions that are described above and in the Wittmer and Kruger works, all cross-depropagation reactions are taken into account. However, instead of using the reactions to estimate the kinetic parameters as defined by Kruger and Wittmer, a different set of parameters were used to estimate monomer consumption and take depropagation into account, and as such the parameter values obtained are not comparable to any defined in the Kruger and Wittmer models. The solution of this system was done using a Monte Carlo method. In a similar methodology using Monte Carlo simulations and probabilities Kang et al. [47] attempt to model the copolymerization of MMA/AMS and later a terpolymerization of MMA/AMS/AN, however in both of these cases Lowry's kinetics for a single depropagating monomer are assumed.

3.3. Ternary Copolymer Composition Models

In the case of a ternary system (3 monomers), the number of reactions to be considered, increases significantly with depropagating behaviour. If all 9 reactions are considered to be reversible, a total of 18 propagation/depropagation reactions need to be taken into account along with the increase in the number of parameters. This being the case, the models required to determine composition will also increase in complexity.



3.3.1. Alfrey-Goldfinger Model

The majority of the modeling work done in the area of ternary copolymerizations has been done with the Alfrey-Goldfinger model or one of its simplifications[48-50]. The model is developed in a similar manner to that of the Mayo-Lewis model which was previously shown. The similarities or symmetry between the two models is apparent. With the 9 equations considered there are 6 parameters (reactivity ratios) to be estimated. 9 or 3^2 equations stem from 3 monomers in the system where as for the binary there were only $2^2 = 4$ (#components²). The number of parameters to be estimated in the binary is 2 (4 equations - 2 components) whereas in the ternary system there are 6 (9 equations - 3 components). The final expression for the Alfrey-Goldfinger model is the following

$$\begin{aligned}
d[M_1] : d[M_2] : d[M_3] = \\
[M_1] \left\{ \frac{[M_1]}{r_{31}r_{21}} + \frac{[M_2]}{r_{21}r_{32}} + \frac{[M_3]}{r_{31}r_{23}} \right\} \left\{ [M_1] + \frac{[M_2]}{r_{12}} + \frac{[M_3]}{r_{13}} \right\} \\
: [M_2] \left\{ \frac{[M_1]}{r_{12}r_{31}} + \frac{[M_2]}{r_{12}r_{32}} + \frac{[M_3]}{r_{32}r_{13}} \right\} \left\{ [M_2] + \frac{[M_1]}{r_{21}} + \frac{[M_3]}{r_{23}} \right\} \\
: [M_3] \left\{ \frac{[M_1]}{r_{13}r_{21}} + \frac{[M_2]}{r_{23}r_{12}} + \frac{[M_3]}{r_{13}r_{23}} \right\} \left\{ [M_3] + \frac{[M_1]}{r_{31}} + \frac{[M_2]}{r_{32}} \right\}
\end{aligned} \tag{35}$$

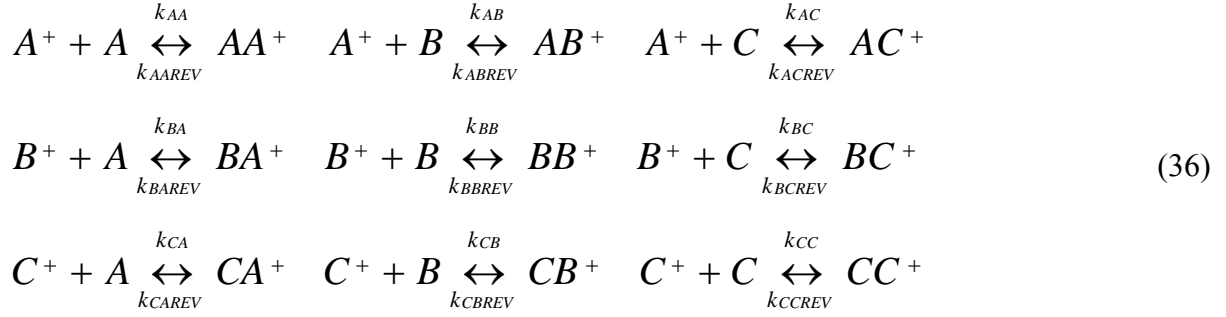
$$\text{where } r_{ab} = \frac{k_{aa}}{k_{ab}}$$

In a similar way that the Mayo-Lewis model was inadequate to predict the composition of a binary system with depropagation, so is the Alfrey-Goldfinger model with respect to a depropagating ternary system. However, the model is quite useful in helping one to understand the symmetry between binary and ternary models and this symmetry should follow when expanding the binary Kruger model to the ternary Kruger model.

3.3.2. Expanded Kruger Model

The symmetry that is seen between the Mayo-Lewis and Alfrey-Goldfinger models should be applicable to the Kruger and expanded Kruger models. The binary Kruger model has 8 reactions ($2n^2$) where 'n' is the number of components. For 3 components one ends up with 18 reactions, which is the case for the fully depropagating ternary system. If this is the case, and it is known that there are 6 parameters to estimate from the binary system (# reactions - #components) then there should be a total of 15 (18 - 3) parameters to be estimated for the expanded Kruger model. If the development of the model is correct there should be 15 parameters to estimate not including the probability values. As is the case with the Mayo-Lewis and Alfrey-Goldfinger models, all of the parameters in the expanded Kruger model should have definitions identical to those found from any of the binary systems, giving the user initial estimates on the parameters based on the work from the binary systems.

For simplicity in the development, and for comparison purposes to the binary model, the definitions of monomers have been changed to what Kruger used in the original publication[41]. Where 'A' represents M_1 , A^+ represents R_1^+ and k_{AC} represents k_{13} and so forth. So the reaction scheme becomes the following.



What is intended to be the final composition equation is the following:

$$F_A = \frac{d[A]}{d[A] + d[B] + d[C]} = \frac{1}{1 + \frac{d[B]}{d[A]} + \frac{d[C]}{d[A]}} \tag{37}$$

Which leads us to find expressions for $d[B]/d[A]$ and $d[C]/d[A]$. The following balances can be written on the monomer concentrations and primary radicals in solution

$$\begin{aligned}
-d[A]/dt &= k_{AA}[A][A^+] + k_{BA}[A][B^+] + k_{CA}[A][C^+] \\
&\quad - k_{AAREV}[AA^+] - k_{BAREV}[BA^+] - k_{CAREV}[CA^+]
\end{aligned} \tag{38}$$

$$\begin{aligned}
-d[B]/dt &= k_{AB}[B][A^+] + k_{BB}[B][B^+] + k_{CB}[B][C^+] \\
&\quad - k_{ABREV}[AB^+] - k_{BBREV}[BB^+] - k_{CBREV}[CB^+]
\end{aligned} \tag{39}$$

$$\begin{aligned}
-d[C]/dt &= k_{AC}[C][A^+] + k_{BC}[C][B^+] + k_{CC}[C][C^+] \\
&\quad - k_{ACREV}[AC^+] - k_{BCREV}[BC^+] - k_{CCREV}[CC^+]
\end{aligned} \tag{40}$$

$$\begin{aligned}
-d[A^+]/dt &= k_{AB}[B][A^+] + k_{AC}[C][A^+] + k_{BAREV}[BA^+] + k_{CAREV}[CA^+] \\
&\quad - k_{ABREV}[AB^+] - k_{ACREV}[AC^+] - k_{BA}[A][B^+] - k_{CA}[A][C^+]
\end{aligned} \tag{41}$$

$$\begin{aligned}
-d[B^+]/dt &= k_{BA}[A][B^+] + k_{BC}[C][B^+] + k_{ABREV}[AB^+] + k_{CBREV}[CB^+] \\
&\quad - k_{BAREV}[BA^+] - k_{BCREV}[BC^+] - k_{AB}[B][A^+] - k_{CB}[B][C^+]
\end{aligned} \tag{42}$$

$$\begin{aligned}
-d[C^+]/dt = & k_{CA}[A][C^+] + k_{CB}[B][C^+] + k_{ACREV}[AC^+] + k_{BCREV}[BC^+] \\
& - k_{CAREV}[CA^+] - k_{CBREV}[CB^+] - k_{AC}[C][A^+] - k_{BC}[C][B^+]
\end{aligned} \tag{43}$$

Based on Kruger's definitions of the probabilities, the following definitions can be used to simplify equations 38-43.

$$\begin{aligned}
[A^+] &= [BA^+] + [AA^+] + [CA^+]; \\
[B^+] &= [AB^+] + [BB^+] + [CB^+]; \\
[C^+] &= [AC^+] + [BC^+] + [CC^+]
\end{aligned} \tag{44}$$

$$[AA^+] = P_{AA}[A^+]; [BA^+] = P_{AB}[A^+]; [CA^+] = P_{AC}[A^+] \tag{45}$$

$$[AB^+] = P_{BA}[B^+]; [BB^+] = P_{BB}[B^+]; [CB^+] = P_{BC}[B^+] \tag{46}$$

$$[AC^+] = P_{CA}[C^+]; [BC^+] = P_{CB}[C^+]; [CC^+] = P_{CC}[C^+] \tag{47}$$

Where P_{AC} is the probability of finding an A^+ primary radical attached to a "C" unit in the polymer chain. Also we define $[BC^+]$ as the overall concentration of radicals ending in BC units.

$$\begin{aligned}
-d[A]/dt = & k_{AA}[A][A^+] + k_{BA}[A][B^+] + k_{CA}[A][C^+] - \\
& k_{AAREV}P_{AA}[A^+] - k_{BAREV}P_{AB}[A^+] - k_{CAREV}P_{AC}[A^+]
\end{aligned} \tag{48}$$

$$\begin{aligned}
-d[B]/dt = & k_{AB}[B][A^+] + k_{BB}[B][B^+] + k_{CB}[B][C^+] - \\
& k_{ABREV}P_{BA}[B^+] - k_{BBREV}P_{BB}[B^+] - k_{CBREV}P_{BC}[B^+]
\end{aligned} \tag{49}$$

$$-d[C]/dt = k_{AC}[C][A^+] + k_{BC}[C][B^+] + k_{CC}[C][C^+] -$$

$$k_{ACREV}P_{CA}[C^+] - k_{BCREV}P_{CB}[C^+] - k_{CCREV}P_{CC}[C^+] \quad (50)$$

$$\begin{aligned} -d[A^+]/dt = & k_{AB}[B][A^+] + k_{AC}[C][A^+] + k_{BAREV}P_{AB}[A^+] + k_{CAREV}P_{AC}[A^+] \\ & - k_{ABREV}P_{BA}[B^+] - k_{ACREV}P_{CA}[C^+] - k_{BA}[A][B^+] - k_{CA}[A][C^+] \end{aligned} \quad (51)$$

$$\begin{aligned} -d[B^+]/dt = & k_{BA}[A][B^+] + k_{BC}[C][B^+] + k_{ABREV}P_{BA}[B^+] + k_{CBREV}P_{BC}[B^+] \\ & - k_{BAREV}P_{AB}[A^+] - k_{BCREV}P_{CB}[C^+] - k_{AB}[B][A^+] - k_{CB}[B][C^+] \end{aligned} \quad (52)$$

$$\begin{aligned} -d[C^+]/dt = & k_{CA}[A][C^+] + k_{CB}[B][C^+] + k_{ACREV}P_{AC}[C^+] + k_{BCREV}P_{CB}[C^+] \\ & - k_{CAREV}P_{AC}[A^+] - k_{CBREV}P_{BC}[B^+] - k_{AC}[C][A^+] - k_{BC}[C][B^+] \end{aligned} \quad (53)$$

Making the assumption of the steady state hypothesis that radical concentrations do not change, one can set equations 51-53 equal to zero and solve the system of equations to determine expressions for each of the radical concentrations $[A^+]$, $[B^+]$, and $[C^+]$ and subsequently substitute these expressions back into the monomer balances (equations 48-50). This will result in the monomer differential equations only being a function of monomer concentrations and kinetic parameters. Dividing the equations by one another will allow us to obtain expressions for $d[B]/d[A]$ and $d[C]/d[A]$ which can then be used to solve for F_A . These expressions once simplified are left with the following kinetic parameters to be solved for:

$$\begin{aligned} r_{AB} = k_{AA}/k_{AB}; r_{AC} = k_{AA}/k_{AC} \\ r_{BA} = k_{BB}/k_{BA}; r_{BC} = k_{BB}/k_{BC} \\ r_{CA} = k_{CC}/k_{CA}; r_{CB} = k_{CC}/k_{CB} \end{aligned} \quad (54)$$

$$\begin{aligned} R_A = k_{ABREV}/k_{BA}; R_B = k_{BAREV}/k_{AB} \\ R_C = k_{CAREV}/k_{AC}; R_D = k_{ACREV}/k_{CA} \\ R_E = k_{BCREV}/k_{CB}; R_F = k_{CBREV}/k_{BC} \\ R_{AA} = k_{AAREV}/k_{AB}; R_{BB} = k_{BBREV}/k_{BA}; R_{CC} = k_{CCREV}/k_{CA} \end{aligned} \quad (55)$$

Upon substitution of these definitions the resulting equations are quite complex. Manipulation of the equations was done in Maple 9.5 and the results are listed in Appendix B. This is of course only half of the solution. The values for the probabilities need to be

estimated. In a similar fashion to the binary model, this set of probabilities will only be dependent on the monomer concentrations and the kinetic parameters defined above. Each update of the kinetic parameters in the NLLS routine will require a new estimation of the 9 different probabilities. 9 probabilities require us to have 9 independent equations. From the definition of the probabilities the following 3 expressions can be obtained:

$$P_{AB} + P_{AC} + P_{AA} = 1 \quad (56)$$

$$P_{BA} + P_{BC} + P_{BB} = 1 \quad (57)$$

$$P_{CA} + P_{CB} + P_{CC} = 1 \quad (58)$$

Six more balances are still required. Balances on the species $[AA^+]$, $[BB^+]$, $[CC^+]$, $[AB^+]$, $[BC^+]$, $[CA^+]$ were used and setting each equation to zero allows for the final 6 algebraic expressions to be created. Substitution of the expressions for the primary radical concentrations and the kinetic parameters leaves the 6 equations being only a function of the probabilities themselves, monomer concentrations and the kinetic parameters. This gives a system of 9 equations and 9 unknowns. Given the size of the system, it has been found that this is the bottleneck in converging on the parameter estimates we are interested in. The expressions can also be found in Appendix B.

Re-examining the final number of kinetic parameters that are to be estimated via the expanded model, there are a total of 15. It should also be noted, that in the context of the binary model, there are no new parameters to be estimated. All 15 parameters that appear in the ternary model appear as parameters from each of the three binary systems. This is useful, since the parameters estimated from the binary system can be used as first guesses when estimating them for ternary system. Ideally, the parameters should not change, but there may be some unaccounted for interaction of the molecules or additional measurement error that would allow for convergence on different values. From here it is time to benchmark the new model by seeing if it will properly predict the composition for published data. This work will be shown in subsequent chapters.

4. Experimental Methods

Polymerization experiments are to be carried out in ampoules. The sections to follow will outline the steps required with selected works [10, 20, 51] taken as a guide.

4.1. Reagent Purification

In order to obtain accurate kinetic data from polymerization experiments, the monomers (and in some cases the initiator) being used must be cleansed of impurities including inhibitors and oligomers. Two separate steps are used to ensure these impurities are removed: washing/drying and distillation. The monomers (BA, MMA and AMS) were obtained from Aldrich Chemical Company and were cleaned using the steps outlined in the following sections. 2,2'- azo-bisisobutyronitrile (AIBN, Polysciences Inc.), was recrystallized three times from absolute methanol. Di-tert-butyl peroxide (Trigonox-B (Trig-B), AKZO), dodecyl mercaptan (NDM) (Aldrich Chemicals) (CTA) and solvents (ethanol, acetone, toluene, dichloromethane, dichloromethane-d₂ and chloroform-d), were used as received without further purification.

4.1.1. Monomer Washing

Monomer is poured into a separatory funnel and to this a volume of 10% wt. NaOH solution is added. The volume of NaOH solution added should be 10% of the volume of the monomer in the funnel. The NaOH reacts with the inhibitor in the monomer phase allowing it to become soluble in the aqueous phase. The funnel is shaken vigorously for 2-3 minutes and then left to stand until the two phases can separate. The aqueous phase can then be removed from the bottom of the funnel. The washing procedure is done 3 times with the NaOH solution and then 3 times with de-ionized water to ensure that all of the NaOH is removed from the monomer. For the final wash with de-ionized water, the mixture is allowed to stand for an extended period of time to allow for any water adhering to the sides of the funnel to agglomerate and collect at the bottom of the funnel. The monomer is then transferred from the funnel to an appropriate storage container and calcium chloride pellets are added to allow

for the removal of any lingering water. The pellets are added progressively until a few pellets are freely floating in the monomer. The “dry” monomer is then refrigerated at -10°C until it is ready for distillation.

4.1.2. Monomer Distillation

Monomer distillation is done at maximum 48 hours before polymerization since even dimers and trimers slowly form at low temperatures. The distillation is carried out using a vertical condenser rotary evaporator that is connected to a vacuum pump. To ensure that no volatiles reach the pump, a liquid nitrogen vacuum trap is used. Once the monomer to be distilled is poured into the source flask, it is heated in a water bath, under vacuum, to initialize the distillation. The first fraction of distillate, as well as the last fraction of the source material, is discarded. These fractions are considered to be high and low volatility impurities. The distilled monomer is now ready for either solution preparation or refrigeration.

4.2. Solution Preparation

Concentrations are back-calculated using temperature corrected densities and molecular weights. Since the smallest mass component is the initiator (if one is used), it is weighed out first and subsequently the amount of monomers and solvent required can be calculated. This solution is then pipetted into the appropriate sized ampoules. The size of the ampoule being used is dependent on the system conditions and the amount of conversion desired. For low conversion solution experiments, it is desired to use a larger ampoule (14mm O.D. vs. 7.5mm O.D.) to create enough copolymer for analysis. Since this solution has been exposed to atmosphere, there will inherently be some dissolved oxygen. Oxygen is an inhibitor for free radical reactions and must be removed if the polymerization kinetics are to be studied accurately. The ampoules are attached to degassing equipment that is connected to the vacuum pump. The ampoules are then frozen in liquid nitrogen and exposed to vacuum until an ultimate vacuum of ~ 0.04 mbar is achieved effectively removing any gas inside the ampoule. The ampoules are then sealed off from the vacuum via valves and thawed to allow any trapped gas to evolve. The cycle is repeated 3 times and then the ampoules are permanently sealed using a torch. The ampoules are now ready for polymerization. If the reaction cannot be started once the ampoules are prepared, they are stored in liquid nitrogen

and then thawed and brought to room temperature before beginning the reaction.

4.3. Polymerization Reaction

A silicone oil bath is used to control the ampoule temperature to within $\pm 0.1^\circ\text{C}$ of the desired reaction temperature. Before placing the ampoules into the bath, they are weighed for gravimetric calculation purposes. Ampoules are then removed at the pre-determined time, wiped clean of silicon oil and then immediately frozen in liquid nitrogen to stop the reaction. The removal process usually takes no longer than 15 seconds. Once the ampoules are completely frozen, and there is little doubt that the reaction has stopped, they are once again thawed, scored, broken open and the contents poured into a pre-weighed flask containing a hydroquinone radical scavenger. The ampoules are rinsed with methylene chloride, acetone and ethanol several times to ensure that all polymer has been removed from the glass ampoule. Once the empty ampoule is dry, it too is weighed. Methylene chloride is then used to ensure that the entire polymer sample is dissolved and ethanol is used to precipitate the polymer inside the flask. In the case of a higher conversion polymerizations where the viscosity is too high to pour the solution out two methods have been used for removing the polymer. For medium viscosities, the ampoule is re-frozen and broken into small pieces and let to sit in methylene chloride until the polymer is dissolved. For very high conversions where the polymer is essentially solid at room temperature, the ampoule can be re-frozen (to shrink the polymer), the ampoule opened at one end and the frozen polymer can be slid out of the ampoule and allowed to dissolve in methylene chloride. Once fully dissolved, the polymer is precipitated with ethanol and a rapid evaporation of solvent/monomer is done. Once a rapid evaporation of the samples has been completed, they can then be placed in a vacuum oven at an appropriate temperature to ensure all volatile components have been removed. Whether the sample is “dry” can be determined by a gravimetric analysis.

4.4. Copolymer Characterization

4.4.1. Gravimetry

Using the measurements mentioned in the previous section, conversion levels are obtained via gravimetry. Once all of the volatiles have been removed from the polymer the following

equation, in conjunction with the four previously obtained weights, is used to determine conversion for a bulk system (a simple modification can be used for solution systems):

$$\text{Conversion} = \frac{(\text{dried polymer plus flask} - \text{empty flask})}{(\text{full ampoule with solution} - \text{dried empty ampoule})} \quad (59)$$

If however the mass of the initiator being used is significant and the initiator is not volatile, it will be necessary to subtract this mass from the amount of polymer produced.

4.4.2. Copolymer Composition: ¹H NMR

The determination of the copolymer composition is achieved through Nuclear Magnetic Resonance (NMR). The particular machines utilized are a 300MHz and 500MHz Bruker FT-H-NMR. The polymer that was created is dissolved in CDCl₃ or CD₂Cl₂ and at least 20mg of polymer is needed in order to achieve a signal strong enough for easy separation from the noise of the baseline. The magnetic pulse reflected back from a proton scan allows for determination of mole fractions of given protons. The idea is to look for those protons on given monomer units that are going to show up outside of the range of the backbone protons. For AMS, the 5 protons of the aromatic ring show up between 6.6 and 7.8ppm. For the acrylates however, the protons being observed fall on the —O—CH_xCH₃ group. For MMA the protons on the —O—CH₃ fall between 2.6 and 3.8ppm [10] while the protons for the —O—CH₂— group of BA fall between 2.5 and 4ppm (see figures 4 and 5). The reason for the range of chemical shifts is thought to stem from different triads and tacticities possible for the copolymer [20]. Typical spectra are shown in Figures 5 and 6.

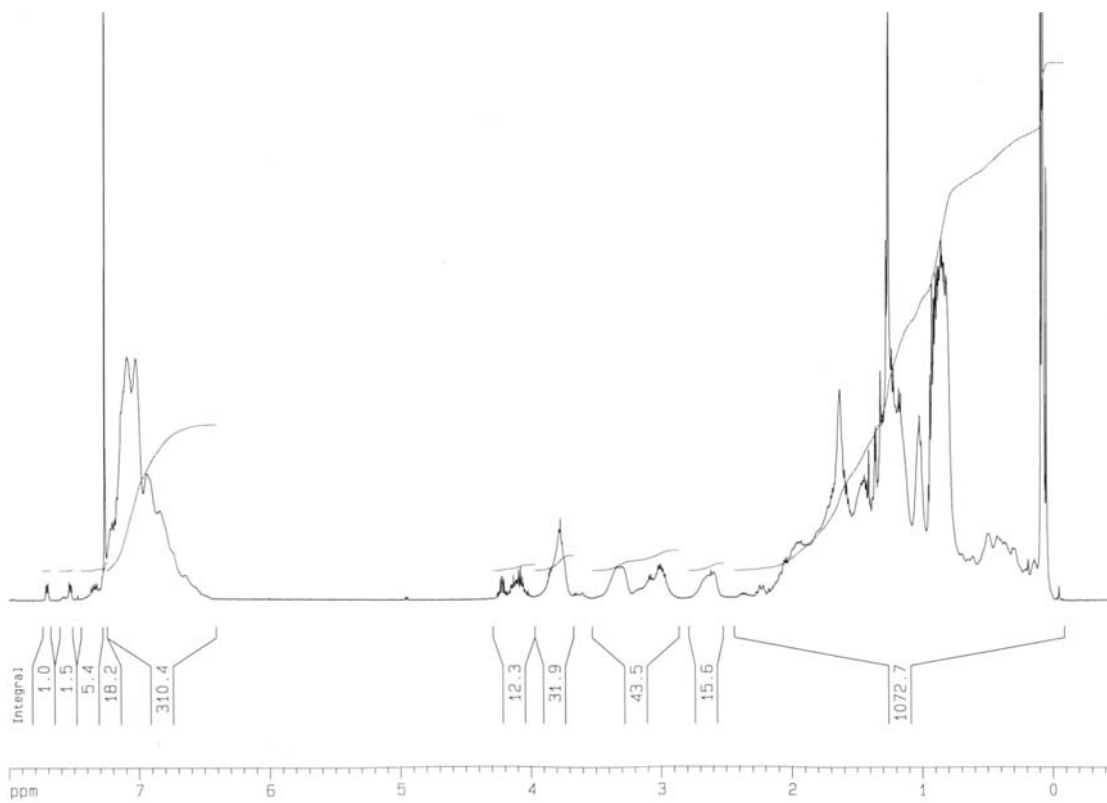


Figure 5: NMR Spectra for Copolymer of BA and AMS

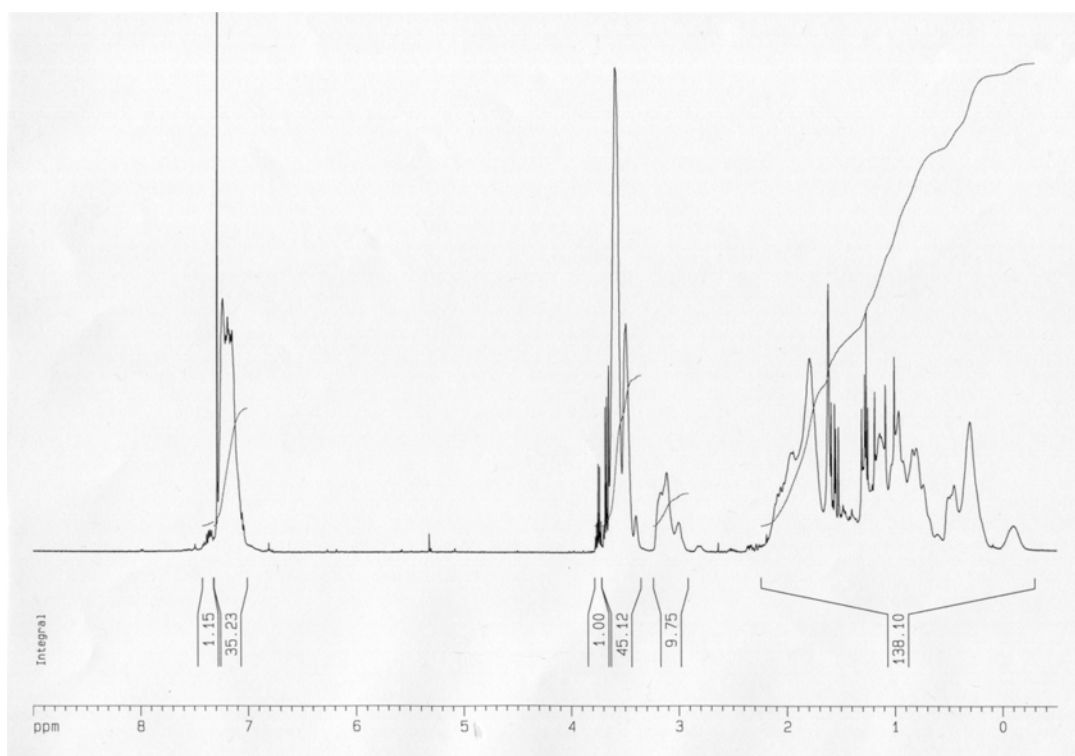


Figure 6: NMR Spectra for Copolymer of MMA and AMS

4.4.3. Copolymer Composition: ^{13}C Carbon NMR

Proton NMR is adequate for analyzing the copolymers of AMS with one of the acrylates and even the BA/MMA spectra can be used to approximate composition as long as care is taken when performing the analysis to achieve a resolution to obtain critical peak separation [28, 52]. However, when all three monomers are combined, there is no absolute method of determining composition from a Proton scan without introducing ambiguity. The proton signals from the backbone of AMS interfere with the signals from the acrylates that would normally allow for composition determination. A method has been devised to use the entire proton signal to ascertain the individual compositions, but there is the potential for significant error propagation [34, 38, 53]. It was therefore decided that in order to determine the terpolymer composition, that ^{13}C NMR would be used instead, which directly allows for unambiguous peak determination of all 3 monomers. The 5 carbons on the aromatic ring fall into a range of 124-130ppm, while the α -carbon for the MMA is distinguishable at 44-46 ppm and the C3 (29.5-31ppm) and C4 (63-65ppm) carbons on the butyl chain in BA are likewise distinguishable[53]. The drawback to ^{13}C NMR is the time required and polymer concentration. The number of carbons in the polymer is significantly less than the number of protons, so for each pass of the magnet a smaller signal is returned. In order to increase the signal, more polymer is required (i.e. more carbons in solution). In order to achieve good peak separation, one must increase the signal to noise ratio. Since each scan produces a weaker signal than that of the proton scan, a significantly larger number of scans are required to obtain this good signal to noise ratio. This, along with using an appropriate relaxation time (10s) increases the number of scans from 64 to nearly 6000. Also, since each polymerization is only to be taken to approximately 5% conversion, and a minimum of 100mg of polymer is required to obtain strong NMR signals, much (if not all) of the polymer created is being used for NMR. Figure 7 shows a typical MMA/BA/AMS Terpolymer ^{13}C spectrum.

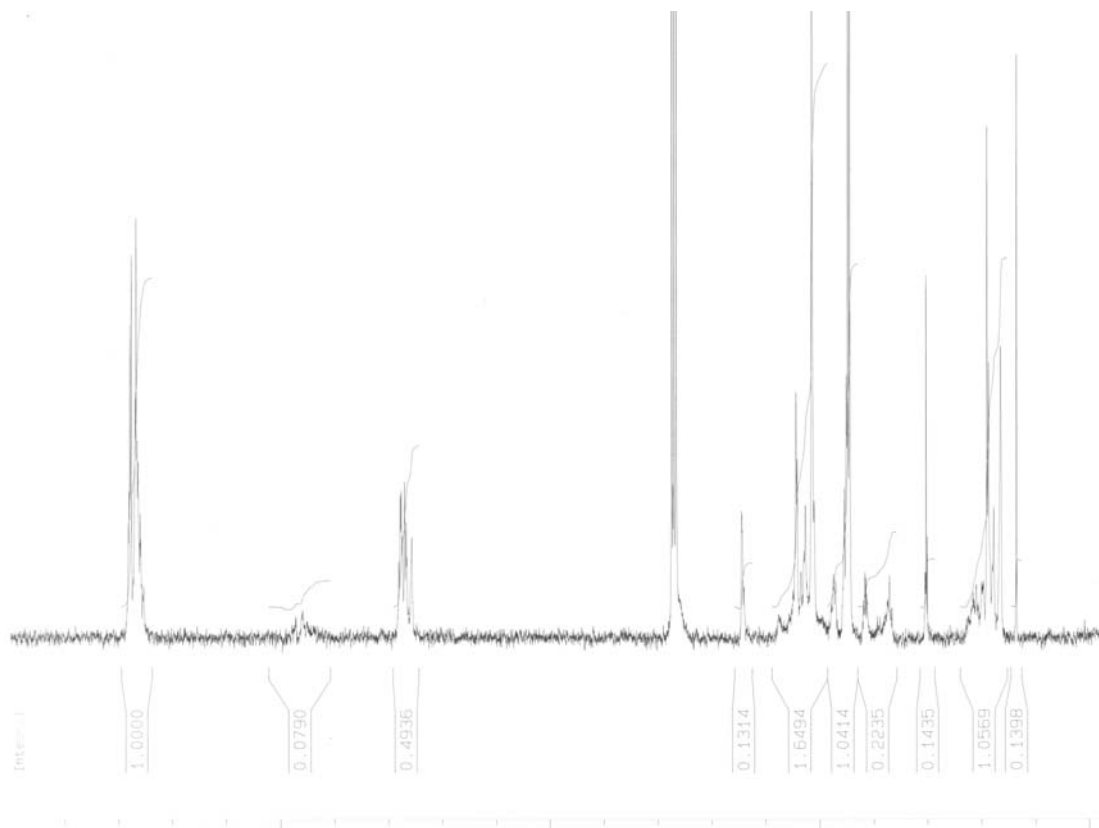


Figure 7: ^{13}C NMR Spectra for MMA/BA/AMS

4.4.4. Molecular Weight

Molecular weights of polymers are typically obtained by Size Exclusion Chromatography (SEC). The most commonly used technique is room temperature SEC or Gel Permeation Chromatography (GPC). GPC is a column fractionation method in which dissolved polymer molecules are separated by size. As the polymer molecules flow through a stationary bed of porous particles, polymer molecules enter the pores or are excluded, based on their size. The larger the polymer molecule, the fewer pores it can enter and consequently the larger molecules exit the column first. As a result, the polymer sample is fractionated according to size and a molecular weight can be determined. Chromatographic grade tetrahydrofuran (THF) is used as a solvent in conjunction with styrene and MMA standards to calibrate the system. As mentioned, elevated temperature polymerizations with depropagation typically result in low molecular weight polymer, so care must be taken to use low-molecular weight standards. The GPC must be able to accurately calculate low molecular weights with as little error as possible.

Two different sets of equipment have been used for molecular weight determination. The first was used for the BA/AMS, BA/MMA systems while the second was used for the MMA/AMS. The first system is a room temperature (25°C) Waters GPC system using THF as the mobile phase. The detectors used were a multi-angle laser light scattering (MALLS; Wyatt Dawn DSP-F) operating at 630nm and a Waters DR401 differential refractive index detector (DRI). Incorporated in this system are 3 PLgel 10µm Mixed-B columns. Data analysis was completed using Wyatt's Astra software. The second system is a room temperature (30°C) Waters solvent/sample delivery system with an in-line degasser (model AF), 515 HPLC pump and 717plus autosampler. The detectors on the system are from Viscotek, contained in the TDA 302 quad detector package that incorporates RALS/LALS (670nm), DRI, viscometer and UV (model 2501) detectors. Incorporated in the detector system are 3 Waters Styragel HR-5E separation columns. Data analysis was completed using Viskotek's OmniSec software. Both pieces of software use the dn/dc of each sample along with the known calibration constant for the equipment to find the polymer concentration (C_i) of each slice. The software then creates a Debye plot which calculates the weight average molecular weight (M_{wi}) for each slice. Assuming each slice is monodisperse $M_{wi} = M_i$ and with the C_i and M_i for each slice, weight average molecular weight (M_w) and number average molecular weight (M_n) can easily be calculated. The dn/dc values for the copolymer products were estimated based on the dn/dc values for the homopolymers and the molar copolymer composition [54-56]. Further work to determine dn/dc values for copolymers has been done using this second GPC setup, see Appendix C [57].

5. Butyl Acrylate/ Alpha-Methyl Styrene Copolymerization in Bulk and Solution

5.1. Introduction

In a previous study that looked purely at the bulk copolymerization of BA and AMS the kinetics and thermodynamics of the system were discussed in detail. It has been found that AMS plays a large role in dictating the rate of polymerization as well as in the development of the molecular weight of the resulting copolymer at elevated temperatures (100°C – 140°C) [5, 10, 11, 20, 21, 24, 35, 40, 58-61].

The purpose of performing these reactions in solution (toluene) is to investigate the effect of decreased monomer concentrations (both global and local) on the kinetics (i.e. rate of polymerization and reactivity ratios) as well as the final polymer properties (i.e. molecular weight and copolymer composition). Previous solution polymerizations [9-11] indicate that the use of toluene has a negligible effect on the resulting reactivity ratios that are obtained. This of course would be true if the solvent in question is inert and plays no role in changing monomer addition/selectivity besides the effects already mentioned.

In the previous study of the BA/AMS copolymerization system, analysis was done using the Mayo-Lewis and Lowry models. However, these models fail to adequately represent the system, as indicated by a significant trend in the AMS reactivity ratio towards zero at increasing temperatures [20]. Logically there is no reason why the reactivity ratio for AMS should approach zero as the temperature increases. For the value to become zero only two options exist: either the forward propagation rate constant of AMS goes to zero or the cross propagation rate constant (where AMS = 1 and BA = 2) becomes orders of magnitude larger than the homopropagation constant (i.e. $k_{12} \gg k_{11}$). Neither case should be true. The only reason that the reactivity ratio for AMS becomes zero is simply because the previously used models ignore the reversibility of the cross propagation reactions. For the previous models to fit the data then, the reactivity ratio for AMS must become zero in order to account for the missing parameters that both Kruger and Wittmer include.

5.2. Results and Discussion

5.2.1. Low Conversion Studies

Estimation of the reactivity ratios (as well as the four cross propagation/depropagation ratios) has been carried out for both the bulk and solution BA/AMS system at five different temperatures ranging from 60°C to 140°C using the Kruger model. All data used for this parameter estimation were taken from samples having conversion levels < 5% in order to maintain the assumption of constant monomer concentrations. Several feed compositions were chosen for each temperature in order to get reliable estimates over the full range of feed compositions. For the solution polymerizations, similar feed ratios were examined while varying the weight fraction of toluene between 23% and 50%[62]. However, due to the production of low molecular weight material at the 50% toluene level, both molecular weight and composition analysis data are unreliable, therefore only the data at 23% toluene were used for parameter estimation.

Figure 8 shows the composition data (mole fraction BA in copolymer vs. mole fraction in the feed) for the bulk copolymers at 60°C and 80°C, while Figure 9 shows analogous data for the experiments at 100°C through 140°C, as well as the fits to the Kruger model. These experimental data have been presented before without the model fits [20]. Similarly in Figures 10 and 11 the same data are shown but for the solution polymerizations. For both systems it is apparent that as the temperature increases to 140°C the system reaches a limiting AMS content of 50%. From these data, it would appear that the effect of the solvent on the localized kinetics plays only a role in the rate of reaction and does not affect the selectivity of monomer addition.

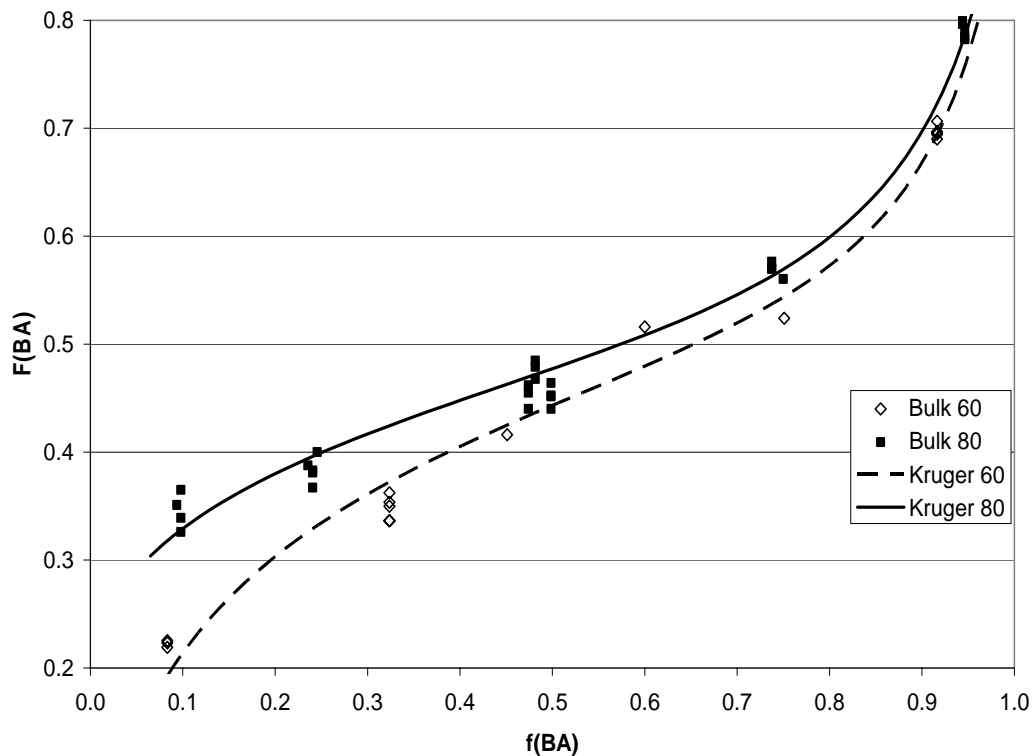


Figure 8: Bulk Composition vs. Feed (60°C & 80°C)

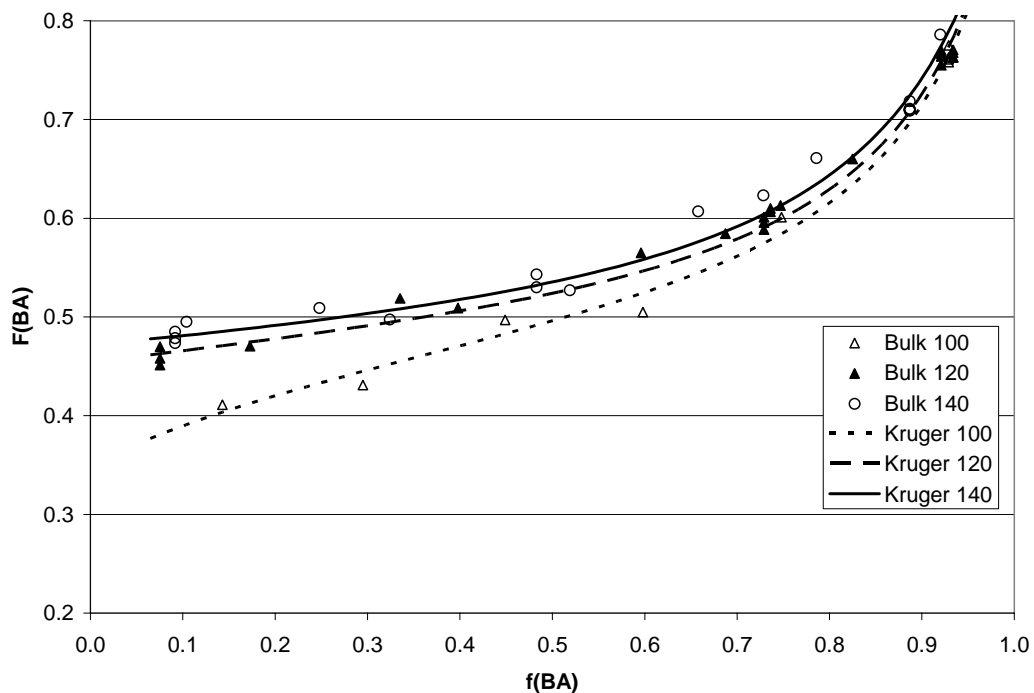


Figure 9: Bulk Composition vs. Feed (100°C , 120°C , 140°C)

Tables 2 and 3 summarize the parameter estimates obtained from the Kruger model for the BA/AMS system under bulk and solution polymerization conditions. It is clear that once depropagation is properly taken into account the forward reactivity ratio for AMS does not approach zero as temperature increases.

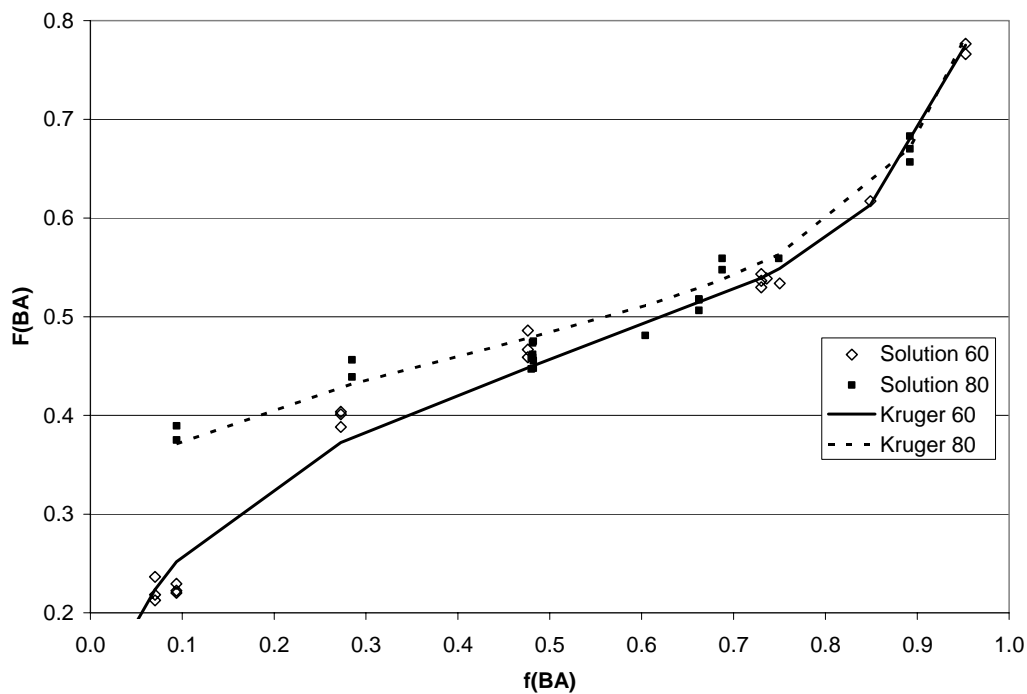


Figure 10: Solution Composition vs. Feed (60°C & 80°C)

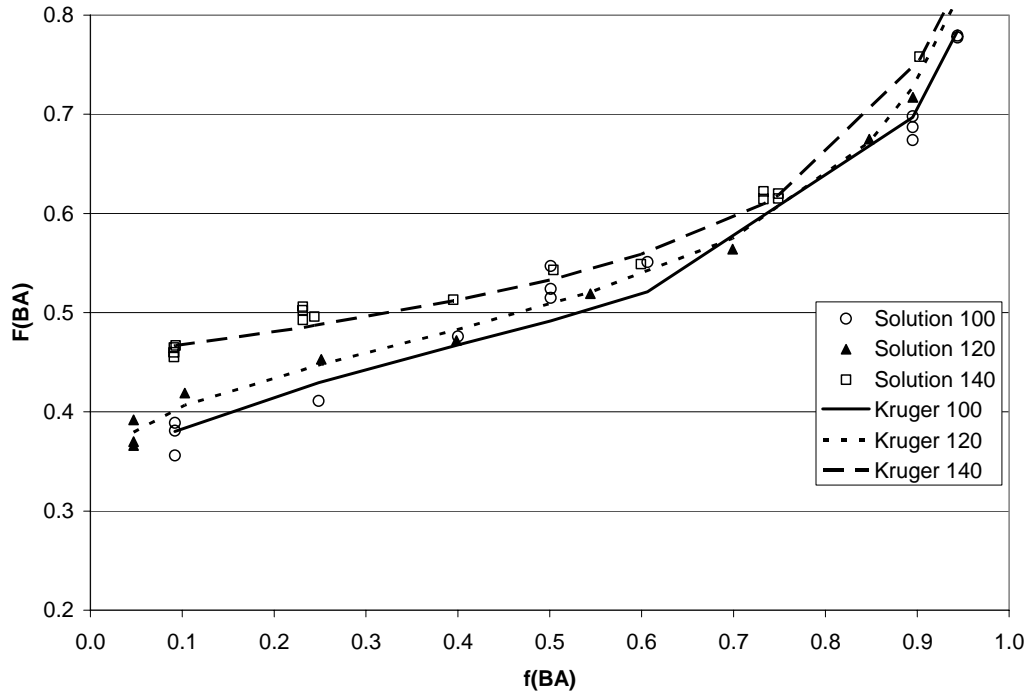


Figure 11: Solution Composition vs. Feed (100°C, 120°C, 140°C)

Table 2: Bulk Parameter Estimates for the Kruger model (1 = AMS, 2 = BA)

Temperature (°C)	r_1	r_2	R_1	R_2	R_{11}	R_{22}
60	0.599	0.123	0.502	0.080	3.003	0.000
80	0.557	0.148	0.674	0.230	6.009	0.000
100	0.546	0.167	0.950	0.251	9.000	0.000
120	0.502	0.171	1.200	0.400	22.000	0.000
140	0.471	0.188	1.499	0.501	30.000	0.000

Table 3: Solution Parameter Estimates for the Kruger model (1 = AMS, 2 = BA)

Temperature ($^{\circ}\text{C}$)	r_1	r_2	R_1	R_2	R_{11}	R_{22}
60	0.570	0.124	0.496	0.050	3.001	0.000
80	0.551	0.125	0.703	0.250	6.101	0.000
100	0.539	0.143	0.990	0.325	6.497	0.000
120	0.524	0.181	1.200	0.351	7.999	0.000
140	0.476	0.189	1.495	0.503	14.999	0.000

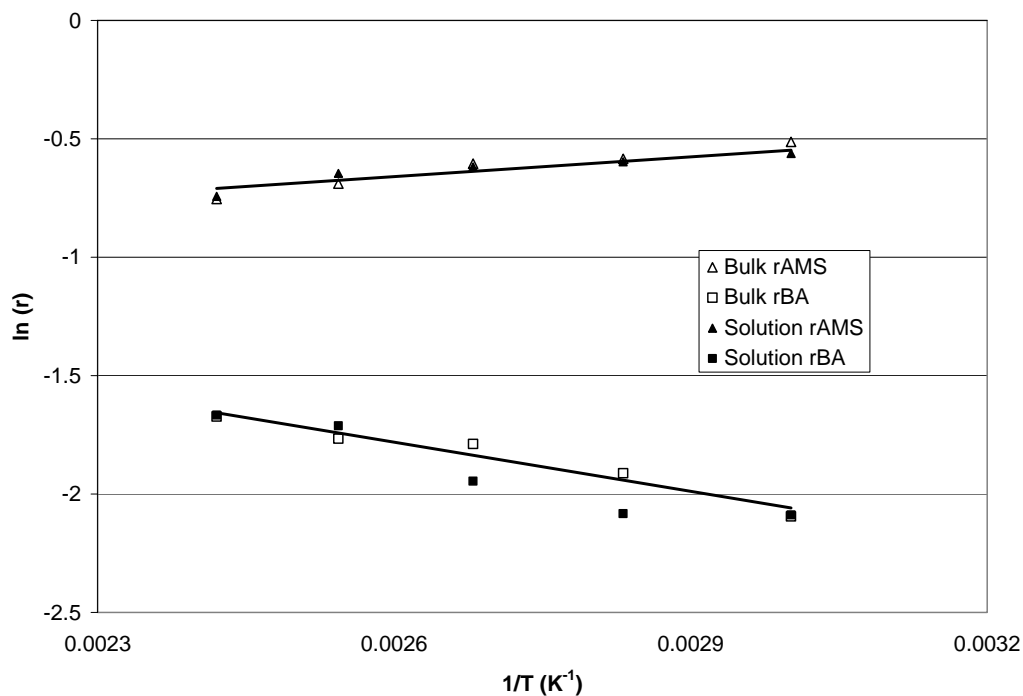


Figure 12: Arrhenius Plot for Reactivity Ratios Obtained Using Kruger Model (Bulk and Solution)

The trends from the Arrhenius plots in Figure 12 are linear as would be expected. Compared with earlier estimates of the reactivity ratios, the slopes of these lines (eq. 60-65) are significantly smaller [20] indicating lower temperature dependence for r_1 and r_2 in both solution and bulk (T in K).

Lowry Estimates (Bulk only):

$$\ln(r_{BA}) = 0.736 - 955/T$$

(60)

$$\ln(r_{AMS}) = -20.9 + 6457/T$$

(61)

Kruger Estimates:

Bulk

$$\ln(r_{BA}) = 0.0131 - 690/T$$

(62)

$$\ln(r_{AMS}) = -1.7091 + 400.75/T$$

(63)

Solution

$$\ln(r_{BA}) = 0.331 - 827.3/T$$

(64)

$$\ln(r_{AMS}) = -1.3817 + 277.81/T$$

(65)

Figure 13 shows r_1 vs. r_2 for 80°C and 140°C along with the 95% joint confidence contours to illustrate the level of confidence in the reactivity ratio estimates. This confirms that the reactivity ratio estimates for the bulk and solution polymerizations are not significantly different from one another.

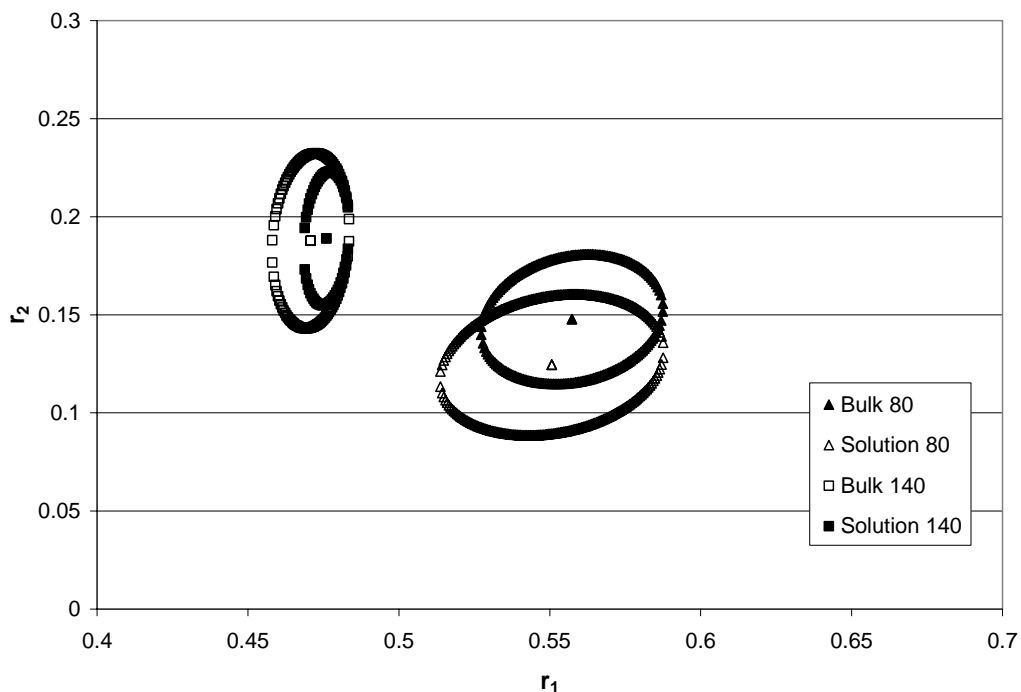


Figure 13: 95% Joint Confidence Contours for r_{AMS} and r_{BA} at $80^{\circ}C$ and $140^{\circ}C$

Similar contours for the other temperatures show that the reactivity ratios obtained for the bulk and solution reactions cannot be considered statistically different from each other due to the overlapping confidence contours. The absolute areas of the contours are listed in Table 4.

Table 4: 95% Joint Confidence Contour Areas

Reaction Conditions	Contour Area
Bulk $60^{\circ}C$	2.10E-02
Solution $60^{\circ}C$	5.38E-03
Bulk $80^{\circ}C$	3.08E-03
Solution $80^{\circ}C$	4.11E-03
Bulk $100^{\circ}C$	3.46E-02
Solution $100^{\circ}C$	1.51E-03
Bulk $120^{\circ}C$	6.97E-04
Solution $120^{\circ}C$	3.20E-03
Bulk $140^{\circ}C$	1.78E-03
Solution $140^{\circ}C$	9.58E-04

From this analysis, multiple points should be made. The belief that the reactivity ratio for AMS is approximately zero at temperatures above $100^{\circ}C$ is not true. The earlier

conclusion is based upon a model that does not adequately describe the system (Mayo-Lewis and/or Lowry). From the parameter estimates obtained using the Kruger model, r_{AMS} is significantly larger than previously predicted and the cross propagation reactions previously discussed have significant reversibility that cannot be ignored. Based upon parameters estimated from the Kruger model, it would appear that toluene does not affect the final copolymer composition. For the most part, the parameters between the two systems (bulk and solution) are virtually identical except for R_{11} . This parameter is especially sensitive to the copolymer compositions at higher levels of AMS incorporation (see Appendix G, Figure 34). Due to the solvent and elevated temperature effect on the molecular weight, it becomes increasingly difficult using NMR to separate the AMS incorporated into copolymer and AMS incorporated into dimers and trimers of poly-AMS. Since NMR is indiscriminate of molecular weight, this error causes scattering in the data at the higher feed ratios of AMS and consequently the estimation of R_{11} is compromised.

Some of the contour areas shown in Table 4 are significantly larger than others. The causes for this may include significant data scattering from the NMR analysis (as previously mentioned), inadequate experimental design or simply not enough data collected. By implementing some model based experiments to generate data and incorporating error into this data, it has been found that if more experiments (between 6 and 12 extra data points) for the 60°C and 100°C are added to the current data generated in this work, then the contour areas can be reduced by an order of magnitude.

5.2.2. Full Conversion Range Studies

The purpose of doing the full conversion range studies is to understand the effect of the AMS depropagation on the overall rate of polymerization and to identify its effects on the copolymer composition and molecular weights. Table 4 outlines the experiments done for the solution polymerizations. Bulk polymerization data have been presented elsewhere [20].

Table 5: Full Conversion Solution Polymerizations

Run #	Temp (°C)	BA/AMS ratio ^a	[Trig B] ^b	[CTA] ^b	[S] ^b
1	115	40/60	1.5	0.26	15
2	115	40/60	1.5	0.2	15
3	140	40/60	1.5	0.2	15
4	115	40/60	1.5	0	15
5	115	55/45	2.5	0.3	15
6	115	60/40	1.5	0	15
7	115	60/40	1.5	0.2	15
8	115	60/40	1.5	0	50
9	115	60/40	1.5	0.2	50
10	115	40/60	1.5	0	50

a = weight ratio; b = weight %; S = solvent (toluene)

Solution polymerizations, with all other factors being equal, due to the dilution effect on the monomers, will ultimately be slower than bulk. They should exhibit little autoacceleration behaviour if the solvent levels are high enough. Data from the bulk system show that the copolymerization of BA/AMS exhibits behaviour of incorporating approximately 50% AMS over a large portion of the conversion range for the selected feed ratios [20]. The purpose of the solution experiments was to show, with both excess BA (60/40) and excess AMS (40/60), how much of an effect either monomer has on the composition drift once the other monomer is consumed. In theory, once the BA is consumed, minimal amounts of AMS should be incorporated into the polymer. Since BA will not depropagate, having an excess amount of BA (for the BA/AMS system at any given temperature) should also increase the rate of reaction.

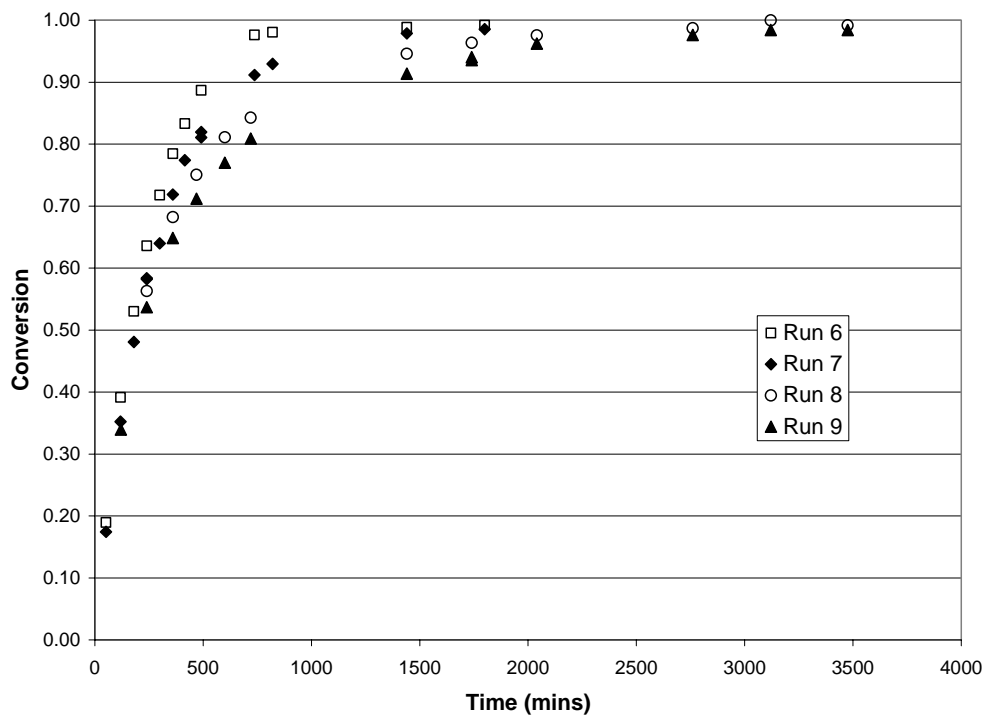


Figure 14: 15% and 50% Toluene at 0% and 0.2% CTA

Figure 14 shows conversion vs. time data from four different reactions that illustrate both the effect of solvent and the effect of CTA. The differences between runs 6/7 and runs 8/9 show how increasing the solvent level to 50% slows the reaction noticeably while introducing 0.2% CTA has only marginal effects on the rate of reaction.

Figure 15 illustrates the effect of the increase in BA on the overall reaction rate at two different levels of solvent: 15% and 50%. It is clear that with lower BA in the feed complete conversion is not possible due to the depropagating effects of AMS. Also as solvent increases (between runs 2 and 10) final conversion drops which signifies that the solvent has an effect on the level of depropagation through its dilution effect. This effect is present for all reactions, and as such does not affect the monomer selectivity. This in turn has no effect on the parameters being estimated in the Kruger model.

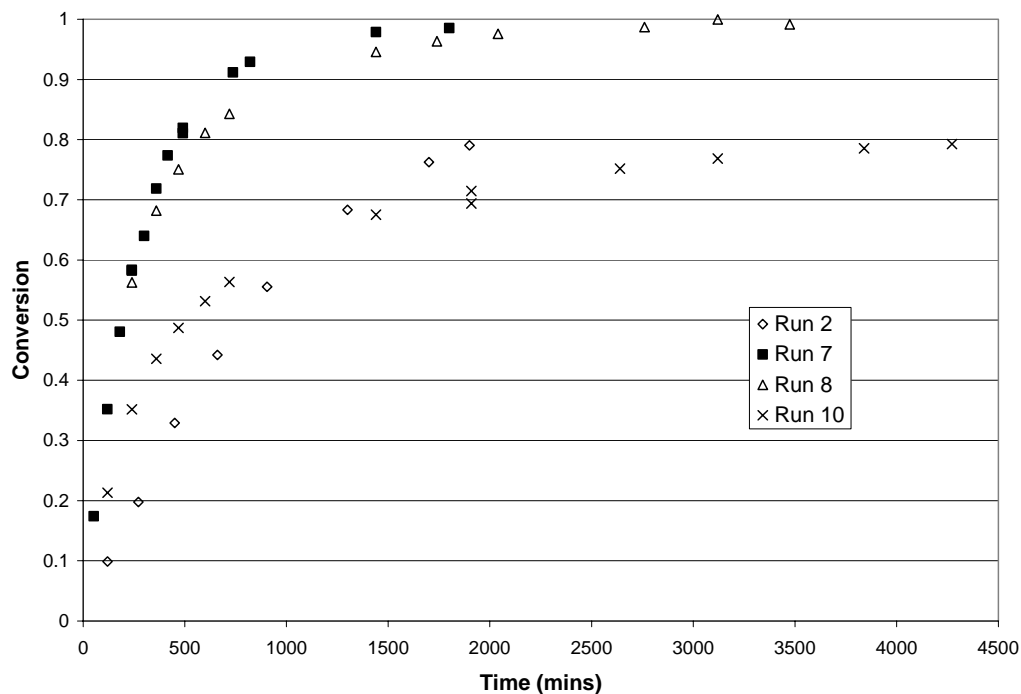


Figure 15: Effect of [BA]

Figure 16 shows the trends in copolymer composition with conversion over the full conversion range for selected experiments. Runs 4 and 10 both have feeds of 40% BA and consequently have lower BA in the resulting copolymer, which reduces the final conversion levels. Once BA has been consumed, polymerization is virtually stopped since AMS does not homopolymerize or cross polymerize forward. We can see by runs 6 and 8 that after about 70% conversion there is a slight drift in composition. It can be calculated at this point that the majority of the AMS has been consumed and so a drift up in BA composition is expected. However, due to the scatter of data in runs 4 and 10, a drop in BA content in the polymer beyond 70% conversion cannot be detected with any level of confidence.

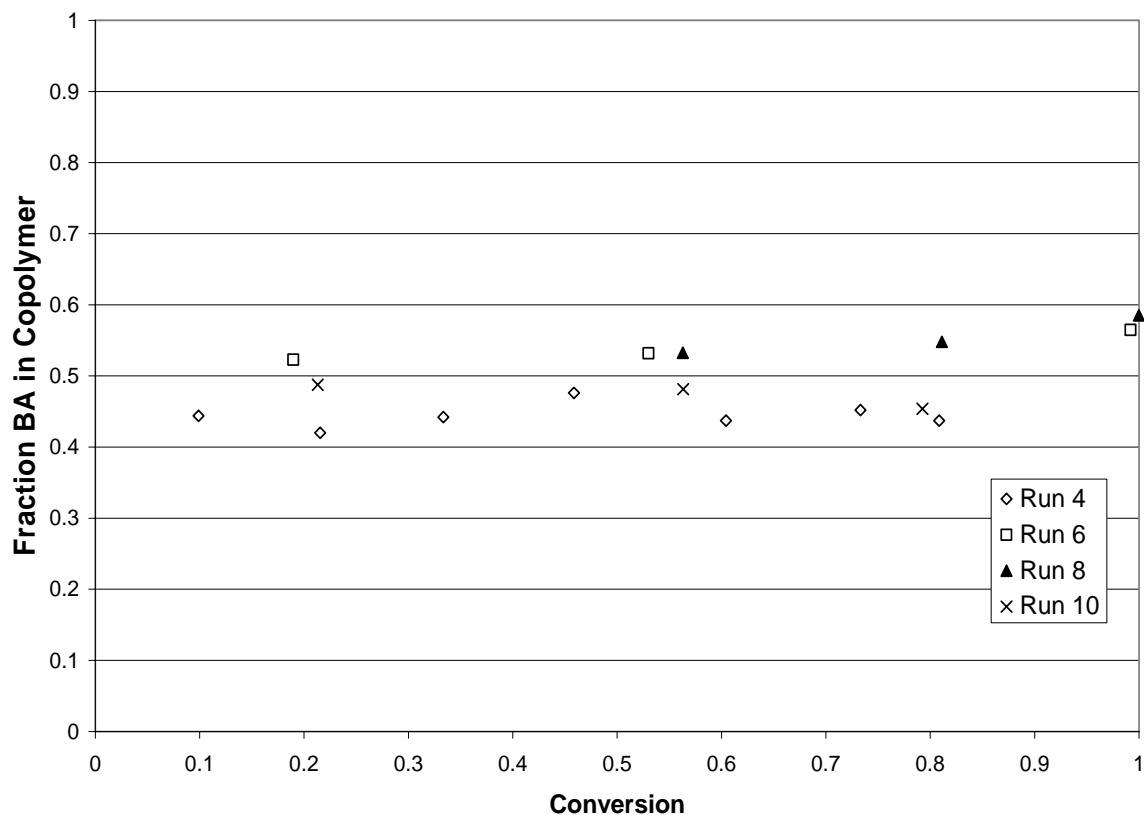


Figure 16: Copolymer Composition vs. Conversion

The effect of a solution polymerization has been documented [6-11] for other systems at high temperatures. It should be noted here that at 50% toluene, the molecular weights of the polymer were too low to be effectively separated with the columns currently installed on the GPC system used. Consequently, the values for weight average molecular weight (M_w) measured are unreliable; however the average values obtained were in the range 5000 - 7000 g/mol.

The molecular weight analysis done for runs 2-5 can be used to draw some conclusions about the effects on molecular weight. Table 6 summarizes the average M_w over the full conversion range as well as the maximum and minimum M_w values.

Table 6: M_w Summary

Run #	M_w (avg)	M_w (max)	M_w (min)
2	22067	26010	16540
3	11285	11500	8050
4	31356	33950	28150
5	32910	52060	18580

As expected, the following trends are seen from this data: Increasing the temperature from 115°C to 140°C effectively decreases the M_w ; increasing the [CTA] to 0.2% decreases the M_w ; increasing the BA content in the feed increases the M_w . It should also be recalled that increasing the level of solvent from 15% to 50% decreased the M_w . Similar results are found in a previous work by Kang and O'Driscoll [63].

5.3. Concluding Remarks

The Kruger model has been used to examine BA/AMS copolymers and estimate the key kinetic parameters. It has been shown that using the Mayo-Lewis or Lowry models for BA/AMS is inadequate. The Kruger model is very successful in explaining the depropagating behaviour of AMS and the model is the most robust of all that have been tested. In the case of BA/AMS, the Kruger model has reaffirmed the fact that BA's ceiling temperature is very high and BA shows no sign of homo-depropagation at temperatures up to 140°C. It can also be concluded that in the BA/AMS system, using toluene as a solvent has seemingly no effect on the copolymer composition. The full conversion range studies solidify the understanding of the effects that changing the feed ratio, solvent and CTA level, as well as temperature have on the rate of reaction and the molecular weight of the resulting material. The results recorded for rate, copolymer composition and molecular weight are what were expected. Increasing the temperature, increasing the [CTA] and increasing [S] all decrease the resulting molecular weight, while increasing the BA content in the feed has the opposite effect. It can be concluded that increasing the BA in the feed increases the overall rate of reaction while increasing [S] decreases the rate of reaction and that changes in [CTA] have seemingly little

effect on the rate. It is apparent from all of these studies that increasing the AMS content in the feed decreases the molecular weight, slows the net production of polymer and limits the overall conversion in the system if the AMS level in the feed climbs beyond 50%. It is evident by examining both the composition results and the full conversion profiles in the bulk and solution systems that significant depropagation of AMS exists. There is no evident reason why the forward reactivity ratio for AMS approaches zero if all depropagation reactions are taken into account properly. The depropagation effects of AMS are significant not only in the homopolymerization reaction but also in the cross-propagation reactions as shown by the magnitude of parameters R_1 and R_2 . Although the homopolymerization of BA is irreversible, it is quite evident that under the right conditions (temperature and concentration) that it will cross depropagate if attached to an AMS unit. If systems that include AMS are to be properly handled, the reversibility of all reactions needs to be considered.

6. Methyl Methacrylate/Alpha-Methyl Styrene Copolymerization in Bulk

6.1. Introduction

Previous studies have looked at the bulk and solution copolymerizations of MMA and AMS [5, 11]. Another study for the MMA/AMS copolymerization system was carried out using full conversion range data in an effort to predict conversion versus time and copolymer composition [64]. The experimental data used for this modelling effort can be seen in Appendix D. The motivation for a return to this system stems from the fact that previous estimates for the kinetic parameters that govern this system take on what appear to be rather unreasonable values as in the case for the BA/AMS system [62]. The reasons for these erroneous values will be discussed.

The purpose in re-examining the MMA/AMS copolymerization system is to better understand the kinetics of this system at various temperatures. In the previous study of the MMA/AMS copolymerization system the analysis done using the Kruger model did not adequately represent the system in a realistic manner, as indicated by a significant trend in the AMS reactivity ratio towards zero at increasing temperatures [5, 11]. Logically there is no reason why the reactivity ratio for AMS should approach zero as the temperature increases. For the value to become zero only two options exist: either the forward propagation rate constant of AMS goes to zero or the cross propagation rate constant (where AMS = 1 and MMA = 2) becomes orders of magnitude larger than the homopropagation constant (i.e. $k_{12} \gg k_{11}$). Neither case should be true. The only reason then for the AMS reactivity ratio to become zero must be due to some sort of a numerical estimation error. Previously, when R_{22} could be considered zero [62], the convergence of the model was such that the remaining 5 parameters were readily resolved while when all 6 parameters are potentially non-zero (an increase in the degrees of freedom) it has been observed that convergence becomes more difficult. It has been documented that highly non-linear models (i.e. Kruger's model) suffer from local optima making convergence on the true parameter values difficult; the more non-zero parameters present the more non-linear the Kruger model becomes [65]. A sensitivity

analysis on the model shows some interesting dependency on temperature for this system. At 60°C the model is quite sensitive to r_1 and r_2 (and somewhat insensitive to R_1 and R_2) while at 140°C the model shows the opposite behaviour (Appendix G, Figure 35). This behaviour from a kinetics stand point is not entirely unexpected (since at elevated temperatures the depropagation parameters should play a larger role in the model) but numerically this behaviour has the potential to create problems that the user needs to be aware of, which may also explain the previous work's trend towards zero in r_{AMS} (r_1) at increasing temperature. Thus, it has been decided to re-visit the system with these issues in mind and make another attempt at determining improved parameter values.

6.2. Results and Discussion

Estimation of the reactivity ratios (as well as the four cross propagation/depropagation ratios) has been carried out for the bulk MMA/AMS system at five different temperatures ranging from 60°C to 140°C using the Kruger model. All data used for this parameter estimation were taken from samples having conversion levels < 5% in order to maintain the assumption of constant monomer concentrations. Multiple feed compositions were chosen for each temperature in order to get reliable estimates over the full range of feed compositions.

Figure 17 shows the composition data (mole fraction MMA in copolymer F_{MMA} vs. mole fraction in the feed f_{MMA}) for the bulk copolymers at 60°C and 80°C, while Figure 18 shows analogous data for the experiments at 100°C through 140°C, as well as the fits of the Kruger model.

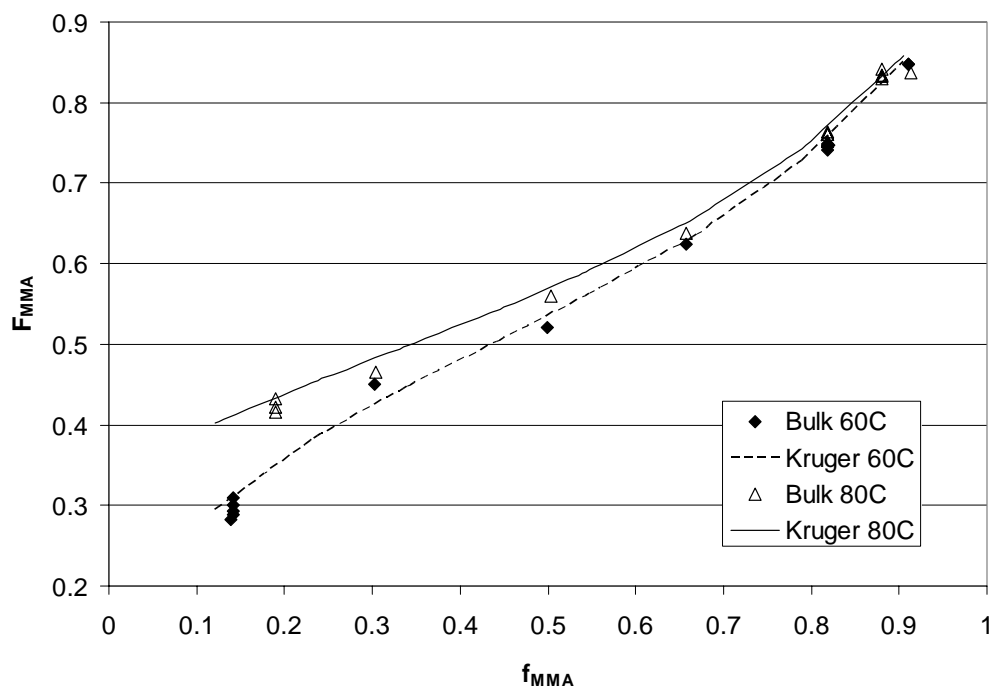


Figure 17: Copolymer Composition versus Feed Composition (60°C & 80°C)

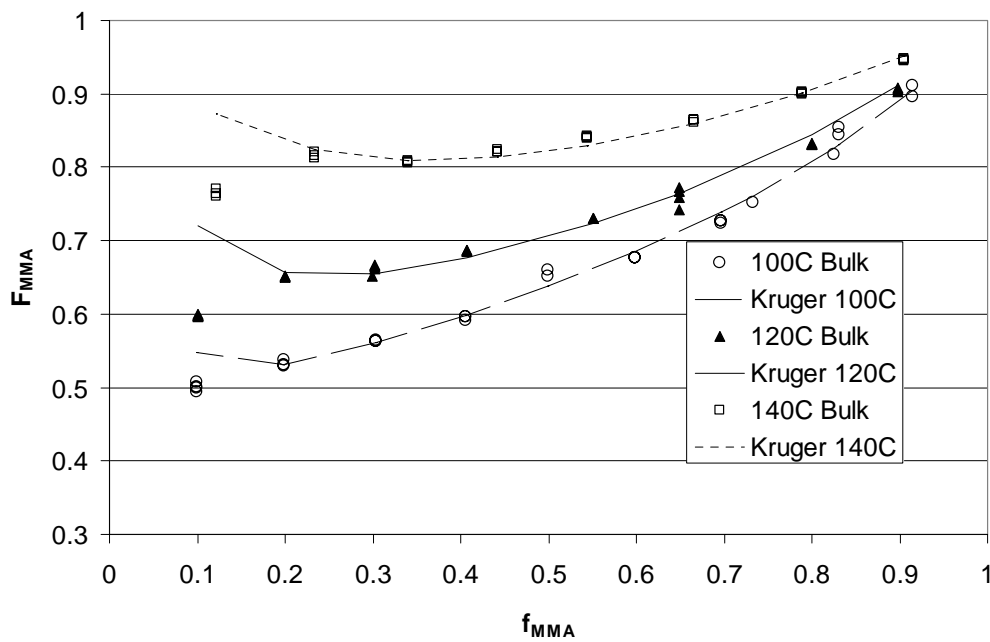


Figure 18: Copolymer Composition versus Feed Composition (100°C, 120°C, 140°C)

In the previous work done with the MMA/AMS system, parameter estimates obtained on the reactivity ratio for AMS showed a trend towards zero at increasing temperatures [5]. With further data acquisition at 100, 120 and 140°C and using the Kruger model again to

estimate the 6 kinetic parameters, the results obtained are summarized in Table 7 for the bulk polymerization of MMA/AMS. It should also be noted that while R_{22} is near zero, it does show a trend towards increasing homo-depropagation for MMA as the temperature increases, indicating that the solution effect of the MMA/AMS mixture does lower the ceiling temperature of MMA.

Table 7: Bulk Parameter Estimates for the Kruger model (1 = AMS, 2 = MMA)

Temperature (°C)	r_1	r_2	R_1	R_2	R_{11}	R_{22}	K_1
60	0.61	0.33	1.40	2.90	4.40	0.0021	7.22
80	0.53	0.33	1.80	3.00	6.25	0.0029	11.85
100	0.47	0.35	2.20	5.00	7.00	0.0049	14.90
120	0.43	0.37	2.99	7.00	8.99	0.0694	20.91
140	0.40	0.40	4.50	11.62	11.26	0.0800	28.14

Based upon the definitions outlined earlier, it is reasonable to assume that all 6 of the kinetic parameters (including the equilibrium constants K_1 and K_2) should follow an Arrhenius type expressions and Figures 19 and 20 show these trends. The equilibrium constant is defined as follows:

$$K_n = \frac{k_{nm}^-}{k_{nn}} = \frac{R_{nm}}{r_n} \quad (66)$$

It should be kept in mind that it is numerically difficult to accurately estimate parameter values that are close to zero. Consequently R_{22} does not follow a linear trend like the remaining parameters and the values of K_2 (as defined in equation 66, which approach zero as well) also do not follow a linear trend.

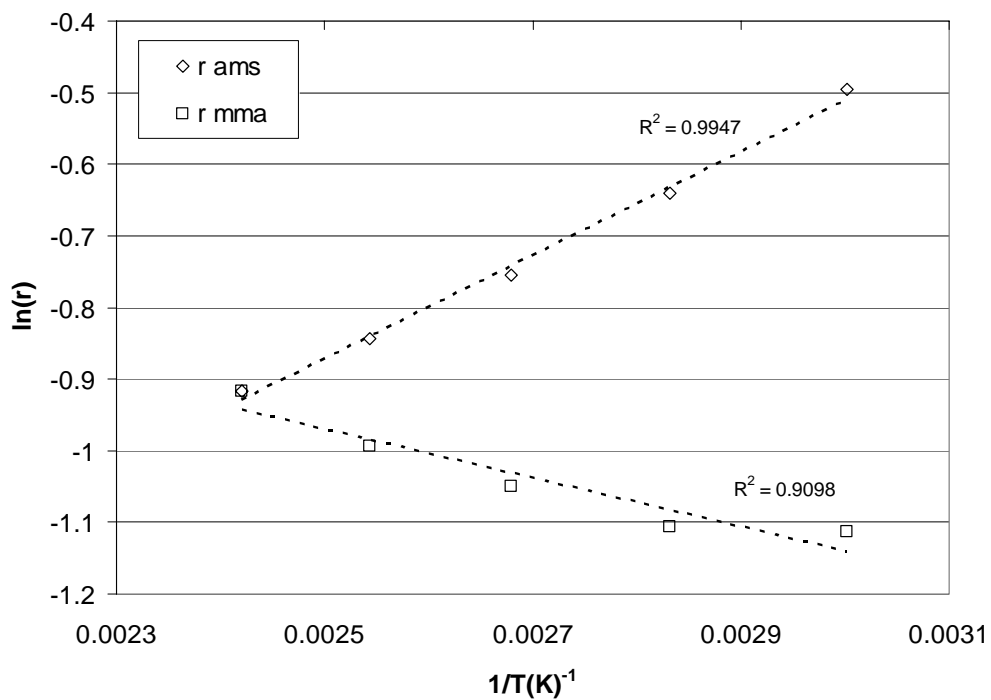


Figure 19: Arrhenius Plot for Reactivity Ratios Obtained Using Kruger Model

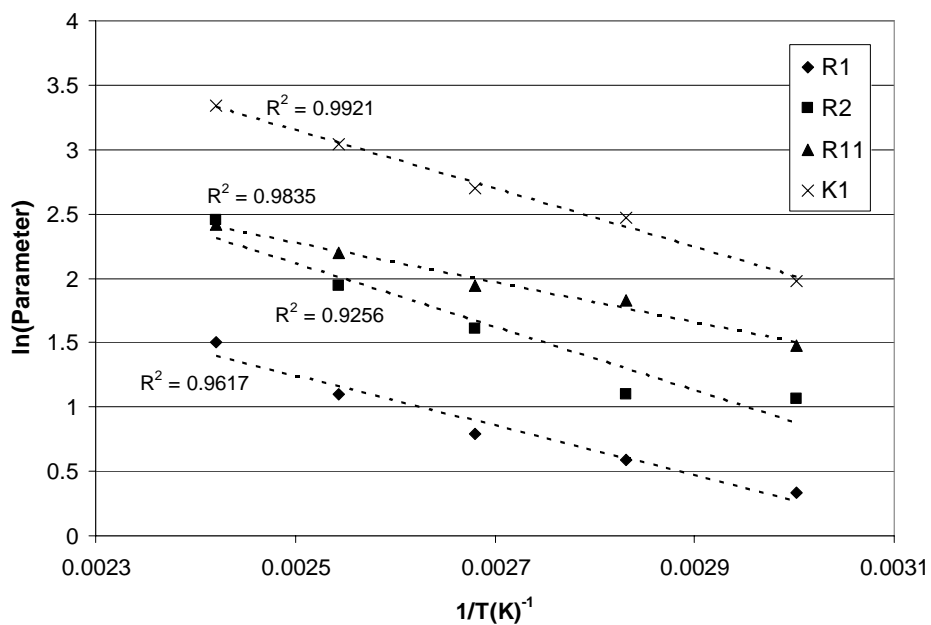


Figure 20: Arrhenius Plots for Cross Propagation Ratios Obtained Using Kruger Model

The trends from the Arrhenius plots in Figures 3 and 4 are linear as would be expected. Equations 67 through 72 outline the Arrhenius equations for each parameter:

$$\ln(r_{AMS}) = -2.6785 + [722.23/T(K)] \quad (67)$$

$$\ln(r_{MMA}) = -0.1142 - [341.95/T(K)] \quad (68)$$

$$\ln(R_1) = 6.0759 - [1934.1/T(K)] \quad (69)$$

$$\ln(R_2) = 8.2568 - [2456.8/T(K)] \quad (70)$$

$$\ln(R_{11}) = 6.1404 - [1545.2/T(K)] \quad (71)$$

$$\ln(K_{AMS}) = 8.8189 - [2268/T(K)] \quad (72)$$

Figure 21 shows r_2 vs. r_1 point estimates for the entire temperature range studied along with the 95% joint confidence contours to illustrate the level of confidence in the reactivity ratio estimates.

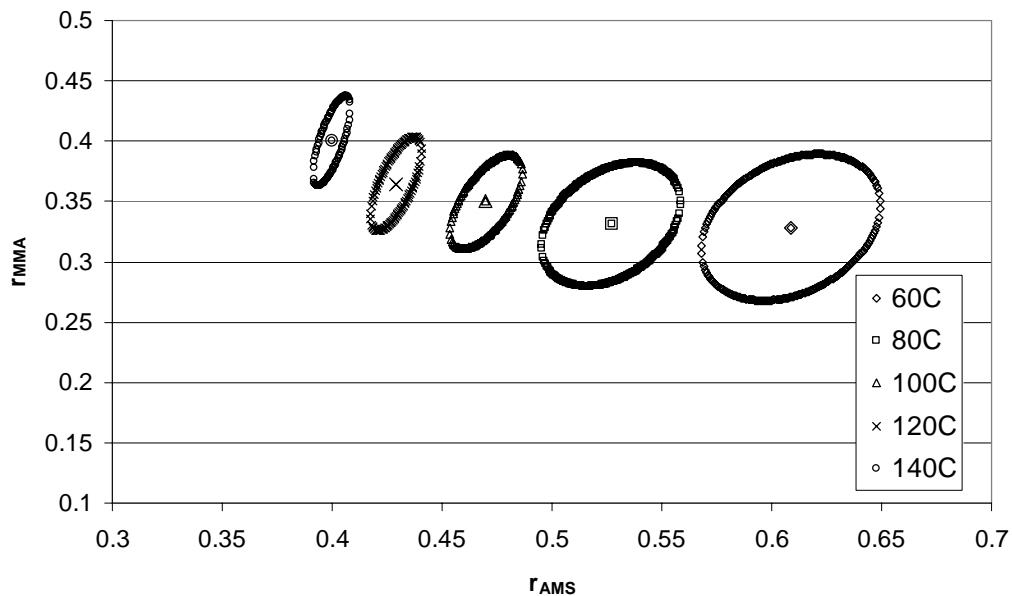


Figure 21: 95% Joint Confidence Contours for r_{AMS} and r_{MMA}

From Figure 21 it is quite obvious that the reactivity ratios are well defined and that there is no overlap of the contours, indicating that the estimates are significantly different for

each temperature. The contours for 60 and 80°C have a slightly larger volume than the contours at higher temperature. This is due to the smaller data set that was used to estimate the kinetic parameters. Additional polymerizations were done at 100, 120 and 140°C in order to investigate what was initially considered to be anomalous results at the low feed concentrations of MMA. When it was found that the new data showed the same behaviour, all the data was included and the data sets for the three higher temperatures were considerably larger.

Looking closely at and comparing Figures 17 and 18, there is an obvious deviation between the Kruger model and the experimental data for 100°C through 140°C at the very low feed concentrations of MMA and this deviation increases with increasing temperature. The Kruger model predicts a higher concentration of MMA in the polymer than what is being seen experimentally. This experimental data has been confirmed as being correct, so what is causing the model to deviate? In both the Mayo-Lewis and Kruger models the key underlying assumptions are the long chain approximations (LCA-I and LCA-II) [41, 66]. In the case of the Kruger model, a modified LCA-II is needed in order to accommodate both depropagating species [41]. Recall that LCA-II is applicable for copolymerizations only. The assumption is that the rate of interconversion (or cross propagation) of the monomers is equivalent. This assumption can only be assumed if the chains are significantly long enough (greater than 10 monomer units) to overcome any lingering effects from the initiation stage on the terminal radical and allow for total random propagation.

What happens then in the case where the level of MMA is low? It has been well documented that the ceiling temperature for a given monomer is directly related to its concentration in solution [4, 5, 10, 23, 24, 31]. This in turn means that at low concentrations of MMA and elevated temperatures, the amount of depropagation of the monomer (while still less than AMS) will have increased. However, an increased depropagation rate of MMA is unlikely to be the cause of such a deviation since depropagation slows down the net propagation of the polymer in turn lowering the rate of monomer consumption which should not have an effect on selectivity in this case. It was also thought that perhaps the polymer chains being produced were not long enough for LCA-II to hold true. GPC analysis of the

polymer at these feed ratios showed the resulting polymer to be of chain length greater than 50 monomer units in all cases. This result then eliminated the potential for LCA-II to be false. However, while the molecular weights of these molecules are large enough to consider them as polymers, the weight average molecular weights are generally small, ranging between 10,000 and 20,000 g/mol.

Recall that LCA-I assumes that 99.9% of all monomer consumption takes place via propagation. In other words:

$$-\frac{d[M]}{dt} = R_{initiation} + R_{propagation} + R_{transfer} \approx R_{initiation} + R_{propagation} \quad (73)$$

In the cases where a deviation is seen, the only species present are the two monomers. The majority of transfer reactions (which are assumed to be minimal) occurring would involve transfer to AMS and not to MMA (based upon the stability of the resulting radicals and by the quantity of AMS in the system). This type of transfer would result in radicals that would be relatively stable and slow to propagate. If the radical is already incorporated into a polymer chain (which would be in the minority given the excess AMS in the system) a reduced propagation rate would result. If the radical produced is primary (in which case monomer is consumed), again the propagation rate would be reduced. Neglecting transfer reactions is conservative on the side of LCA-I and if such reactions are significant in quantity, this would tend to exacerbate the situation.

For LCA-I to hold true,

$$\frac{R_{initiation} + R_{transfer}}{R_{propagation}} \approx \frac{R_{initiation}}{R_{propagation}} \ll 1 \quad (74)$$

In the polymerizations run at 100°C through 140°C, initiation is carried out thermally. In this case it is well documented that MMA will undergo a coupling reaction to create a bi-radical [14, 67-71]. However, what is uncertain is whether AMS will undergo a similar

adduct reaction that is seen with styrene [17, 18] to also produce radicals. Since studies for homopolymerizations of AMS cannot be done under free radical conditions at these temperatures, it is impossible to know for certain. However, the type of radical produced under this reaction (if at all) may not be as reactive as an MMA radical (given the structure of the AMS adduct) and consequently may not significantly contribute to the thermal initiation. Since the rate of MMA radical production is directly proportional to the square of MMA's concentration, the rate of decomposition of MMA to form radicals would be low at such low concentrations, but given the length of time required for the reaction to proceed to reach only 5% conversion (ranging from 20hrs at 140°C to over 50 hours at 100°C), it is quite possible that a significant fraction of the MMA (when compared with other feed ratios) is consumed via $R_{\text{initiation}}$. This being considered, along with the fact that $R_{\text{propagation}}$ for this feed level is small, it is possible that LCA-I may no longer hold true. In the cases at 60°C and 80°C AIBN was used to initiate the reaction. It is not apparent at these lower temperatures that this phenomenon is occurring. It may be that the amount of deviation at these temperatures is insignificant at the lowest feed ratios studied, while if even lower feed ratios of MMA were used it might be detected. If one is to propose that this phenomenon will only occur for low molecular weights (where the amount of monomer consumed via propagation per chain is lower than that for higher molecular weight polymers), then the addition of an initiator should succeed in exacerbating the situation. This would lead one to believe that at 60°C and 80°C the molecular weights are large enough, even with the use of initiator, that LCA-I holds or nearly holds true.

Under these conditions of high temperatures and high concentrations of AMS the production of dimers and trimers is a distinct possibility [22]. This type of molecule production, which may or may not include the consumption of MMA, can distort the results that are seen in GPC and NMR. NMR does not discriminate based on molecular weight while GPC does. There is potential in this case that we are producing many smaller chain molecules that we cannot easily detect by GPC but are still present, and hence, as a source of monomer consumption their presence may be skewing the NMR results. The quantitative effect of this on both LCA-I and LCA-II can only be estimated, and work should be done to properly take

such a phenomenon's effects into account. However, if this is taking place, it most certainly would increase the ratio $R_{\text{initiation}}/R_{\text{propagation}}$ and invalidate LCA-I.

In addition, looking at two other systems (BA/AMS and BA/MMA) [20, 28, 62], such behaviour is not observed in either case. In both of these other systems, initiator was used at all temperature levels. It should be noted that for the BA/MMA system feed ratios were only studied to a minimum of 15 mol% of MMA while for the BA/AMS system in bulk and solution the levels of BA were studied to 10 mol% BA and in some cases below this. It has been well documented that BA will not undergo any depropagation under homopolymerization conditions [20, 28, 32, 62]. In this case, the use of BA with either MMA or AMS will only increase the rate of propagation. However, results from the solution copolymerization of BA/AMS using 50 wt% toluene as a solvent, produced molecular weights in a lower range (5000 – 7000 g/mol) than what was being observed in the MMA/AMS bulk system at 10 wt% MMA.

If this is so, then why is this phenomenon not being observed with the BA/AMS solution system? It has been noted in other work that BA will undergo self initiation under various temperature conditions and that the rate of polymerization is significant (Appendix A). It is one of the properties of BA homopolymerization to produce gel at even low conversion levels (the higher the temperature the sooner the gel is created). This early gel formation subsequently ramps the observed polymerization rate beyond that which MMA is capable of for the same level of conversion. Under closer observation at very low conversion levels [12], it is apparent that the initial rate of propagation (and hence initiation) of MMA is greater than that of BA. This may be the reason why the phenomenon is being observed in the MMA/AMS system but with neither of the other two binary systems mentioned.

If one were to add an initiator agent to the system, it would potentially relieve the stress placed on the MMA to initiate the majority of the polymer chains throughout the reaction. The initiator should not be able to discriminate and would initiate a large portion of the AMS molecules to start the chain leaving more MMA readily available for propagation reactions, in turn leading to a higher $R_{\text{propagation}}$. So then addition of initiator may in fact help

to eliminate this phenomenon. If experiments were conducted using initiator, the molecular weights should be less than what would be observed from a purely thermal initiation (for the same level of conversion) of MMA/AMS (since there would be more chains being initiated), and if this deviation from the model were not seen, it might indicate that what has been theorized is true and that the rate of monomer consumption via initiation under thermal conditions may be of significance, thus invalidating LCA-I.

In summary then, the deviations between the Kruger model and the experimental data observed for the temperatures of 100, 120 and 140°C are possibly a result of a breakdown of LCA-I. However, to be certain, more work needs to be done at the low feed fractions of MMA using initiator to study the effect on composition of the copolymer as well as on the resulting molecular weights. More work should also be done to determine how much (if any) low-molecular weight material is being produced to quantify the effects on NMR results.

6.3. Concluding Remarks

The MMA/AMS copolymerization system has been re-investigated using the Kruger model to estimate the 6 key kinetic parameters used by Kruger to describe a system with two depropagating monomers. It is obvious from the parameter estimates that a trend towards zero for r_{AMS} is incorrect. It is also apparent that there is significant depropagation in the reactions described by equations 2 and 3, while it is confirmed that the solution effect on the homo-depropagation of MMA (equation 4) is not insignificant. An interesting effect of thermal polymerization with this system has been uncovered: at sufficiently low concentrations of MMA, the Kruger model will not be able to properly predict the copolymer composition since at these low concentrations it is proposed that LCA-I no longer holds. Care should be taken when using the Kruger model to estimate the kinetic parameters mentioned. The models' sensitivity towards each parameter can change at various temperatures leading to numerical pitfalls and the possibility of erroneous parameter estimates.

7. Butyl Acrylate/Methyl Methacrylate Copolymerization in Bulk

7.1. Introduction

While the use of AMS in the other two copolymer systems causes a distinct increase on the T_g for the systems, the copolymerization of MMA and BA together has the opposite effect. The relatively low T_g of BA will lower the average T_g from the MMA homopolymer. The work done by McManus et al. [28] was detailed enough in the estimation of the reactivity ratio values as well as the experimental design and raw data collected that further experimental work was deemed unnecessary. As with most of the past work done with reactivity ratios, the monomer concentrations were calculated at room temperature without taking into account the density changes that occur when running the reactions at elevated temperatures. At temperatures of 100°C through 140°C the changes in the respective monomer concentrations are not insignificant and in cases where depropagation is a considerable factor, these changes can ultimately have an effect on the parameter estimates.

7.2. Results

Taking the data from the bulk system and correcting for the temperature effect, it was possible to recalculate the parameter estimates (using Kruger's model [41]) for the BA/MMA system. In this case the changes in the parameter estimates were not significant for the reactivity ratios. However, at elevated temperatures minor amounts of MMA depropagation is noticed as seen via the slightly elevated values of R_2 and R_{11} , which is to be expected given what was seen for the MMA/AMS system. The resulting parameter estimates, shown here in Table 8, match well with the estimates in the previous work [28] and show only a slight temperature dependency.

Table 8: Bulk Parameter Estimates for the Kruger model (1 = MMA, 2 = BA)

Temp (°C)	r_1^*	r_2^*	r_1	r_2	R_1	R_2	R_{11}	R_{22}	K_1
60	2.2384	0.3802	2.204	0.342	0.000	0.000	0.000	0.000	0.000
80	1.8324	0.3048	2.134	0.353	0.000	0.000	0.000	0.000	0.000
100	1.8484	0.3735	1.799	0.352	0.000	0.000	0.034	0.000	0.019
120	1.6165	0.3731	1.635	0.366	0.000	0.002	0.069	0.000	0.042
140	1.6669	0.4257	1.687	0.431	0.000	0.008	0.085	0.000	0.050

* Previous estimates [28]

Given the fact that the Kruger model was able to match the results from the Mayo-Lewis model, this proves once again that the Kruger model is robust enough to handle even systems with minimal or no depropagating behaviour. Unlike the previous two systems, these parameter estimates show some interesting behaviour in that the reactivity ratio values do not show the same type of Arrhenius temperature dependency. This behaviour might be explained through errors associated with the NMR spectra. It has been documented that an overlap of the BA and MMA peaks [28, 72] is possible and while the previous work appears to have separated the peaks, perhaps the separation was not as distinct as previously thought. However, this does not pose a problem since these values are only going to be used as first guesses for the terpolymer system, and while these values may or may not have error in them, they will be appropriate enough to allow convergence.

8. MMA/BA/AMS Terpolymerization in Bulk

8.1. Introduction and Experimental Considerations

Since the terpolymer model is so large and has so many parameters, it is unrealistic to expect convergence on the correct parameter values without a reasonable set of initial estimates. Recalling the definitions of the parameters defined for the terpolymer model earlier, it is seen that all of the parameters in the terpolymer model have already been estimated by studying the binary systems. As mentioned earlier, composition analysis on a terpolymer sample is significantly more time consuming and requires more polymer than for the binary systems that have been studied. This is the difference between doing a ^{13}C analysis, which may take from 8-12 hours, and a ^1H analysis which may take 8-12 minutes depending on the relaxation time used for running the analysis. Industrially speaking, typical AMS copolymerizations would not contain significant amounts of AMS in the feed (typically only up to 10%). This is due to the fact that only small amounts of AMS are needed to increase the T_g of a polymer while too much AMS results in brittle polymer that takes a significant amount of time to produce by free radical methods, as has been seen for the BA/AMS full conversion polymerizations. For this reason, the feed protocol for the terpolymer system was chosen to operate over only a small range of AMS feed concentrations while increasing the range of BA and MMA concentrations. Besides the fact that upwards of five times the amount of polymer is required for a ^{13}C NMR analysis compared to a ^1H NMR analysis, and the time required to produce this amount of polymer at higher AMS concentrations, the actual scans produced by a ^{13}C NMR analysis also play a role in determining the feed concentrations being used. The peaks produced by the aromatic AMS carbons (5) outnumber those associated with the BA and MMA molecules (1). This means that in order to get comparative signals from BA and MMA it would mean having at least five times the incorporation of BA and MMA into the polymer. A past study [34] showed that if the BA level in the feed was too small (below a feed fraction of about 10%), then it became very difficult to accurately separate and integrate the resulting BA peaks. For all of these reasons, it was decided to run experiments with AMS feed fractions between 0.065 - 0.1, BA feed fractions between 0.15 - 0.45 and MMA feed fractions between 0.5 - 0.8. Using these feed ratios should ensure that a) the feeds would

reflect what would be done in industry b) enough polymer was created for analysis c) the composition of the terpolymer would allow for easy separation of peaks on the ^{13}C NMR spectra, and d) the molecular weights would be large enough to not have any concerns with respect to long chain approximations.

8.2. Experimental Results

Given the amount of time it would take to properly analyze all of the samples created in a run with 12 distinct data points (with 3 replicates at each feed ratio), it was decided that only one temperature would be studied here for the terpolymer case. The amount of NMR time to get all 36 samples analyzed took almost 2 months. For multiple reasons a temperature of 140°C was chosen to run the experiments at. It has been seen in the binary systems that as temperature increases, there is a greater response in the cross depropagation parameters. While the absolute values of the gradients are not large, they are larger than what was seen at lower temperatures. This allows better estimates of the cross depropagation parameters as well as the standard reactivity ratios[62, 73]. As well as showing better numerical results, operating at 140°C allows for easier experimental operation. The reactions reach a 5% conversion much faster, allows for easier separation of the polymer from the ampoules and the resulting polymer (which has a lower molecular weight) is much easier to work with for NMR. A lower molecular weight will result in a lower viscosity for the same weight of material, allowing for a more concentrated solution to be used for analysis resulting in stronger peaks in the spectra.

The results from the NMR analysis are shown in Figure 22.

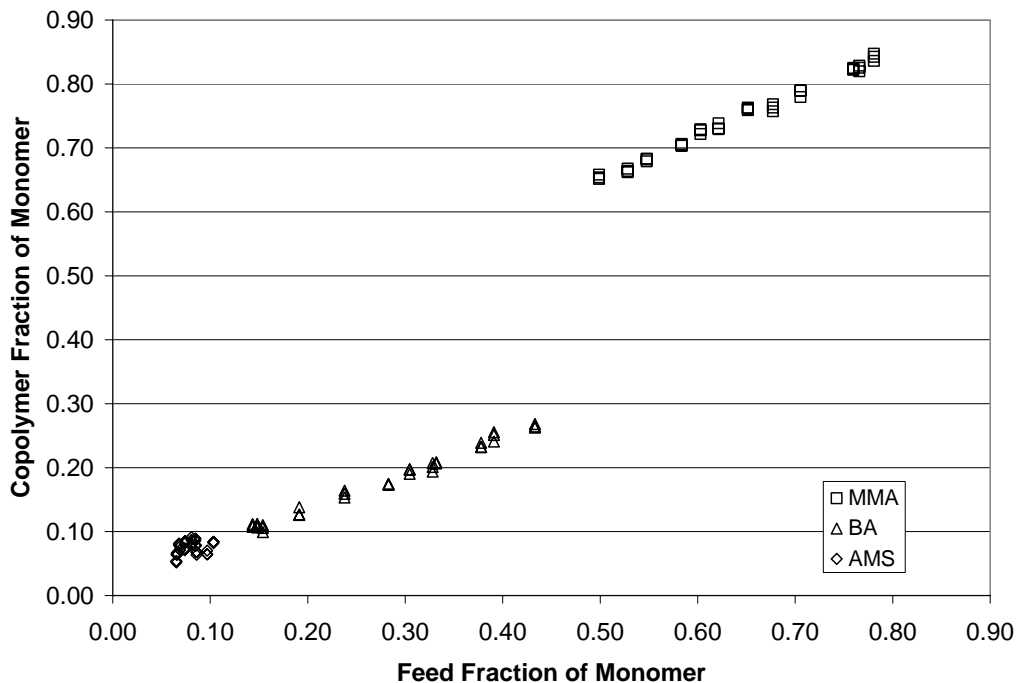


Figure 22: Terpolymer NMR results

It is to be expected that with such a small range of AMS concentrations the terpolymer fraction of AMS does not change much. However, it is quite apparent that there is a linear trend with both the BA and MMA compositions that shows a tendency for MMA to be incorporated more readily than BA. This is not surprising. From looking at the binary system parameters, it is obvious that MMA has a higher affinity for polymerizing with itself than BA does, and consequently more MMA will be incorporated at higher MMA concentrations.

8.3. Modeling

As in the case with other models with many parameters, there are problems when it comes to converging on estimates for the parameters [74], especially when the data set is limited and there is only one or possibly two responses that can be used to fit the parameters such that the model matches the experimental data. In the case of the binary model the NMR data was only good for estimating one of the composition values since the second was linearly dependent upon the first. In the case of the terpolymer model, two of the copolymer composition values (e.g. F_{MMA} and F_{BA}) are independent from one another and therefore both can be used in the

estimation of the parameters. Using these two responses, parameter estimates were obtained from a non-linear least squares technique using a sum of squared differences.

8.3.1. Sensitivity Analysis

Since a sensitivity analysis done for the binary Kruger model revealed interesting results, a similar procedure should be done for the ternary model in an attempt to reveal information about the ability to estimate parameters as well as confidence regions for those parameter estimates. The binary sensitivity analysis showed significant model sensitivity to certain parameters in regions of higher monomer concentration directly associated to that parameter. For example, heightened sensitivity was seen for r_A in regions of higher concentrations of A. This made estimating parameters relatively straightforward and consequently estimation of the joint confidence regions was easily achieved since the resulting Jacobian matrix consisted of elements that were significantly large leading to a relatively tight interval in many cases. The sensitivity analysis for the ternary model was not as encouraging. In many cases there were no clearly defined regions where the model was more sensitive to a given parameter (within the range predetermined by the binary Kruger estimates) over the entire range of concentrations being considered. Examples of these contours are shown in Figures 23 - 25.

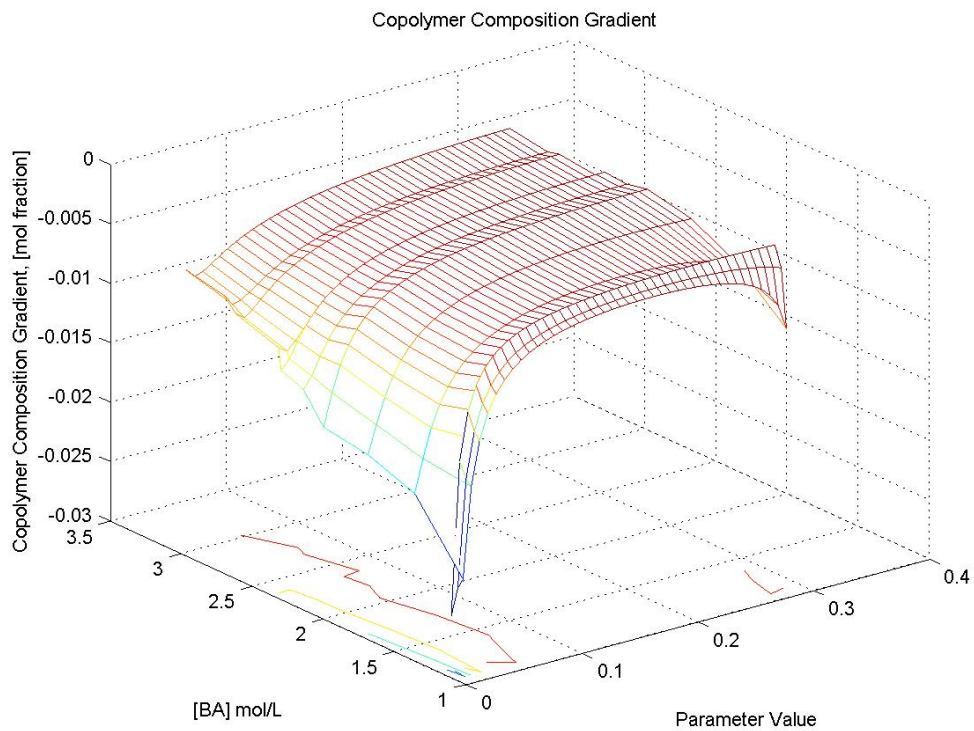


Figure 23: Terpolymer Model Gradient for r_{AB} ($A = BA$, $B = AMS$)

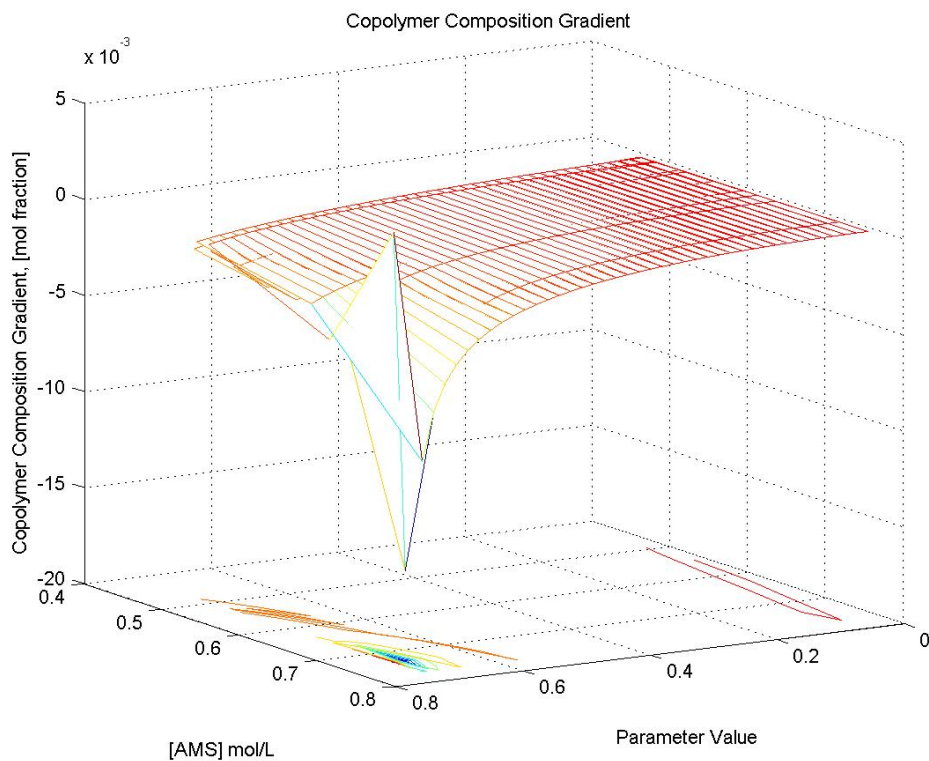


Figure 24: Terpolymer Model Gradient for r_{BC} ($B = AMS$, $C = MMA$)

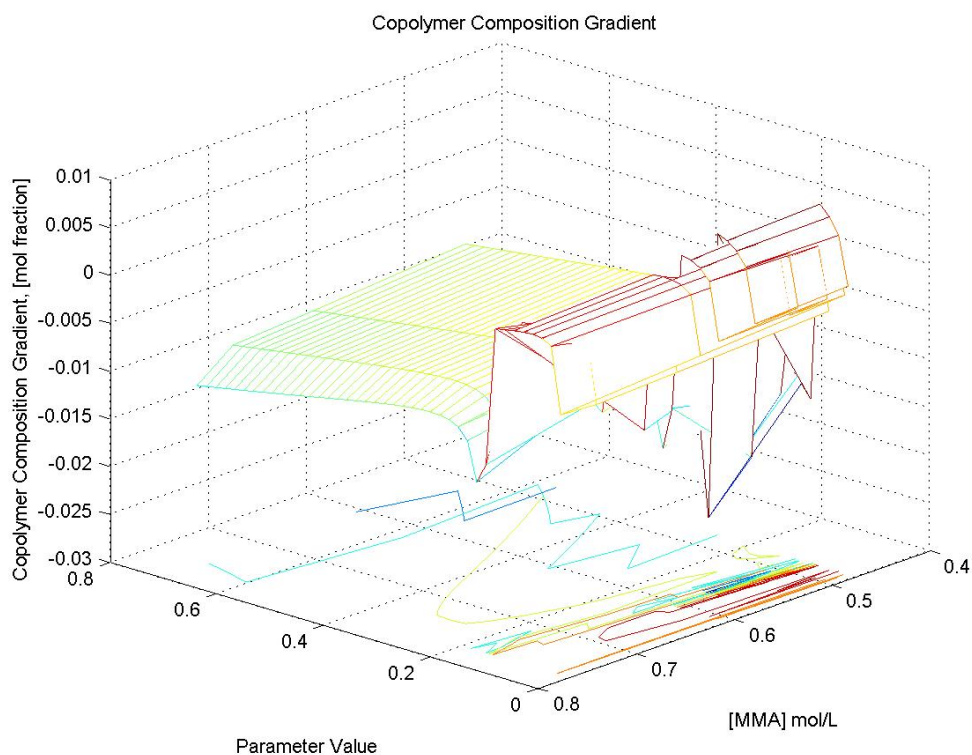


Figure 25: Terpolymer Model Gradient for r_{AC} ($A = BA$, $C = MMA$)

From all three contours, it is apparent that there are large regions where the model is not very sensitive to changes in monomer feed concentration as indicated by the large flat areas. Each contour does show an area of sensitivity, but these are unstable regions that exist outside of the probable regions for the parameter values. Problems of this type are inherent in complex models such as this where there are so many parameters that the model's sensitivity is spread such that sensitivity to any one parameter becomes diminished. This was even the case with the binary Kruger model when compared to the Mayo-Lewis model and the trend apparently has continued into the terpolymer model. However, this does not mean that the model will not work; it simply indicates that the creation of meaningful joint confidence regions for the parameters may not be possible. In order to properly predict the composition of a terpolymer, good initial estimates of the parameters will be required.

8.3.2. Benchmarking

It should be noted here that the ternary model will not reduce to predict depropagating binary copolymer systems. If a monomer is removed from the system entirely, some of the parameters become indeterminate (non-zero) and some of the initial monomer balances disintegrate. Since the binary Kruger model has already been studied and used successfully, it is of no concern that the model will not reduce. Given that the terpolymer model is derived from the binary model methodology, the terpolymer model should be capable of handling terpolymer systems without depropagation. To ensure that the ternary model was in fact working correctly and was able to predict the composition of any terpolymer system, it was decided to benchmark it against some published values for a variety of different systems and compare the estimates to that of the Alfrey Goldfinger model. The major pitfalls with this type of analysis are that often literature has limited data sets and assumptions about conversion levels and actual monomer concentrations in solution need to be made (i.e. temperature corrections). Other publications do not list the temperatures being used to generate the data, making the data set unusable[75]. Along with these other issues, the accuracy of the composition data using less accurate NMR methods is also often in question.

With these factors considered, the terpolymer model was successful in duplicating the work from several sources of literature. Data sets from publications by Hocking [76], Braun and Cei [77], Valvassori and Sartori [78], and Koenig [79] were used to test the terpolymer model. In multiple cases, specifically with respect to the data sets from Valvassori and Koenig, the terpolymer model was able to match the NMR data more closely with minor changes in some of the parameter values. An example of this benchmarking for a Styrene/Acrylonitrile(AN)/MMA system is shown in Figure 26 and 27 where a system from Valvassori is used. Multiple Styrene/AN/MMA data sets were obtained from the literature and every set of parameters that are estimated to fit the data are different from one publication to the next (see Table 13 and Table 19 in Appendix E), supporting the previous statement about using literature data for benchmarking. The specifics of the parameters estimated from this system are shown in Table 9 and while the others can be found in Appendix E.

Table 9: Expanded Kruger Fit vs. Alfrey-Goldfinger Fit

Parameter	Updated Kruger Estimates	Original Alfrey-Goldfinger Estimates
r_{AB}	0.51464	0.5
r_{AC}	0.23113	0.41
r_{BA}	0.49914	0.5
r_{BC}	0.98176	1.2
r_{CA}	0.063528	0.04
r_{CB}	0.25712	0.15
R_A	0	n/a
R_B	0	n/a
R_C	0	n/a
R_D	0	n/a
R_E	0	n/a
R_F	0	n/a
R_{AA}	0	n/a
R_{BB}	0	n/a
R_{CC}	0	n/a

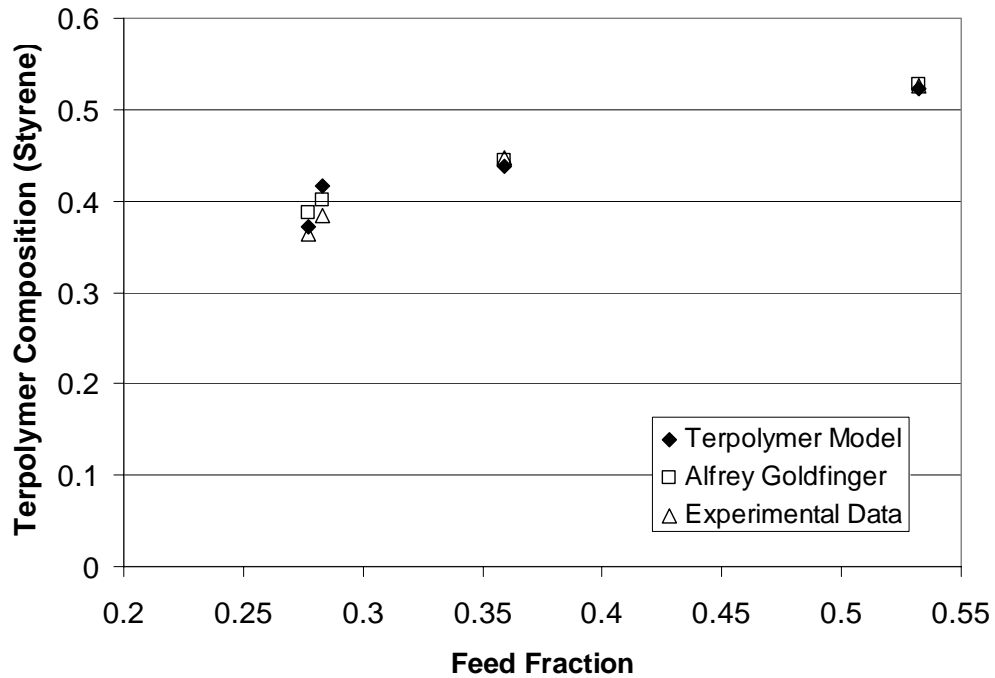


Figure 26: Terpolymer Composition Comparisons (Styrene)

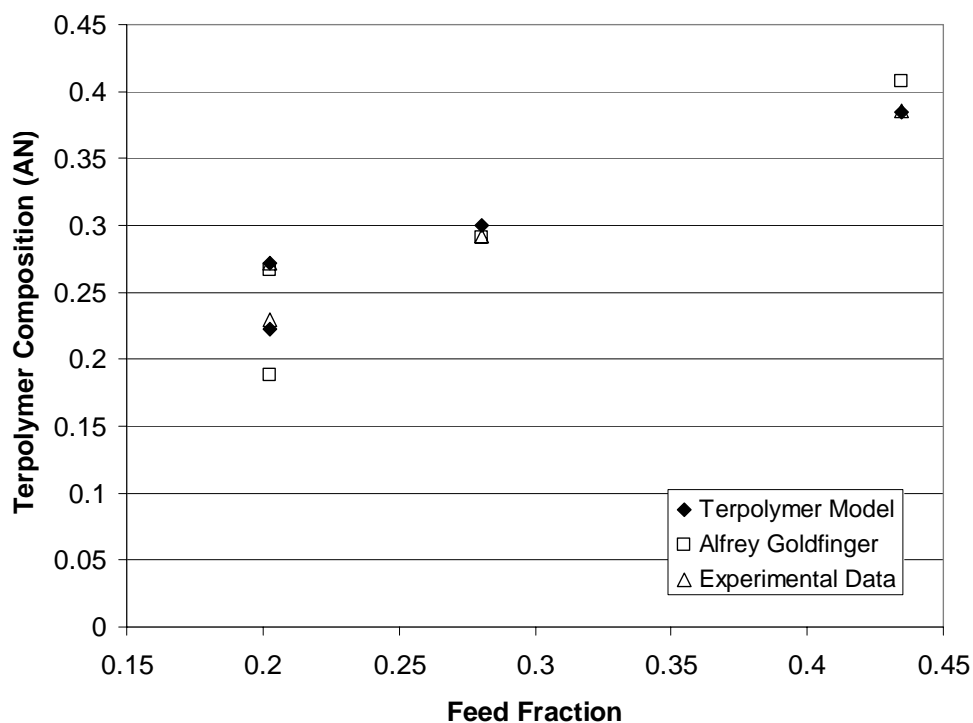


Figure 27: Terpolymer Composition Comparisons (Acrylonitrile)

8.4. MMA/BA/AMS Parameter Estimation: Results and Discussion

Moving on to the fully depropagating MMA/BA/AMS system, the initial parameter estimates required have already been estimated from the binary systems. The following is a list of the initial estimates along with the values estimated from the least squares fitting.

Table 10: Parameter Estimates for Binary and Ternary Systems

Parameter (A=BA,B=AMS,C= MMA)	Initial Parameter Estimates (from Binary Model)	Estimated Values (from Terpolymer Model)
r_{AB}	0.1814	0.14299
r_{AC}	0.4308	0.34841
r_{BA}	0.5511	0.5575
r_{BC}	0.33	0.35956
r_{CA}	1.6871	1.905
r_{CB}	0.65	0.70698
R_A	0.5101	0.50796
R_B	1.4599	1.4629

R_C	0	0
R_D	0	0
R_E	4.0409	4.0401
R_F	14.045	14.041
R_{AA}	0	0
R_{BB}	33	33
R_{CC}	0.05	0

From Table 10 it is obvious there are some discrepancies between what was estimated from the binary systems and what parameters are estimated from the ternary system. This is not unexpected given the increased complexity of the system which may not behave identically to the binary systems as well as the potential for differences in NMR results between proton and carbon analysis. It is encouraging to note however that the ternary estimates do fall into the ranges of each confidence region calculated from the binary systems for each parameter. This may indicate there is no numerically significant difference between the parameter sets. One should also note the relative indifference in the cross depropagation parameters (R_A , R_B , R_C , R_D , R_E , R_F). This follows what was being seen for the binary systems as well. While the sensitivity of the crosspropagation/depropagation ratios increases with temperature, the relative sensitivity in these parameters was still lower than that of the reactivity ratios. From the sensitivity analysis done on the ternary model it can be seen that while the average absolute sensitivity values for the reactivity ratios are typically of the order 10^{-2} , the cross depropagation parameters have average values of the order 10^{-4} . The fit to the terpolymer composition data can be seen here in Figure 28.

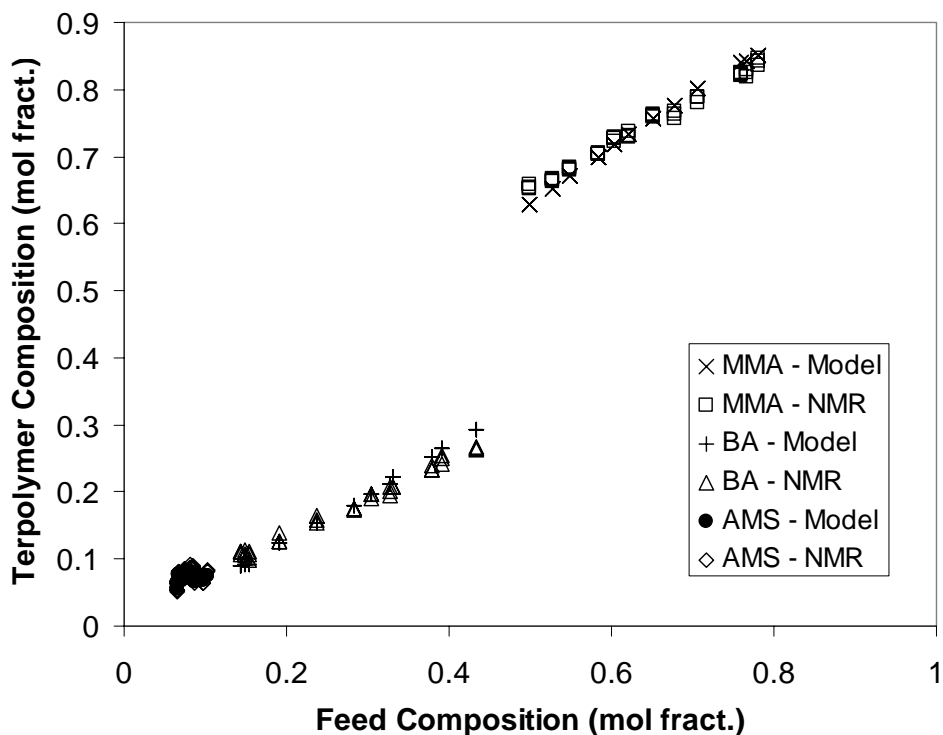


Figure 28: Model Prediction vs. Experimental Data

From Figure 28, it is seen that the model does match the experimental data reasonably well using the parameters listed above in Table 10. However, when going to estimate the joint confidence regions for the reactivity ratios the expected problems did occur. Due to the apparent low numerical sensitivity of the model, the values found in the Jacobian matrix (i.e. the matrix representing the change in function value with a change in parameter) were relatively small, in fact an order of magnitude too small in order to produce meaningful estimates on the relative amount of error for each parameter. This means that when the joint confidence contours are created, they encompass zero.

However, there are other indicators besides a joint confidence contour that point to the fact that the parameters estimated may be correct. The first is that they are very nearly close to the values obtained from the binary system analyses and fall into the ranges dictated by the previously obtained joint confidence contours. Besides this the NLLS subroutine converges on these values and fits the NMR data closely. A small manual change in any of these key reactivity ratio parameters, as well as a change in any of R_C , R_D , or R_{AA} , significantly moves

the model estimates away from the NMR values. In addition to these indicators, anything but a small deviation from these estimates leads to erroneous estimates of the probability values. Recall that in the ternary model there are 9 probabilities to be estimated. Due to the complexity of the model, these 9 equations must be solved simultaneously. For the probabilities to have physical meaning, they must fall between the values of zero and one. Not only do these values need to fall between zero and one, their values must also follow an educated line of logic. For example, at 140°C, $P_{BB} \approx 0$ (the probability of AMS attaching itself to another AMS molecule) simply due to the thermodynamics of the system. Also $P_{CC} > P_{AA} \gg P_{BB}$ since from the previously estimated parameters as well as from the feed compositions being used MMA will homopolymerize more readily than BA. Other such logic can be derived by observing the parameters from the binary systems that were shown earlier. The probability values obtained using these parameter estimates are shown in Appendix F. By observing the values of these probabilities when deviating from the estimated values in Table 10, a large fraction of them fall outside of this range and consequently the model does not converge to match the NMR data. It is therefore believed that these parameter estimates are accurate, even though it is not at this time possible to put a numerical value on their accuracy.

8.5. Concluding Remarks

The expanded Kruger model is a complex mechanistic model that is as robust as the binary Kruger model since it requires no special cases to allow for convergence. At the same time, it can estimate the parameters for less complicated systems without difficulty. The terpolymer model does however suffer from issues with insensitivity which leads to difficulty in properly determining error on parameter estimates. From the work done with the model, it is apparent that the model does fit NMR data well using parameters that are not very different from those estimated from the binary systems. Some possible future work that might be done with the terpolymer model might be to expand into regions with higher AMS concentrations taking into consideration the issue already mentioned with respect to the potential NMR difficulties.

9. Conclusions and Recommendations

9.1. Concluding Remarks

Depropagating systems are not straightforward and many factors must be taken into account. How many monomers in the system are depropagating? What are the relative rates of depropagation? Are both homopropagation reactions reversible? Are the cross propagation reactions reversible? What feed temperatures and concentrations are required to produce a desirable product in a reasonable amount of time? One of the biggest misconceptions with depropagating systems is that it is often assumed that if one works below the ceiling temperature for a given monomer no depropagating effects will be exhibited. Since the ceiling temperature is defined such that the reverse reaction is of *equal* rate to the forward reaction, it is quite possible that the reverse reaction is occurring even at lower temperatures. This misconception must be dispelled and depropagation properly taken into account if a realistic representation of the system is to be achieved.

The binary Kruger model takes into account every propagation reaction being reversible with the only restrictions those being imposed by the user. It is the most comprehensive and robust model that is currently available for use since it overcomes the shortcomings of the Mayo-Lewis, Lowry and Wittmer models. It can be used to estimate kinetic parameters for both bulk and solution systems as well as the parameters for non-depropagating systems. However, in special cases as seen with the MMA/AMS system, the Kruger model cannot predict proper compositions when the system does not follow the underlying long chain approximations.

The expanded Kruger model for terpolymer systems was also a success. Given how the model was developed, it has similar properties and the same robustness as the binary Kruger model. No special cases are required and all reactions are considered reversible. From benchmarking work, the model has proven itself to work well for non-depropagating systems and in some cases improve upon the existing parameter estimates from the literature.

Using the parameter estimates from the three binary systems (MMA/AMS, BA/AMS and MMA/BA), the model was able to match NMR data well with small adjustments to the binary parameter estimates as well as come up with reasonable reaction probabilities. Since the expanded model uses the same long chain approximation assumptions that the binary model does, the user should realize that if for any reason a system would not follow these assumptions, then the model becomes invalid.

Caution should be used when using either the binary or expanded Kruger models. Both models suffer from their own unique sensitivity issues and with the increased complexity of the terpolymer model, the problems are exacerbated. This has led to issues in estimating error contours for the parameter estimates from the terpolymer model. In some cases, these sensitivity issues may lead to potential problems with parameter estimation for certain systems and feed fractions.

9.2. Recommendations

To expand upon the work presented here there are some areas of these depropagating systems that could be explored further. The discrepancy seen at low feed fractions of MMA at elevated temperatures should be looked at more closely using peroxide initiators. It is quite possible that if one were to use an additional initiator instead of relying on the MMA to start all of the polymer chains, the apparent invalidation of LCA-I might be eliminated or at the very least the discrepancy between the data and model prediction would be minimized.

It would also be interesting to do further work with the terpolymer system at some higher feed fractions of AMS to complete the overall composition picture for the system. The reader should realize however the complications associated with such an endeavour. The reactions would take a significantly longer time to achieve the 5% conversion level desired. Since it is required that at least 100 mg of polymer is used for ^{13}C NMR, a 5% level of conversion is almost a requirement. There is also the difficulty with properly reading the NMR spectra. Having higher levels of AMS removes BA and MMA from the system, leading

to smaller peaks from the BA and MMA, thus leading to difficulty in accurately integrating the peaks. Increased AMS content will also significantly reduce the molecular weight of the final product making accurate NMR determination more difficult still since NMR does not discriminate between dimers/trimers/oligomers and polymeric chains. Investigation of lower temperature polymerizations (100°C and 120°C) would also be interesting to see if the same types of Arrhenius trends in the binary systems are seen in the terpolymer system.

Since both the binary and ternary/extended Kruger model are instantaneous equations, they are only applicable for low conversion (< 5%) data. It would be interesting to see the results from a fully integrated form of both equations. One would have to take the models back to the base differential equations and reconstruct them using the definition of conversion and redo the derivation for the substitution of parameter definitions. This would allow the models to work for the full conversion range. However, the newly derived models would be considerably more complex than the instantaneous versions and the problems with convergence seen for the ternary model might be exacerbated.

9.3. Contributions

The contributions that this work has made in the area of high temperature polymerizations with depropagation are many. I have identified the inadequacy of many of the models in the literature used for depropagating systems. The Lowry models for these systems simply do not describe enough of the reactions occurring and the Wittmer model can be awkward to handle under certain conditions. This can be found in chapter 3 of the thesis. As well as identifying models that are inadequate, there are also some misconceptions about ceiling temperatures and reactivity ratios that have been brought to light. I have also determined kinetic parameters for two binary depropagating systems (BA/AMS and MMA/AMS) that properly take into account depropagation characteristics. This can be found in chapters 5 and 6. I have also identified a potential pitfall in the Kruger and other instantaneous copolymer composition models in the apparent invalidation of the long chain approximation. This invalidation can lead to erroneous prediction by the models. This can be found in chapter 6. I have also confirmed the kinetic parameters for the BA/MMA copolymer system using the Kruger

model. This can be found in chapter 7. I have developed, benchmarked and tested a new model for fully depropagating terpolymer systems as well as determine kinetic parameters for the BA/MMA/AMS terpolymer system. It is these contributions that I hope will go to further the understanding for depropagating systems.

9.4. Publications

- Ziaee, F., A. Kavousian, M. H. Nekoomanesh, M. J. Leamen, and A. Penlidis (2004). Determination of monomer reactivity ratios in styrene/2-ethylhexylacrylate copolymer. *Journal of Applied Polymer Science*, **92** (5), 3368-3370.
- Wang, T. J., M. J. Leamen, N. T. McManus, and A. Penlidis (2004). Copolymerization of Alpha Methyl Styrene with Butyl Acrylate: Parameter Estimation Considerations. *Journal of Macromolecular Science, Part A: Pure and Applied Chemistry*, **41** (11), 1205-1220.
 - Published “As is”: Chapter 5
- Leamen, M. J., N. T. McManus, and A. Penlidis (2004). Refractive index increment (dn/dc) using GPC for the α -methyl styrene/methyl methacrylate copolymer at 670 nm in tetrahydrofuran. *Journal of Applied Polymer Science*, **94** (6), 2545-2547.
 - Published “As is”: Appendix C
- Leamen, M. J., N. T. McManus, and A. Penlidis (2005). Binary Copolymerization with Full Depropagation: A Study of Methyl Methacrylate/Alpha-Methyl Styrene Copolymerization. *Journal of Polymer Science: Part A: Polymer Chemistry*, **43** (17), 3868-3877.
 - Chapter 6
- Leamen, M.J., N.T. McManus, and A. Penlidis (2005). Kinetic Investigation and Modelling of a Terpolymer Systems with Depropagation (BA/MMA/AMS) [in preparation for publication]
 - Chapter 3 and 8
- Leamen, M.J. and A. Penlidis (2005). A Tutorial on Depropagation: Misconceptions and New Concepts. [in preparation for publication]

10. References

- [1] Tullo, A. H. (2002). Automotive Coatings. *Chemical and Engineering News*, **80** (42), 27-30.
- [2] Sharma, K. R. (2002). Thermal Terpolymerization of Alkylmethylstyrene, Acrylonitrile and Styrene. *Polymer*, **41** (4), 1305-1308.
- [3] Odian, G. (1991). *Principles of Polymerization*. John Wiley and Sons, Inc., New York,
- [4] Hoppe, S. and A. Renken (1998). Modelling of the Free Radical Polymerization of Methylmethacrylate Up to High Temperature. *Polymer Reaction Engineering Journal*, **6** (1), 1-39.
- [5] Palmer, D. E., N. T. McManus, and A. Penlidis (2000). Copolymerization with Depropagation: A Study of Alpha-Methyl Styrene/Methyl Methacrylate in Bulk at Elevated Temperatures. *Journal of Polymer Science: Part A: Polymer Chemistry*, **38** (11), 1981-1990.
- [6] Fernandez-Garcia, M., L. L. Martinez, and E. L. Madruga (1998). Solvent Effects on the Free-Radical Polymerization of Methyl Methacrylate. *Polymer*, **39** (4), 991-995.
- [7] Fernandez-Garcia, M., M. Fernandez-Sanz, and E. L. Madruga (2000). A Kinetic Study of Butyl Acrylate Free Radical Polymerization in Benzene Solution. *Macromolecular Chemistry and Physics*, **201** (14), 1840-1845.
- [8] Fernandez-Garcia, M., J. L. De la Fuente, M. Fernandez-Sanz, and E. L. Madruga (2001). An Analysis of the Solvent Effects on the Monomer Reactivity Ratios Using the Copolymer Glass Transition Temperatures. *Macromolecular Rapid Communications*, **22** (6), 451-455.
- [9] Hakim, M., V. Verhoeven, N. T. McManus, M. A. Dubé, and A. Penlidis (2000). High-Temperature Solution Polymerization of Butyl Acrylate / Methyl Methacrylate: Reactivity Ratio Estimation. *Journal of Applied Polymer Science*, **77** (3), 602-609.
- [10] Martinet, F. and J. Guillot (1997). Copolymerization with Depropagation: Experiments and Prediction of Kinetics and Properties of Alpha-Methylstyrene/Methyl Methacrylate Copolymers. I. Solution Copolymerization. *Journal of Applied Polymer Science*, **65** (12), 2297-2313.
- [11] Palmer, D. E., N. T. McManus, and A. Penlidis (2001). Copolymerization with Depropagation: A Study of Alpha-Methyl Styrene/Methyl Methacrylate in Solution at Elevated Temperatures. *Journal of Polymer Science: Part A: Polymer Chemistry*, **39** (10), 1753-1763.
- [12] Clouet, G., P. Chaumont, and P. Corpart (1993). Studies on Bulk Polymerization of Methyl Methacrylate. I. Thermal Polymerization. *Journal of Polymer Science: Part A: Polymer Chemistry*, **31** (11), 2815-2824.

- [13] Fenouillot, F., J. Terrisse, and T. Rimlinger (1998). Thermal Polymerization of Methyl Methacrylate at High Temperature. *International Polymer Processing*, **13** (2), 154-161.
- [14] Lingnau, J. and G. Meyerhoff (1984). Spontaneous Polymerization of Methyl Methacrylate. 8. Polymerization Kinetics of Acrylates Containing Chlorine Atoms. *Macromolecules*, **17** (4), 941-945.
- [15] Walling, C. and E. R. Briggs (1946). The Thermal Polymerization of Methyl Methacrylate. *Journal of the American Chemical Society*, **68** (7), 1141-1149.
- [16] Levy, L. B. (1996). The Inhibition of Butyl Acrylate by p-methoxyphenol. *Journal of Applied Polymer Science*, **60** (13), 2481-2487.
- [17] Hui, A. W. and A. E. Hamielec (1972). Thermal Polymerization of Styrene at High Conversions and Temperatures. An Experimental Study. *Journal of Applied Polymer Science*, **16**, 749-769.
- [18] Husain, A. and A. E. Hamielec (1978). Thermal Polymerization of Styrene. *Journal of Applied Polymer Science*, **22** (5), 1207-1223.
- [19] Mark, H. F., Bikales, N. M., Overberger, C. G., Menges, G., and Kroschwitz, J. I. Encyclopedia of Polymer Science and Engineering Oligomers. Wiley, New York, 1986. 440-440.
- [20] McManus, N. T., A. Penlidis, and M. A. Dubé (2002). Copolymerization of Alpha-Methyl Styrene with Butyl Acrylate in Bulk. *Polymer*, **43** (5), 1607-1614.
- [21] Martinet, F. and J. Guillot (1999). Copolymerization with Depropagation: Experiments and Prediction of Kinetics and Properties of Alpha-Methylstyrene/Methyl Methacrylate Copolymers. II. Bulk Copolymerization. *Journal of Applied Polymer Science*, **72** (12), 1611-1625.
- [22] Gridnev, A. A. (2002). Kinetics of Alpha-Methylstyrene Oligomerization by Catalytic Chain Transfer. *Journal of Polymer Science: Part A: Polymer Chemistry*, **40** (9), 1366-1376.
- [23] O'Driscoll, K. F. and F. P. Gasparro (1967). Copolymerization with Depropagation. *Journal of Macromolecular Science: Chemistry*, **A1** (4), 643-652.
- [24] Izu, M. and K. F. O'Driscoll (1970). Copolymerization with Depropagation. V. Copolymerization of Alpha-Methylstyrene and Methyl Methacrylate between Their Ceiling Temperatures. *Journal of Polymer Science: Part A-1*, **8**, 1687-1691.
- [25] O'Driscoll, K. F. and A. F. Burczyk (1992). Kinetics of Styrene and Methyl Methacrylate Polymerizations in a Starved Feed Reactor. *Polymer Reaction Engineering Journal*, **1** (1), 111-144.

- [26] Villalobos, M. A. and J. A. Debling (2001). Modeling and Simulation of Continuous Free Radical Polymerization with Multiple Monomers Exhibiting Reversible Propagation. *DECHEMA Monographien*, **137** (7th International Workshop on Polymer Reaction Engineering), 107-115.
- [27] Hutchinson, R. A., D. A. Paquet, S. Beuermann, and J. H. McMinn (1998). Investigation of Methacrylate Free-Radical Depropagation Kinetics by Pulsed-Laser Polymerization. *Industrial and Engineering Chemistry Research*, **37**, 3567-3574.
- [28] McManus, N. T., M. A. Dubé, and A. Penlidis (1999). High Temperature Bulk Copolymerization of Butyl Acrylate/Methyl Methacrylate: Reactivity Ratio Estimation. *Polymer Reaction Engineering Journal*, **7** (1), 131-145.
- [29] Mark, H. F., Bikales, N. M., Overberger, C. G., Menges, G., and Kroschwitz, J. I. *Encyclopedia of Polymer Science and Engineering Polymerization Thermodynamics*. Wiley Interscience, New York, 1986. 561-568.
- [30] Brandrup, J. and Immergut, E. H. *Polymer Handbook 4th: Heats and Entropies of Polymerization, Ceiling Temperatures*. Wiley, New York, 1998. 394-401.
- [31] Odian, G. (2004). *Principles of Polymerization 4th Edn.* Wiley, New York, 275-282.
- [32] Dubé, M. A., K. Rilling, and A. Penlidis (1991). A Kinetic Investigation of Butyl Acrylate Polymerization. *Journal of Applied Polymer Science*, **43** (11), 2137-2145.
- [33] McManus, N. T. (2002). Terpolymerization of BA/MMA/AMS at Elevated Temperatures. *Unpublished Paper*, University of Waterloo, Waterloo Ontario, CANADA.
- [34] McManus, N. T., G. Hsieh, and A. Penlidis (2004). Free Radical Terpolymerization of Butyl Acrylate/Methyl Methacrylate and Alpha Methyl Styrene at High Temperature. *Polymer*, **45** (17), 5837-5845.
- [35] Ito, K. and K. Kodaira (1986). Kinetics of Radical Copolymerization between Alpha-Methylstyrene and Methyl Methacrylate. *Polymer Journal*, **18** (9), 667-672.
- [36] Christiansen, R. L. (1990). Computer-Aided Design of Polymerization Reactors. *PhD. Thesis*, Department of Chemical Engineering, University of Wisconsin-Madison, Madison, Wisconsin, United States of America, 146-158.
- [37] Sanders, J. K. M. and B. K. Hunter (1994). *Modern NMR Spectroscopy: A Guide for Chemists*. Oxford University Press, Toronto, 10-16.
- [38] McManus, N. T., L. M. F. Lona, and A. Penlidis (2002). Comparative Trends of Copolymerizations Involving Alpha Methyl Styrene at Elevated Temperatures. *Polymer Reaction Engineering Journal*, **10** (4), 285-309.

- [39] Lowry, G. G. (1960). The Effect of Depropagation on Copolymer Composition. I. General Theory for One Depropagating Monomer. *Journal of Polymer Science*, **42**, 463-477.
- [40] Wittmer, P. (1970). Copolymerization in the Presence of Depolymerization Reactions. *Advances in Chemistry Series*, **99**, 140-174.
- [41] Kruger, H., J. Bauer, and J. Rubner (1987). Ein Modell zur Beschreibung reversibler Copolymerisationen. *Makromolekulare Chemie*, **188**, 2163-2175.
- [42] Howell, J. A., M. Izu, and K. F. O'Driscoll (1970). Copolymerization with Depropagation. III. Composition and Sequence Distribution from Probability Considerations. *Journal of Polymer Science: Part A-1*, **8**, 699-710.
- [43] Barson, C. A. and D. R. Fenn (1987). A Method for Determining Reactivity Ratios in Copolymerizations in the Presence of a Ceiling Temperature Effect. *European Polymer Journal*, **23** (11), 835-837.
- [44] Georgiev, G. S. (1976). Use of Markov Chains in Treating Depropagation in Copolymerization. II. Distribution of Monomer Units in Copolymers. *Journal of Macromolecular Science: Chemistry*, **A10** (6), 1081-1092.
- [45] Georgiev, G. S. (1976). Use of Markov Chains in Treating Depropagation in Copolymerization. I. Composition of Copolymers. *Journal of Macromolecular Science: Chemistry*, **A10** (6), 1063-1080.
- [46] Meakin, P. and G. A. Abraham (1983). Effects of Depropagation on Free Radical Copolymerization Kinetics. *Macromolecules*, **16** (10), 1661-1669.
- [47] Kang, B. K., K. F. O'Driscoll, and J. A. Howell (1972). Copolymerization with Depropagation. VIII. A General Solution for Reversible Multicomponent Polymerization. *Journal of Polymer Science: Part A-1*, **10**, 2349-2363.
- [48] Alfrey, T. and G. Goldfinger (1946). Copolymerization of Systems Containing Three Components. *The Journal of Chemical Physics*, **14**, 115-116.
- [49] Alfrey, T. and G. Goldfinger (1944). Copolymerization of Systems of Three and More Components. *The Journal of Chemical Physics*, **12**, 322-322.
- [50] Chien, J. C. W. and A. L. Finkenaur (1985). A Simplification of the Terpolymerization Equation. *Journal of Polymer Science: Polymer Chemistry*, **23** (8), 2247-2254.
- [51] Wang, T. J. (1999). Kinetic Investigation of Copolymerization of Butyl Acrylate / Alpha-Methyl Styrene in Solution at Elevated Temperatures. *MASc Thesis*, University of Waterloo, Waterloo, Ontario, CANADA, 13-29.
- [52] Dubé, M. A. and A. Penlidis (1995). A Systematic Approach to the Study of Multicomponent Polymerization Kinetics - the Butyl Acrylate/Methyl

- Methacrylate/Vinyl Acetate example: 1. Bulk copolymerization. *Polymer*, **36** (3), 587-598.
- [53] McManus, N. T. and A. Penlidis (2005). Terpolymer Composition Analysis: A case study of the BA/MMA/AMS Terpolymer. *Submitted to Journal of Applied Polymer Science*,
- [54] Brandrup, J. and Immergut, E. H. In *Polymer Handbook 4th Ed.: Solution Properties: Specific Refractive Index Increment of Polymers in Dilute Solution*. Wiley Interscience, New York, 1989. 547-614.
- [55] Podzimek, S. (1994). The use of GPC coupled with a multiangle laser light scattering photometer for the characterization of polymers. On the determination of molecular weight, size, and branching. *Journal of Applied Polymer Science*, **54**, 91-103.
- [56] McManus, N. T. and A. Penlidis (1998). The Refractive Index Increment for Poly-Alpha-Methylstyrene at 633nm in Tetrahydrofuran. *Journal of Applied Polymer Science*, **70** (6), 1253-1254.
- [57] Leamen, M. J., N. T. McManus, and A. Penlidis (2004). Refractive index increment (dn/dc) using GPC for the α -methyl styrene/methyl methacrylate copolymer at 670 nm in tetrahydrofuran. *Journal of Applied Polymer Science*, **94** (6), 2545-2547.
- [58] Badeen, C. and M. A. Dube (2003). Modeling the copolymerization of methyl methacrylate/ α -methyl styrene at elevated temperatures using Java. *Polymer Reaction Engineering Journal*, **11** (1), 53-77.
- [59] Ham, G. E. (1960). Application of an Expanded Copolymerization Theory to Systems Involving α -Methylstyrene. *Journal of Polymer Science*, **45**, 183-187.
- [60] Kukulj, D., T. P. Davis, and R. G. Gilbert (1998). Chain Transfer to Monomer in the Free-Radical Polymerizations of Methyl Methacrylate, Styrene, and Alpha Methyl Styrene. *Macromolecules*, **31** (4), 994-999.
- [61] McCormick, H. W. (1957). Ceiling Temperature of α -Methylstyrene. *Journal of Polymer Science*, **25** (111), 488-490.
- [62] Wang, T. J., M. J. Leamen, N. T. McManus, and A. Penlidis (2004). Copolymerization of Alpha Methyl Styrene with Butyl Acrylate: Parameter Estimation Considerations. *Journal of Macromolecular Science, Part A: Pure and Applied Chemistry*, **41** (11), 1205-1220.
- [63] Kang, B. K. and K. F. O'Driscoll (1974). Copolymerization with Depropagation. IX. Molecular Weights in Copolymerization with Depropagation. *Macromolecules*, **7**, 886-893.

- [64] Cheong, S. I. and A. Penlidis (2004). Modelling of the Copolymerization, with Depropagation, of alpha-Methyl Styrene and Methyl Methacrylate at an Elevated Temperature. *Journal of Applied Polymer Science*, **93** (1), 261-270.
- [65] Polic, A. L., L. M. F. Lona, T. A. Duever, and A. Penlidis (2004). A protocol for the estimation of parameters in process models: case studies with polymerization scenarios. *Macromolecular Theory and Simulations*, **13** (2), 1022-1344.
- [66] Mayo, F. R. and F. M. Lewis (1944). Copolymerization. I. A Basis for Comparing the Behaviour of Monomers in Copolymerization; The Copolymerization of Styrene and Methyl Methacrylate. *Journal of the American Chemical Society*, **66**, 1594-1601.
- [67] Lingnau, J., M. Stickler, and G. Meyerhoff (1980). The Spontaneous Polymerization of Methyl Methacrylate 4: Formation of Cyclic Dimers and Linear Trimers. *European Polymer Journal*, **16**, 785-791.
- [68] Lingnau, J. and G. Meyerhoff (1983). The spontaneous polymerization of methyl methacrylate 6: Polymerization in solution: participation of transfer agents in the initiation reaction. *Polymer*, **24**, 1473-1478.
- [69] Lingnau, J. and G. Meyerhoff (1984). The spontaneous polymerization of methyl methacrylate: 7 External Heavy Atom effect on the initiation. *Makromolekulare Chemie*, **185**, 587-600.
- [70] Stickler, M. and G. Meyerhoff (1978). Die thermische Polymerisation von Methylmethacrylat, I: Polymerisation in Substanz. *Makromolekulare Chemie*, **179**, 2729-2745.
- [71] Stickler, M. and G. Meyerhoff (1981). The Spontaneous Thermal Polymerization of Methyl Methacrylate 5: Experimental Study and Computer Simulation of the High Conversion Reaction at 130 Centigrade. *Polymer*, **22**, 928-933.
- [72] Dube, M. A., M. Hakim, N. T. McManus, and A. Penlidis (2002). Bulk and solution copolymerization of butyl acrylate/methyl methacrylate at elevated temperatures. *Macromolecular Chemistry and Physics*, **203** (17), 2446-2453.
- [73] Leamen, M. J., N. T. McManus, and A. Penlidis (2005). Binary Copolymerization with Full Depropagation: A Study of Methyl Methacrylate/Alpha-Methyl Styrene Copolymerization. *Journal of Polymer Science: Part A: Polymer Chemistry*, **43** (17), 3868-3877.
- [74] Polic, A. L., T. A. Duever, and A. Penlidis (1998). Case Studies and Literature Review on the Estimation of Copolymerization Reactivity Ratios. *Journal of Polymer Science: Part A: Polymer Chemistry*, **36** (5), 813-822.
- [75] Brar, A. S. and S. K. Hekmatyar (1999). Microstructure Determination of the Acrylonitrile-Styrene-Methyl Methacrylate Terpolymers by NMR Spectroscopy. *Journal of Applied Polymer Science*, **74** (13), 3026-3032.

- [76] Hocking, M. B. and K. A. Klimchuk (1996). A Refinement of the Terpolymer Equation and Its Simple Extension to Two- and Four-Component Systems. *Journal of Polymer Science: Part A: Polymer Chemistry*, **34** (12), 2481-2497.
- [77] Braun, D. and G. Cei (1987). Kinetics of the Free Radical Terpolymerization of Diethyl Maleate with Methyl Methacrylate and Styrene. *Makromolekulare Chemie*, **188** (1), 171-187.
- [78] Valvassori, A. and G. Sartori (1967). Present Status of the Multicomponent Copolymerization. *Fortschritte Der Hochpolymeren-Forschung*, **5** (1), 28-58.
- [79] Koenig, J. L. (1980). *Chemical Microstructure of Polymer Chains*. Wiley-Interscience, New York, 47-48.
- [80] Brandolin, A., M. H. Lacunza, P. E. Urgan, and N. J. Capiatik (1996). High pressure polymerization of ethylene. An improved mathematical model for industrial tubular reactors. *Polymer Reaction Engineering Journal*, **4** (4)
- [81] Zabisky, R. C. M., W. M. Chan, P. Gloor, and A. E. Hamielec (1992). A kinetic model for olefin polymer in high-pressure tubular reactors: A review and update. *Polymer*, **33** (11), 2243-2262.
- [82] Stickler, M., D. Panke, and A. E. Hamielec (1984). Polymerization of Methyl Methacrylate up to High Degrees of Conversion: Experimental Investigation of the Diffusion-Controlled Polymerization. *Journal of Polymer Science: Polymer Chemistry*, **22** (9), 2243-2253.
- [83] Wunderlich, W. and M. Stickler (1984). The Free Radical Polymerization of Some Methacrylates at Very High Degrees of Conversion. *Polymer Preprints*, **25** (2), 7-8.

APPENDIX A: THERMAL POLYMERIZATION OF BUTYL ACRYLATE

Thermal Homopolymerizations

The bulk thermal homopolymerization of certain monomers has been well documented. Both styrene (Sty) and methyl methacrylate (MMA) have been intensively studied and reaction mechanisms proposed. Ethylene is also known to thermally polymerize under high temperature, high pressure conditions in a continuous tubular reactor. [80, 81]

At elevated temperatures (100 – 230 centigrade) it is proposed that the thermal initiation of Sty undergoes a Diels-Alder reaction to produce a species with a free radical capable of sustaining polymerization [17, 18]. The proposed mechanism involves the combination of two monomers to create a 3-ringed complex which then reacts with another styrene monomer to produce two distinct species capable of creating primary radicals. Experiments done were conducted in a similar manner as to what is done in our group by using sealed glass ampoules for a batch reaction. Modeling for the polymerization included expressions for the thermal initiation of Sty, rate of polymerization, diffusion controlled kinetics as well as molecular weight determinations. The mechanism shows a third order dependency upon the monomer concentration and modeling under this assumption has been successful. The model was based upon tracking conversion with time (and hence monomer concentration and volume contraction) and molecular weight versus conversion. The model parameters were based upon a Bayesian criterion of minimizing the determinant of the difference in squares matrix. A Rosenbrock multivariable search routine was used.

Thermal polymerization of MMA is different. Past work has shown that MMA undergoes a very rapid thermal polymerization at elevated temperatures [4, 12], yet the structure of MMA is not conducive to such initiation rates. It has been proposed by several groups [13, 67, 70, 71, 82, 83] that there is in fact more than one reaction occurring that initiates the polymerization reaction. In the past, multiple methods of monomer purification have led to different rates of polymerization that coincides with the theory that within the MMA there is another molecule that is much more thermally susceptible to producing primary radicals[15, 16]. Such a species is very similar to MMA since many separation techniques (simple distillation being among them) are unable to separate the two. Work has been done

with MMA in an attempt to ascertain the true thermal polymerization potential of MMA without this extra molecule or “impurity”. Stickler’s group [71] has done modeling in an attempt to model the reaction without taking into account the “impurity”. Fennouillot’s group [13] takes the next step and separates the impurity from the thermal polymerization of MMA. The reaction for the pure MMA portion is thought to be 2nd order dependent upon monomer concentration with the mechanism involving the creation of a bi-molecular species capable of supporting two initiation sites. The impurity is treated like a standard mono-functional initiator. The work has been done in a dilatometric reactor working at temperatures up to 200 centigrade and pressures reaching 50 bar. This work is detailed and the modeling successful. The group used a set of differential equations to model the system and tracked conversion versus time as well as molecular weight. The differential equations were solved using a 4th order Runge-Kutta method coupled with a simplex method while minimizing a mean squared error function.

The thermal polymerization of butyl acrylate (BA) is another reaction of interest in industry. At elevated temperatures the thermal polymerization of BA is evident from work done in our group. Given the nature of BA it is also thought that some form of impurity is responsible for the high rates of reaction. Another feature of the homopolymerization of BA at elevated temperatures is gel formation which in turn leads to decreased levels of monomer conversion. The creation of gel leads to analysis issues since GPC cannot be used for molecular weight determination and a soxhlet extraction must be used to determine the gel content. Due to the differences in equipment, it will not be possible to run the exact same types of experiments done above in order to determine parameter values for such a model. However, since the reaction mechanism being proposed for BA is virtually identical to that of MMA, it may be possible that such elaborate experiments are unnecessary. In the case that a quantitative analysis of the reaction is not possible with our equipment, a qualitative study might be done in order to support the model/mechanisms being proposed. It may be possible to negate the effects of the impurity by using a radical scavenger like hydro-quinone (or 2,2'-diphenyl-1-picrylhydrazyl, 4-tert-butylcatechol) to consume the radicals produced by the impurity, hence delaying the reaction long enough that all impurity is consumed leaving only the BA to undergo its own pure thermal polymerization[16].

Other issues to be taken into consideration are reproducible industrial type polymerizations. It is unlikely that in industry such elaborate cleansing of the monomer is done as performed in the lab. Most monomers already come with a stabilizing agent to prevent spontaneous thermal polymerizations while in storage. Leaving these agents in the mix while running the reaction may produce a lowered rate of reaction and the concentration of this agent must be taken into account while running reactions. It is unknown if there is enough of this agent to consume all or only part of the impurity. More radical scavenger will need to be added to be sure of this. If adding more hydroquinone only delays the reaction and does not change the actual polymerization rate, then purification of the monomer will need to be done and varying levels of scavenger be added to determine the critical concentration.

An interesting application is the use of alpha-methyl styrene (AMS) in the mixture of either a MMA or BA thermal polymerization. AMS is thought to have the potential to undergo its own thermal initiation; however, due to the low ceiling temperature of the monomer, the production of poly(AMS) via thermal initiation would not be realized. However, using AMS with either MMA or BA might allow one to be able to determine if AMS does have this property. If one can separate the thermal initiation of an impurity from the pure MMA/BA thermal initiation, then why not separate the thermal initiation of AMS from the other two? The addition of AMS may also conceivably act as a chain transfer agent (CTA) for the BA and reduce the level of branching/gel formation to make the polymer more usable. It is also quite possible that AMS would be a less expensive agent than CTA itself and in small amounts it would not greatly affect the properties of the poly(BA).

Work has been done to investigate the effects of CTA on BA reactions. Preliminary runs have been completed using pure BA that has had the inhibitor removed at 80, 100, 120 and 140 centigrade (figure 29). The runs are done to what was thought would give the highest limiting conversion, however from the data it looks like the higher temperature runs could be extended further. The amount of gel formation however makes the determination of conversion values difficult which is why there is considerable scattering in the data. The gel

content has not been quantified from these samples. Qualitatively though, the amount of gel formed was considerable even at what appears to be the lower conversion samples.

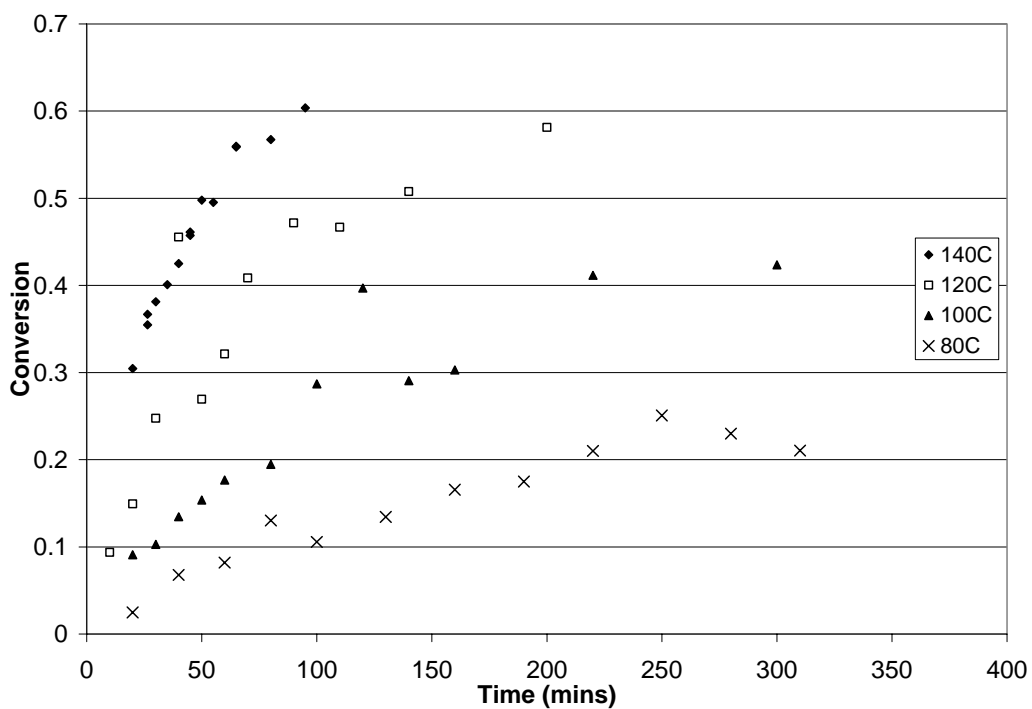


Figure 29: BA Thermal Homopolymerization (Conversion vs. Time)

Bulk reactions at 90 (figure 30) and 100 centigrade (figure 31) using purified BA have been performed independently from the reactions discussed above.

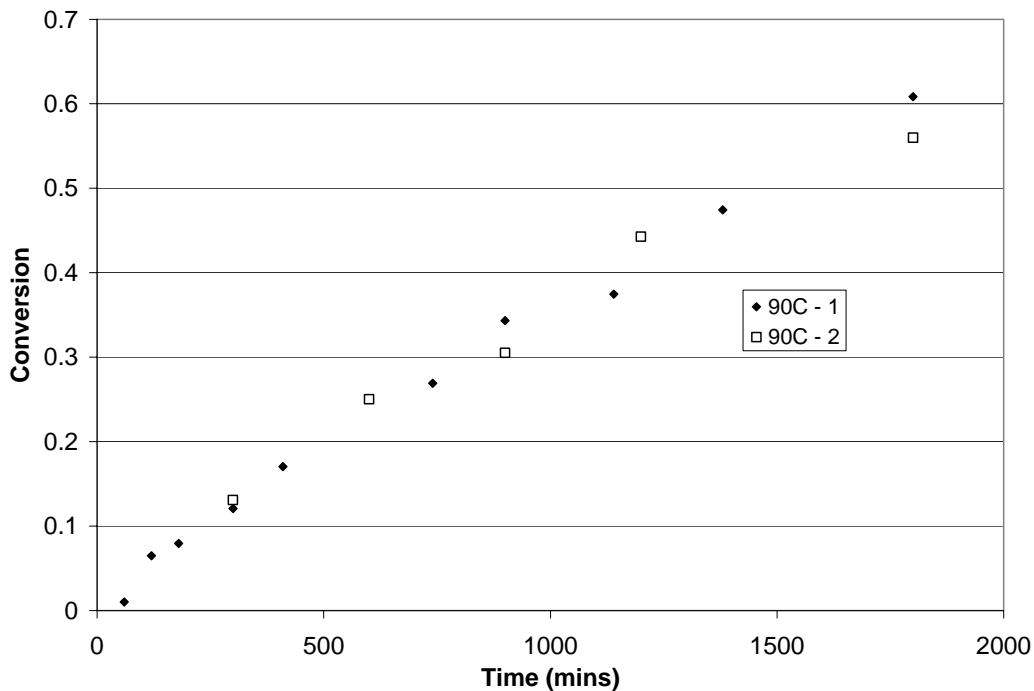


Figure 30: BA Homopolymerizations at 90C

From figure 30, it would appear that good agreement has been met from the two runs at 90C, however, if one is to observe figure 31, there is a discrepancy in the conversion levels for the runs done independently at 100C. If more work is to be pursued in this area, then the use of inhibitors will be necessary in order to determine if the discrepancy is from the experimental technique, or resulting from a varying level of “impurity” in the monomer stock.

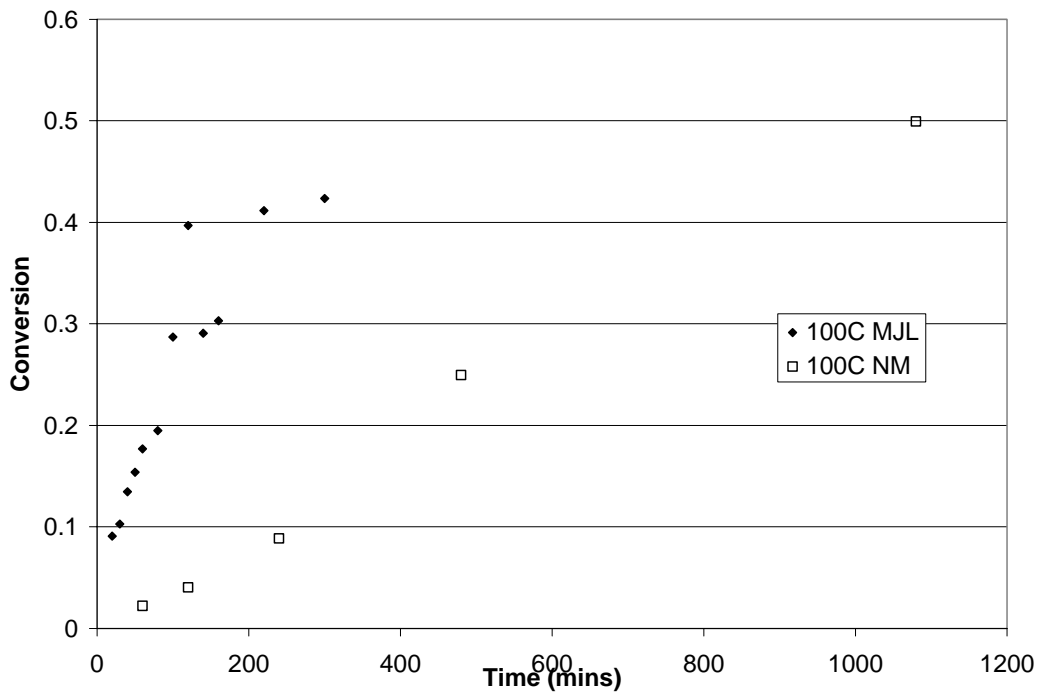


Figure 31: BA Thermal Homopolymerization Comparison at 100C

The other reactions run, shown in figure 32, are the following:

Bulk reaction at 140 centigrade using 0.05% CTA

Solution reaction (41% Xylene) at 140 centigrade using 0.01% DPPH (inhibitor)

Solution reaction (Xylene) at 140 centigrade using un-purified BA

Solution reaction (Xylene) at 140 centigrade using un-purified BA with CTA

APPENDIX B: TERPOLYMER MODEL DEVELOPMENT USING MAPLE

Taking the equations that were displayed in Chapter 8 for the terpolymer system, a mechanistic model was developed using Maple. Maple was used primarily as a tool for algebraic substitution and simplification and was not used to actually estimate the parameters for the terpolymer system. Taking the final differential and probability equations from Maple and using them in Matlab, the final parameter estimates were obtained.

Samples of the types of equations that were developed are shown below. The first equation relates to the base composition equation while the second relates to the determination of the probabilities.

```
> dAdt := -
kaa*A*Br*(kba*A^2*kca+kba*A*kcb*B+kba*A*kacrev*Pac+kba*A*kbcrev*Pcb+kbc*C*kca*A+kbc*C*kacrev*Pac+kabrev*Pba*kca*A+kabrev*Pba*kcb*B+kabrev*Pba*kacrev*Pac+kabrev*Pba*kbcrev*Pcb+kcbrev*Pbc*kca*A+kcbrev*Pbc*kacrev*Pac)/(kbarev*Pab*kca*A+kbarev*Pab*kcb*B+kbarev*Pab*kacrev*Pac+kbarev*Pab*kbcrev*Pcb+kbcrev*Pcb*kcarev*Pac+kbcrev*Pcb*kac*C+kab*B*kca*A+kab*B^2*kcb+kab*B*kacrev*Pac+kab*B*kbcrev*Pcb+kcb*B*kcarev*Pac+kcb*B*kac*C)-kba*A*Br-kca*A*Br*(kabrev*Pba*kca*A*kac*C+kabrev*Pba*kca*A*kcarev*Pac+kabrev*Pba*kacrev*Pac*kac*C+kabrev*Pba*kacrev*Pac^2*kcarev+kcbrev*Pbc*kca*A*kab*B+kcbrev*Pbc*kca*A*kac*C+kcbrev*Pbc*kca*A*kbarev*Pab+kcbrev*Pbc*kca*A*kcarev*Pac+kcbrev*Pbc*kacrev*Pac*kab*B+kcbrev*Pbc*kacrev*Pac*kac*C+kcbrev*Pbc*kacrev*Pac*kbarev*Pab+kcbrev*Pbc*kacrev*Pac^2*kcarev+kba*A^2*kca*kac*C+kba*A^2*kca*kcarev*Pac+kba*A*kacrev*Pac^2*kcarev+kbc*C*kca*A*kab*B+kbc*C^2*kca*A*kac+kbc*C*kca*A*kbarev*Pab+kbc*C*kca*A*kcarev*Pac+kbc*C*kacrev*Pac*kab*B+kbc*C^2*kacrev*Pac*kac+kbc*C*kacrev*Pac*kbarev*Pab+kbc*C*kacrev*Pac^2*kcarev)/((kbarev*Pab*kca*A+kbarev*Pab*kcb*B+kbarev*Pab*kacrev*Pac+kbarev*Pab*kbcrev*Pcb+kbcrev*Pcb*kcarev*Pac+kbcrev*Pcb*kac*C+kab*B*kca*A+kab*B^2*kcb+kab*B*kacrev*Pac+kcb*B*kcarev*Pac+kcb*B*kac*C)*(kacrev*Pca+kca*A))+kaarev*Paa*Br*(kba*A^2*kca+kba*A*kcb*B+kba*A*kacrev*Pac+kba*A*kbcrev*Pcb+kbc*C*kca*A+kbc*C*kacrev*Pac+kabrev*Pba*kca*A+kabrev*Pba*kcb*B+kabrev*Pba*kacrev*Pac+kabrev*Pba*kbcrev*Pcb+kcbrev*Pbc*kca*A+kcbrev*Pbc*kacrev*Pac)/(kbarev*Pab*kca*A+kbarev*Pab*kcb*B+kbarev*Pab*kacrev*Pac+kbarev*Pab*kbcrev*Pcb+kbcrev*Pcb*kcarev*Pac+kbcrev*Pcb*kac*C+kab*B*kca*A+kab*B^2*kcb+kab*B*kacrev*Pac+kab*B*kbcrev*Pcb+kcb*B*kcarev*Pac+kcb*B*kac*C)+kbarev*Pab*Br*(kba*A^2*kca+kba*A*kcb*B+kba*A*kacrev*Pac+kba*A*kbcrev*Pcb+kbc*C*kca*A+kbc*C*kacrev*Pac+kabrev*Pba*kca*A+kabrev*Pba*kcb*B+kabrev*Pba*kacrev*Pac+kabrev*Pba*kbcrev*Pcb+kcbrev*Pbc*kca*A+kcbrev*Pbc*kacrev*Pac)/(kbarev*Pab*kca*A+kbarev*Pab*kcb*B+kbarev*Pab*kbcrev*Pcb+kbcrev*Pcb*kcarev*Pac+kbcrev*Pcb*kacrev*Pac+kab*B*kca*A+kab*B^2*kcb+kab*B*kacrev*Pac+kab*B*kbcrev*Pcb+kcb*B*kcarev*Pac+kcb*B*kac*C)+kcarev*Pac*Br*(kba*A^2*kca+kba*A*kcb*B+kba*A*kacrev*Pac+kba*A*kbcrev*Pcb+kbc*C*kca*A+kbc*C*kacrev*Pac+kabrev*Pba*kca*A+kabrev*Pba*kcb*B+kabrev*Pba*kacrev*Pac+kabrev*Pba*kbcrev*Pcb+kcbrev*Pbc*kca*A+kcbrev*Pbc*kacrev*Pac)/(kbarev*Pab*kca*A+kbarev*Pab*kcb*B+kbarev*Pab*kbcrev*Pcb+kbcrev*Pcb*kcarev*Pac+kbcrev*Pcb*kacrev*Pac+kab*B*kca*A+kab*B^2*kcb+kab*B*kacrev*Pac+kab*B*kbcrev*Pcb+kcb*B*kcarev*Pac+kcb*B*kac*C)
```

> 0 = Br*kbc*(-Pca*C^2*RD*Pac*RB*Pab*rba*rac*rcb*rca-
 Pca*RA*rb*c*Pba*A*RC*rab*Pac*r\cb*C*rca-
 Pca*RF*Pbc*RD*Pac*B*rba*rac*rcb*C*rca-
 Pca*RF*Pbc*A*RC*rab*Pac*rba*rcb*C*rca-
 Pca*RA*rb*c*Pba*RD*Pac*rab*C^2*rcb*rca-
 Pca*RA*rb*c*Pba*RD*Pac^2*RC*rab*rcb*C*rca-rcb*Pcb*C^2*rca*rb*c*A^2*rab-
 rcb*Pcb*C*rca*rb*c*A^2*RC*rab*Pac-rcb*Pcb*C^2*rca*rb*c*A*RD*Pac*rab-
 rcb*Pcb*C*rca*rb*c*A*RD*Pac^2*RC*rab-rcb*Pcb*C^2*rca*A*B*rba*ra\c-
 rcb*Pcb*C^3*rca*A*rab*rba-rcb*Pcb*C^2*rca*A*RB*Pab*rba*rac-
 rcb*Pcb*C^2*rca*A*R\
 C*rab*Pac*rba-rcb*Pcb*C^2*rca*RD*Pac*B*rba*rac-
 rcb*Pcb*C^3*rca*RD*Pac*rab*rba-rc*b*Pcb*C^2*rca*RD*Pac*RB*Pab*rba*rac-
 rcb*Pcb*C^2*rca*RD*Pac^2*RC*rab*rba+rcb*Pcc*\A^2*RA*rb*c*Pba*rab*C+rcb*Pcc*A
 *RA*rb*c*Pba*RD*Pac*rab*C+rcb*Pcc*A^2*RF*Pbc*rab*C*rba+rcb*Pcc*A*RF*Pbc*RD*
 Pac*rab*C*rba+rcb*Pcc*A^3*rb*c*rab*C+rcb*Pcc*A^2*rb*c*RD*P\ac*rab*C+rcb*Pcc*A
 ^2*C*B*rba*rac+rcb*Pcc*A^2*C^2*rab*rba+rcb*Pcc*A^2*C*RB*Pab*rb*a*rac+rcb*Pc
 c*A*C*RD*Pac*B*rba*rac+rcb*Pcc*A*C^2*RD*Pac*rab*rba+rcb*Pcc*A*C*RD*P\ac*RB*
 Pab*rba*rac+Pcc*B*rca*RA*rb*c*Pba*A*rab*C+Pcc*B*rca*RA*rb*c*Pba*RD*Pac*rab*C\
 +Pcc*B*rca*RA*rb*c*Pba*RD*Pac^2*RC*rab+Pcc*B^2*rca*RF*Pbc*RD*Pac*rba*rac+Pcc
 *B*rc*a*RF*Pbc*RD*Pac*rab*C*rba+Pcc*B*rca*RF*Pbc*RD*Pac*RB*Pab*rba*rac+Pcc*
 B*rca*RF*Pb\c*RD*Pac^2*RC*rab*rba+Pcc*B*rca*rb*c*A^2*rab*C+Pcc*B*rca*rb*c*A*R
 D*Pac*rab*C+Pcc*B*rca*rb*c*A*RD*Pac^2*RC*rab+Pcc*B^2*rca*C*A*rba*rac+Pcc*B*
 rca*C^2*A*rab*rba+Pcc*B*rca*C*A*RB*Pab*rba*rac+Pcc*B*rca*C*A*RC*rab*Pac*rb
 a+Pcc*B^2*rca*C*RD*Pac*rba*ra\c+Pcc*B*rca*C^2*RD*Pac*rab*rba+Pcc*B*rca*C*RD
 *Pac*RB*Pab*rba*rac+Pcc*B*rca*C*RD*\Pac^2*RC*rab*rba+RCC*rcb*Pcc*Pcb*RA*rb*c
 *Pba*A*rab*C+RCC*rcb*Pcc*Pcb*RA*rb*c*Pba*A*RC*rab*Pac+RCC*rcb*Pcc*Pcb*RA*rb
 c*Pba*RD*Pac*rab*C+RCC*rcb*Pcc*Pcb*RA*rb*c*Pba*R\D*Pac^2*RC*rab+RCC*rcb*Pcc*
 Pcb*RF*Pbc*A*B*rba*rac+RCC*rcb*Pcc*Pcb*RF*Pbc*A*rab*C*rba+RCC*rcb*Pcc*Pcb*
 RF*Pbc*A*RB*Pab*rba*rac+RCC*rcb*Pcc*Pcb*RF*Pbc*A*RC*rab**rba+RCC*rcb*Pc
 c*Pcb*RF*Pbc*RD*Pac*B*rba*rac+RCC*rcb*Pcc*Pcb*RF*Pbc*RD*Pac*rab*C*rba+RCC*
 rcb*Pcc*Pcb*RF*Pbc*RD*Pac*RB*Pab*rba*rac+RCC*rcb*Pcc*Pcb*RF*Pbc*RD*Pac^\2*R
 C*rab*rba+RCC*rcb*Pcc*Pcb*rb*c*A^2*rab*C+RCC*rcb*Pcc*Pcb*rb*c*A^2*RC*rab*Pac+
 RC\C*rcb*Pcc*Pcb*rb*c*A*RD*Pac*rab*C+RCC*rcb*Pcc*Pca*RF*Pbc*RD*Pac*rab*C*rba
 +RCC*rcb**Pcc*Pca*RF*Pbc*RD*Pac*RB*Pab*rba*rac+RCC*rcb*Pcc*Pca*RF*Pbc*RD*Pa
 c^2*RC*rab*rba\+RCC*rcb*Pcc*Pca*rb*c*A^2*rab*C+RCC*rcb*Pcc*Pca*rb*c*A^2*RC*ra
 b*Pac+RCC*rcb*Pcc*Pc*a*rb*c*A*RD*Pac*rab*C+RCC*rcb*Pcc*Pca*rb*c*A*RD*Pac^2*RC
 *rab+RCC*rcb*Pcc*Pca*C*A*B*rba*rac+RCC*rcb*Pcc*Pca*C^2*A*rab*rba+RCC*rcb*P
 cc*Pca*C*A*RB*Pab*rba*rac+RCC*rc*b*Pcc*Pca*C*A*RC*rab*Pac*rba+RCC*rcb*Pcc*P
 ca*C*RD*Pac*B*rba*rac+RCC*rcb*Pcc*Pca*\C^2*RD*Pac*rab*rba+RCC*rcb*Pcc*Pca*C
 *RD*Pac*RB*Pab*rba*rac+RCC*rcb*Pcc*Pca*C*RD\
 Pac^2*RC*rab*rba-Pca*RF*Pbc*RD*Pac*rab*C^2*rba*rcb*rca-
 Pca*RF*Pbc*RD*Pac*RB*Pab**rba*rac*rcb*C*rca-Pca*rb*c*A^2*rab*C^2*rcb*rca-
 Pca*RF*Pbc*RD*Pac^2*RC*rab*rba*rcb*C*rca-Pca*rb*c*A^2*RC*rab*Pac*rcb*C*rca-
 Pca*rb*c*A*RD*Pac*rab*C^2*rcb*rca-Pca*rb*c*A*RD*Pac^2*RC*rab*rcb*C*rca-
 Pca*RF*Pbc*A*RB*Pab*rba*rac*rcb*C*rca-Pca*C^2*A*B*r*ba*rac*rcb*rca-
 Pca*C^3*A*rab*rba*rcb*rca-Pca*C^2*A*RB*Pab*rba*rac*rcb*rca-Pca*C^\2
 *A*RC*rab*Pac*rba*rcb*rca-Pca*C^2*RD*Pac*B*rba*rac*rcb*rca-
 Pca*C^3*RD*Pac*rab*r*ba*rcb*rca+RCC*rcb*Pcc*Pcb*rb*c*A*RD*Pac^2*RC*rab+RCC*r
 cb*Pcc*Pcb*C*A*B*rba*rac+R\CC*rcb*Pcc*Pcb*C^2*A*rab*rba+RCC*rcb*Pcc*Pcb*C*A
 *RB*Pab*rba*rac+RCC*rcb*Pcc*Pcb*\C*A*RC*rab*Pac*rba+RCC*rcb*Pcc*Pcb*C*RD*Pa
 c*B*rba*rac+RCC*rcb*Pcc*Pcb*C^2*RD*Pac*rab*rba+RCC*rcb*Pcc*Pcb*C*RD*Pac*RB
 *Pab*rba*rac+RCC*rcb*Pcc*Pcb*C*RD*Pac^2*RC*r*ab*rba-
 RC*rab*Pcc*Pac*rb*c*A^2*rcb*RD*Pca-RC*rab*Pcc*Pac*rb*c*A*B*rca*RD*Pca-RC*ra\
 b*Pcc*Pac^2*rb*c*A*RD^2*rcb*Pca-RC*rab*Pcc*Pac*rb*c*A*RE*Pcb*rca*RD*Pca-
 RC*rab*Pcc**Pac*rb*c*A^2*RE*Pcb*rca-RC*rab*Pcc*Pac*C*rcb*A*rba*RD*Pca-
 RC*rab*Pcc*Pac^2*C*RD^\2*rcb*rba*Pca-
 RC*rab*Pcc*Pac*RA*rb*c*Pba*rcb*A*RD*Pca-

```

RC*rab*Pcc*Pac*RA*rbc*Pba*B\*rca*RD*Pca-
RC*rab*Pcc*Pac^2*RA*rbc*Pba*RD^2*rbc*Pca-RC*rab*Pcc*Pac*RA*rbc*Pba*R\
E*Pcb*rca*RD*Pca-RC*rab*Pcc*Pac*RA*rbc*Pba*RE*Pcb*rca*A-
RC*rab*Pcc*Pac*RF*Pbc*rc\b*A*rba*RD*Pca-
RC*rab*Pcc*Pac^2*RF*Pbc*RD^2*rbc*rba*Pca-RF*Pcc*Pbc*rba*RB*Pab*rc\
b*A*rac*RD*Pca-RF*Pcc*Pbc*rba*RB*Pab*B*rca*rac*RD*Pca-
RF*Pcc*Pbc*rba*RB*Pab*RD^2\*rbc*Pac*rac*Pca-
Pca*RA*rbc*Pba*A*rab*C^2*rbc*rca-
Pca*C^2*RD*Pac^2*RC*rab*rba*rc\b*rca+RCC*rbc*Pcc*Pca*RA*rbc*Pba*A*rab*C+RCC
*rbc*Pcc*Pca*RA*rbc*Pba*A*RC*rab*Pac\+RCC*rbc*Pcc*Pca*RA*rbc*Pba*RD*Pac*rab
*C+RCC*rbc*Pcc*Pca*RA*rbc*Pba*RD*Pac^2*RC*\rab+RCC*rbc*Pcc*Pca*RF*Pbc*A*B*r
ba*rac+RCC*rbc*Pcc*Pca*RF*Pbc*A*rab*C*rba+RCC*rc\b*Pcc*Pca*RF*Pbc*A*RB*Pab*
rba*rac+RCC*rbc*Pcc*Pca*RF*Pbc*A*RC*rab*Pac*rba+RCC*rc\b*Pcc*Pca*RF*Pbc*RD*
Pac*B*rba*rac-rbc*Pcb*C^2*rca*RA*rbc*Pba*A*rab-
rbc*Pcb*C*rca\*RA*rbc*Pba*A*RC*rab*Pac-
rbc*Pcb*C^2*rca*RA*rbc*Pba*RD*Pac*rab-rbc*Pcb*C*rca*RA*\
rbc*Pba*RD*Pac^2*RC*rab-rbc*Pcb*C*rca*RF*Pbc*A*B*rba*rac-
rbc*Pcb*C^2*rca*RF*Pbc*\A*rab*rba-rbc*Pcb*C*rca*RF*Pbc*A*RB*Pab*rba*rac-
rbc*Pcb*C*rca*RF*Pbc*A*RC*rab*Pa\c*rba-
rbc*Pcb*C*rca*RF*Pbc*RD*Pac*B*rba*rac-
rbc*Pcb*C^2*rca*RF*Pbc*RD*Pac*rab*rb\ a-
rbc*Pcb*C*rca*RF*Pbc*RD*Pac*RB*Pab*rba*rac-
rbc*Pcb*C*rca*RF*Pbc*RD*Pac^2*RC*ra\
b*rba-Pca*RF*Pbc*A*B*rba*rac*rbc*C*rca-
RF*Pcc*Pbc*rba*RB*Pab*RE*Pcb*rca*rac*RD*P\
ca-RF*Pcc*Pbc*rba*RB*Pab*RE*Pcb*rca*rac*A-
RF*Pcc*Pbc*rba*RE*Pcb*RC*rab*Pac*rca*R\D*Pca-
RF*Pcc*Pbc*rba*RE*Pcb*RC*rab*Pac*rca*A-RF*Pcc*Pbc*rba*RE*Pcb*rab*C*rca*RD*\
Pca-RF*Pcc*Pbc*rba*RE*Pcb*rab*C*rca*A-RF*Pcc*Pbc*rba*B*rbc*A*rac*RD*Pca-
RF*Pcc*Pbc*rba*B^2*rca*rac*RD*Pca-RF*Pcc*Pbc*rba*B*RD^2*rbc*Pac*rac*Pca-
RF*Pcc*Pbc*rba*B\*RE*Pcb*rca*rac*RD*Pca-RF*Pcc*Pbc*rba*B*RE*Pcb*rca*rac*A-
RF*Pcc*Pbc*rba*B*RC*rab\*Pac*rca*RD*Pca-RF*Pcc*Pbc*rba*B*rab*C*rca*RD*Pca-
Pca*RF*Pbc*A*rab*C^2*rba*rbc*r\
ca)/(rba*(RB*Pab*rbc*A*rac+RB*Pab*B*rca*rac+RB*Pab*RD*rbc*Pac*rac+RB*Pab*RE
*Pcb*\rca*rac+RE*Pcb*RC*rab*Pac*rca+RE*Pcb*rab*C*rca+B*rbc*A*rac+B^2*rca*ra
c+B*RD*rbc*\Pac*rac+B*RE*Pcb*rca*rac+B*RC*rab*Pac*rca+B*rab*C*rca)*(RD*Pca+
A))

```

The model development work done in Maple (which outlines the final sets of equations) as well as the Matlab routine used for estimating the parameters can be obtained by contacting Professor Alex Penlidis at the following address:

Prof. A. Penlidis (penlidis@cape.uwaterloo.ca)

Department of Chemical Engineering
University of Waterloo
Waterloo, Ontario, CANADA
N2L 3G1

APPENDIX C: COPOLYMER REFRACTIVE INDEX

The Refractive Index Increment (dn/dc) using GPC for the Alpha-Methyl Styrene/Methyl Methacrylate Copolymer at 670nm in Tetrahydrofuran

The dn/dc values for the copolymer system Alpha-Methyl Styrene (AMS)/Methyl Methacrylate (MMA) have been determined for varying composition using GPC at 670nm in THF. A linear model with dependence on the square of the mole fraction of AMS in the copolymer is successful in modelling dn/dc values over this composition range.

While much work has been published about the dn/dc values for homopolymers, including alpha-methyl styrene (AMS) and methyl methacrylate (MMA) [54, 56] there has been little in the way of published work to determine the dn/dc values for copolymers. It is generally accepted that the dn/dc value for a homopolymer is almost entirely dependent upon the monomer and weakly dependent on (or independent of) molecular weight [54].

Copolymers however may be very different. Since molecular weight and composition can be closely linked (especially for systems with depropagating monomers like AMS and to a lesser extent MMA), some correlation may be present. Another factor that is going to affect molecular weight, besides the reaction conditions, is the feed fraction of monomers. Will this have an effect on the dn/dc values obtained?

From the Polymer Handbook there is a historical recording of dn/dc values primarily at wavelengths below 633nm with new data appearing for 633nm He-Ne Lasers but with none at the wavelength that current equipment uses: 670nm. Another incentive to embark on this work is to show whether the assumption of a *linear* relationship between dn/dc and copolymer composition is valid [5, 11, 20, 28, 54] and whether the relationship works better for the mole or weight fraction composition.

To determine the dn/dc of the copolymers and of the two homopolymers, a GPC setup including a Waters solvent/sample delivery system with an in-line degasser (model AF), 515 HPLC pump and 717plus autosampler was used. The detectors on the system are from Viscotek, contained in the TDA 302 quad detector package that incorporates RALS/LALS

(670nm), DRI, viscometer and UV (model 2501) detectors. The analysis software included with the detectors is the OmniSEC v2.0.

The samples analyzed in this study had been produced by free radical polymerizations at temperatures ranging from 100°C to 140°C. Consequently, the AMS content in the copolymer reached a maximum of approximately 20%. To produce polymer with a higher AMS content we would have to greatly sacrifice both yield and molecular weight, making the polymer undesirable for practical applications.

For determination of dn/dc it is possible to use this equipment along with the following expression based on the DRI response:

$$RI_i = \frac{RI_{cal} \cdot C_i}{n_o} \cdot \frac{dn}{dc} \quad (75)$$

RI_{cal} is the calibration constant for the RI detector, established by analyzing samples of known dn/dc and known concentrations. RI_i is the measured response from the detector, C_i is the sample concentration and n_o is the refractive index of the solvent. Since we already have the RI_{cal} , and we know C_i and n_o , then the dn/dc can be calculated for the sample. Alternatively, the dn/dc can be calculated by plotting the RI_{area} (integrated from the RI signal) vs. C_i . The slope of this line, since RI_{area} is assumed directly proportional to the refractive index of the sample in solution, will be dn/dc . For the work discussed here, this second technique has been used.

In our study the objective was to assess the validity of this method using samples of polymer with realistic compositions of MMA and AMS. For each sample that has a given copolymer composition, a variety of concentrations must be made. Each solution, at different polymer concentration, while having the same copolymer composition, is sent through the detectors mentioned above where a full analysis is done. For example, from Table 1, sample 2-1 had 5 subsequent solutions made at varying concentrations of the same polymer. When

using the OmniSEC software for dn/dc analysis (using the second method mentioned above), the integration of the DRI signal should be done very precisely since this is the primary source of data for the dn/dc calculation.

Previously published data for the homopolymers [54, 56] indicated that at 633nm the dn/dc for poly(MMA) is 0.083 mL/g while that for poly(AMS) is 0.2056 mL/g. The values of Table 11 were obtained for the homopolymers and copolymers.

Table 11: dn/dc Values for AMS/MMA Copolymers

Sample	Mole fraction AMS	Mw (g/mol)	PDI	dn/dc (mL/g)
2-1	0.204	131063	1.47	0.1045
2-2	0.206	121724	1.50	0.1080
3-1	0.105	95849	1.40	0.0916
3-2	0.096	96677	1.42	0.0910
4-1	0.153	389582	1.49	0.0985
4-2	0.114	348629	1.57	0.0932
5-1	0.147	388780	1.76	0.0970
6-1	0.042	254556	2.13	0.0872
6-2	0.041	255612	1.54	0.0900
AMS _{STD}	1.000	72000	~1	0.1924
MMA _{STD}	0.000	100000	~1	0.0843

Mw = weight-average molecular weight

Mole fraction AMS = copolymer composition

From Table 11, the dn/dc values for the two homopolymers are not significantly different from the published values (6.4% difference for AMS and 1.5% difference for MMA).

Since the data available reach up to 20% AMS content, models using the data will only be applicable for this composition range. Initial investigations of the data show a linear trend between dn/dc and the square of the mole fraction of AMS in the copolymer (MFAMS). Modelling efforts have included many different models that take into account both MFAMS and the molecular weight of the polymer. Most exhibited curvature in the model predictions, some with a quadratic and others with a cubic dependence. Included in these modelling efforts is the simple weighted average model, where the dn/dc is predicted by the mole

fraction of the monomers in the copolymer and the dn/dc 's of the two homopolymers. This weighted average model was not successful either. Once a model that appeared linear was obtained using MFAMS and the molecular weight, it turned out that the parameter for the molecular weight term was potentially zero. This indicates that the dependence of dn/dc on molecular weight (at least for the range that was used here) is insignificant.

The best fit that was obtained is shown in the simple $y = mx^2 + b$ model (equation 2) obtained from linear regression:

$$\frac{dn}{dc} = C_1(MFAMS^2) + C_2 \quad (76)$$

where: $C_1 = 0.449 \pm 0.396$

$$C_2 = 0.087 \pm 0.061$$

The R^2 value for this regression is 0.973. Residual analysis does not show any significant patterns, however the error is not centered about zero. This is mainly imparted by two data points at higher MFAMS values indicating that at higher MFAMS there is the potential for curvature and that equation 2 may not be as useful for AMS compositions much above 20%.

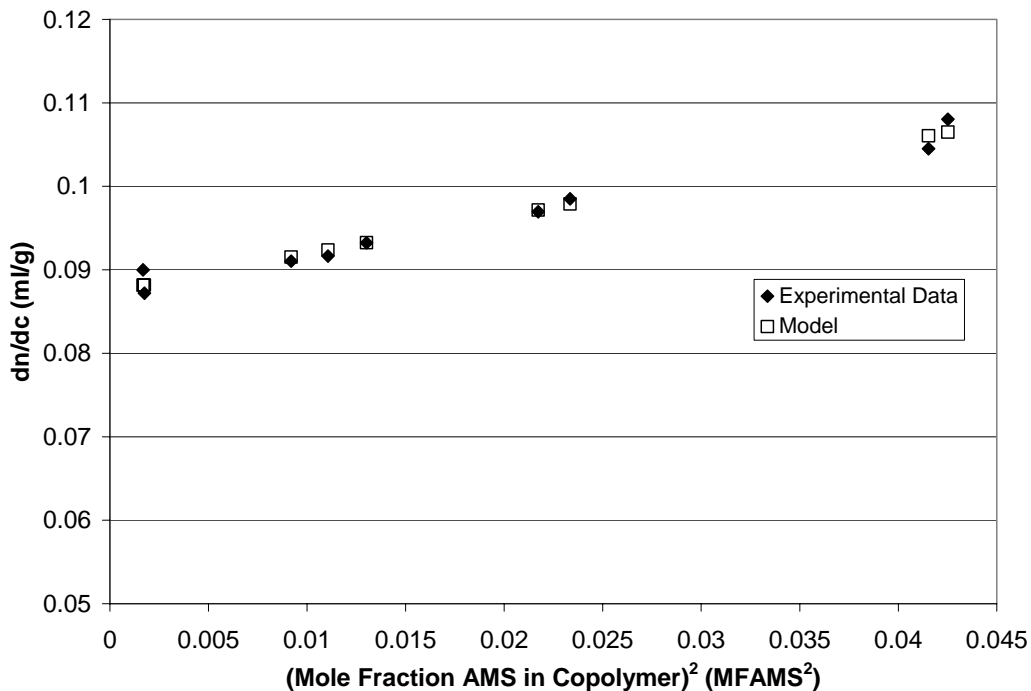


Figure 33: dn/dc Model vs. Experimental Data

Figure 33 shows the experimental data plotted against the model. There is good agreement and like all the other models attempted, the dependence on MFAMS is significant. From this analysis it would appear that dn/dc is almost entirely independent of molecular weight for the range in consideration and dependent alone on the mole fraction of AMS in the copolymer.

Our study has included only one copolymer system, a system that we are currently working with for other research purposes. The MMA/AMS system is well behaved in that there are no issues with dissolving the polymer in THF (i.e. no gel-portion). The main advantage of this type of analysis is that it is expedient and simple. However, from the parameter uncertainty, it is recommended that more data for the system be analysed. In order to be certain that this GPC technique is in fact accurate and reliable more copolymer systems using wider ranges of composition with more data points will need to be studied.

APPENDIX D: FULL CONVERSION MMA/AMS DATA

Table 12: Full Conversion MMA/AMS Data for 100, 115 and 140°C

Sample	Time (min)	Conversion	Mn (Daltons)	Mw (Daltons)	mol% AMS
100-1	30	0.24%	262498	404700	0.174
100-2	30	0.23%	288552	424748	0.150
100-3	60	0.55%	159171	405710	0.154
100-4	90	0.90%	119274	376230	0.143
100-5	90	0.90%	248161	369290	0.140
100-6	120	1.22%	165580	344567	0.147
100-7	180	1.92%	261222	348301	0.144
100-8	240	2.74%	248734	396511	0.155
100-9	240	2.80%	260971	389582	0.153
100-10	360	4.27%	220686	388780	0.147
115-1	20	0.51%	189956	310303	0.1119
115-2	20	0.47%	214882	316504	0.1194
115-3	60	1.21%	196690	326322	0.1093
115-4	90	3.01%	193733	327698	0.1027
115-5	90	3.05%	220963	329049	0.0996
115-6	120	4.36%	192220	314596	0.1080
115-7	180	4.72%	191663	328196	0.1133
115-8	180	6.80%	205878	331066	0.1080
115-9	240	9.16%	216438	339075	0.1049
115-10	360	14.17%	240500	348629	0.1141
115-11	360	14.04%	232138	348546	0.1009
140-1	15	2.23%	112397	229551	0.0435
140-2	30	5.04%	142417	260751	0.0393
140-3	30	5.13%	197694	279971	0.0448
140-4	45	7.89%	192933	273840	0.0414
140-5	60	10.19%	168159	261531	0.0320
140-6	90	15.05%	147321	240846	0.0453
140-7	90	15.11%	176697	260175	0.0414
140-8	120	19.71%	119725	254556	0.0418
140-9	150	23.93%	166034	255612	0.0410

APPENDIX E: BENCHMARKING RESULTS

Data from Hocking [76]
Styrene/MMA/AN system

Table 13: Hocking Parameter Estimates

Parameter (A=Styrene, B=MMA, C= AN)	Parameter Values
r_{AB}	0.5
r_{AC}	0.41
r_{BA}	0.5
r_{BC}	1.2
r_{CA}	0.04
r_{CB}	0.15
R_A	0
R_B	0
R_C	0
R_D	0
R_E	0
R_F	0
R_{AA}	0
R_{BB}	0
R_{CC}	0

Table 14: Hocking NMR Results/Kruger Results

Component	[M] mol/L	F(Alfrey-Goldfinger)	F(Exp. Kruger)
Styrene	3.641896	0.4519	0.4464
MMA	3.653048	0.3134	0.3182
AN	2.843964	0.2347	0.2355

Data from Braun and Cei [77]

Styrene/MMA/DEM system

DEM \equiv Diethyl Maleate

Table 15: Braun and Cei Parameter Estimates

Parameter (A=DEM,B =MMA, C= Styrene)	Parameter Values
r_{AB}	370
r_{AC}	6.59
r_{BA}	0.46
r_{BC}	0.52
r_{CA}	0
r_{CB}	0
R_A	0

R _B	0
R _C	0
R _D	0
R _E	0
R _F	0
R _{AA}	0
R _{BB}	0
R _{CC}	0

Table 16: Braun and Cei NMR Results/Kruger Results

Component	[M] mol/L	NMR results	F(Alfrey-Goldfinger)	F(Exp. Kruger)
Styrene	8.090848	0.849	0.91484	0.8212
Styrene	4.521953	0.721	0.82639	0.70873
Styrene	5.47501	0.631	0.7367	0.63822
Styrene	3.376256	0.512	0.50099	0.50052
Styrene	2.190004	0.495	0.47525	0.48121
Styrene	4.562508	0.517	0.50565	0.50673
Styrene	2.362366	0.36	0.24433	0.37003
Styrene	1.034169	0.245	0.11332	0.26547
Styrene	0.953057	0.174	0.035434	0.1753
MMA	1.003752	0.103	0.079113	0.16611
MMA	0.983474	0.198	0.13172	0.22099
MMA	2.331949	0.339	0.24725	0.33973
MMA	3.366117	0.414	0.47374	0.47419
MMA	2.281254	0.431	0.46745	0.46214
MMA	4.592925	0.433	0.48866	0.4876
MMA	5.444593	0.594	0.74337	0.61971
MMA	4.562508	0.731	0.86408	0.71581
MMA	8.242932	0.788	0.9626	0.82301
DEM	1.034169	0.048	0.006042	0.012687
DEM	4.633481	0.081	0.04189	0.07028
DEM	2.331949	0.03	0.016046	0.022048
DEM	3.396534	0.074	0.025271	0.025295
DEM	5.667649	0.074	0.057301	0.056651
DEM	0.983474	0.05	0.005685	0.005673
DEM	2.32181	0.046	0.012301	0.010255
DEM	4.542231	0.024	0.022596	0.018719
DEM	0.942918	0.038	0.001969	0.001683

Data from Valvassori and Sartori [78]
 AN/Methyl Acrylate (MA)/2-vinyl pyridine (2VP)

Table 17: Valvassori and Sartori Parameter Estimates

Parameter (A=AN,B=MA, C= 2VP)	Original Parameter Values	Exp. Kruger Updated Parameters
r_{AB}	0.51	0.50877
r_{AC}	0.087	0.14632
r_{BA}	0.51	0.50787
r_{BC}	0.26	0.26348
r_{CA}	2.13	2.1284
r_{CB}	2.38	2.3803
R_A	0	0
R_B	0	0
R_C	0	0
R_D	0	0
R_E	0	0
R_F	0	0
R_{AA}	0	0
R_{BB}	0	0
R_{CC}	0	0

Table 18: Valvasorri and Sartori NMR Results/Kruger Results

Component	[M] mol/L	NMR results	F(Alfrey- Goldfinger)	F(Exp. Kruger)
AN	13.2047	0.711	0.72413	0.72413
AN	11.43038	0.583	0.58405	0.58405
AN	9.746544	0.475	0.48651	0.48651
AN	6.834412	0.484	0.36753	0.35567
MA	0.733594	0.089	0.063716	0.063716
MA	1.428797	0.11	0.098866	0.098866
MA	2.088545	0.107	0.12512	0.12512
MA	4.100647	0.129	0.22063	0.21351
2VP	0.733594	0.2	0.21215	0.21215
2VP	1.428797	0.307	0.31709	0.31709
2VP	2.088545	0.418	0.38837	0.38837
2VP	2.733765	0.387	0.41184	0.43081

Data from Koenig [79]
Styrene/MMA/AN system

Table 19: Koenig Parameter Estimates

Parameter (A=Styrene, B=MMA, C= AN)	Original Parameter Values	Exp. Kruger Updated Parameters
r_{AB}	0.5	0.58249
r_{AC}	0.41	0.23293
r_{BA}	0.5	0.51043
r_{BC}	1.2	1.1817
r_{CA}	0.04	0.057212
r_{CB}	0.15	0.17448
R_A	0	0
R_B	0	0
R_C	0	0
R_D	0	0
R_E	0	0
R_F	0	0
R_{AA}	0	0
R_{BB}	0	0
R_{CC}	0	0

Table 20: Koenig NMR Results/Kruger Results

Component	[M] mol/L	NMR results	F(Alfrey- Goldfinger)	F(Exp. Kruger)
Styrene	3.639868	0.447	0.44033	0.43343
Styrene	5.393899	0.526	0.52836	0.52369
Styrene	2.869311	0.384	0.39068	0.40921
Styrene	2.818616	0.364	0.38436	0.36532
MMA	3.650007	0.261	0.27259	0.26832
MMA	2.686811	0.202	0.20401	0.2022
MMA	2.859172	0.23	0.2027	0.21231
MMA	5.272232	0.406	0.43784	0.41616
AN	2.849033	0.292	0.28707	0.29824
AN	2.058198	0.272	0.26764	0.27411
AN	4.410425	0.386	0.40662	0.37847
AN	2.048059	0.23	0.1778	0.21852

APPENDIX F: TERPOLYMER PROBABILITY VALUES

Table 21: Terpolymer Probability Values: A=BA, B = AMS, C = MMA

Paa	Pab	Pac	Pba	Pbb	Pbc	Pca	Pcb	Pcc
0.056967	0.016808	0.92623	0.81689	0.007022	0.17609	0.090455	0.077229	0.83232
0.056967	0.016808	0.92623	0.81689	0.007022	0.17609	0.090455	0.077229	0.83232
0.056967	0.016808	0.92623	0.81689	0.007022	0.17609	0.090455	0.077229	0.83232
0.0537	0.023804	0.9225	0.77089	0.009257	0.21985	0.087541	0.097447	0.81501
0.0537	0.023804	0.9225	0.77089	0.009257	0.21985	0.087541	0.097447	0.81501
0.0537	0.023804	0.9225	0.77089	0.009257	0.21985	0.087541	0.097447	0.81501
0.051364	0.034167	0.91447	0.74801	0.010451	0.24154	0.084848	0.10756	0.80759
0.051364	0.034167	0.91447	0.74801	0.010451	0.24154	0.084848	0.10756	0.80759
0.051364	0.034167	0.91447	0.74801	0.010451	0.24154	0.084848	0.10756	0.80759
0.068747	0.022385	0.90887	0.74257	0.011021	0.24641	0.11407	0.11497	0.77096
0.068747	0.022385	0.90887	0.74257	0.011021	0.24641	0.11407	0.11497	0.77096
0.068747	0.022385	0.90887	0.74257	0.011021	0.24641	0.11407	0.11497	0.77096
0.089271	0.012134	0.8986	0.78265	0.008971	0.20838	0.14356	0.09911	0.75734
0.089271	0.012134	0.8986	0.78265	0.008971	0.20838	0.14356	0.09911	0.75734
0.089271	0.012134	0.8986	0.78265	0.008971	0.20838	0.14356	0.09911	0.75734
0.11135	0.014915	0.87374	0.82543	0.006861	0.16771	0.17362	0.080639	0.74574
0.11135	0.014915	0.87374	0.82543	0.006861	0.16771	0.17362	0.080639	0.74574
0.11135	0.014915	0.87374	0.82543	0.006861	0.16771	0.17362	0.080639	0.74574
0.12047	0.012082	0.86745	0.81093	0.007679	0.1814	0.18894	0.089808	0.72125
0.12047	0.012082	0.86745	0.81093	0.007679	0.1814	0.18894	0.089808	0.72125
0.12047	0.012082	0.86745	0.81093	0.007679	0.1814	0.18894	0.089808	0.72125
0.13252	0.013408	0.85408	0.82248	0.007136	0.17038	0.20579	0.085336	0.70888
0.13252	0.013408	0.85408	0.82248	0.007136	0.17038	0.20579	0.085336	0.70888
0.13252	0.013408	0.85408	0.82248	0.007136	0.17038	0.20579	0.085336	0.70888
0.13196	0.007139	0.8609	0.79433	0.008745	0.19693	0.20848	0.10169	0.68982
0.13196	0.007139	0.8609	0.79433	0.008745	0.19693	0.20848	0.10169	0.68982
0.13196	0.007139	0.8609	0.79433	0.008745	0.19693	0.20848	0.10169	0.68982
0.15702	0.01023	0.83275	0.8177	0.007587	0.17471	0.24296	0.092272	0.66477
0.15702	0.01023	0.83275	0.8177	0.007587	0.17471	0.24296	0.092272	0.66477
0.15702	0.01023	0.83275	0.8177	0.007587	0.17471	0.24296	0.092272	0.66477
0.16281	0.006493	0.8307	0.80816	0.00823	0.18361	0.25308	0.099594	0.64733
0.16281	0.006493	0.8307	0.80816	0.00823	0.18361	0.25308	0.099594	0.64733
0.16281	0.006493	0.8307	0.80816	0.00823	0.18361	0.25308	0.099594	0.64733
0.18886	0.011896	0.79925	0.83419	0.006869	0.15894	0.28681	0.087169	0.62602
0.18886	0.011896	0.79925	0.83419	0.006869	0.15894	0.28681	0.087169	0.62602
0.18886	0.011896	0.79925	0.83419	0.006869	0.15894	0.28681	0.087169	0.62602

**APPENDIX G: SENSITIVITY CONTOURS FOR THE BINARY
KRUGER MODEL**

Sensitivity Plots

In order to converge on model parameter estimates that have high certainty (i.e. a small confidence region), it is ideal if the parameter itself is sensitive to a model input in a region where experiments can and will be run. For example, it would be advantageous if r_{AMS} (a.k.a. r_1) is sensitive at a large range of AMS concentrations in regions where the parameter (r_{AMS}) would take on meaningful values. Sensitivity is measured by the magnitude of the gradient. The larger the absolute value of the gradient (positive or negative) leads to areas of heightened sensitivity. Representative examples of these types of contours can be seen in the figures below. It can be seen in these two figures regions where the gradient values have the largest magnitudes. These areas are of different shapes certainly, but each plots indicates an area of increased sensitivity for the parameters being considered.

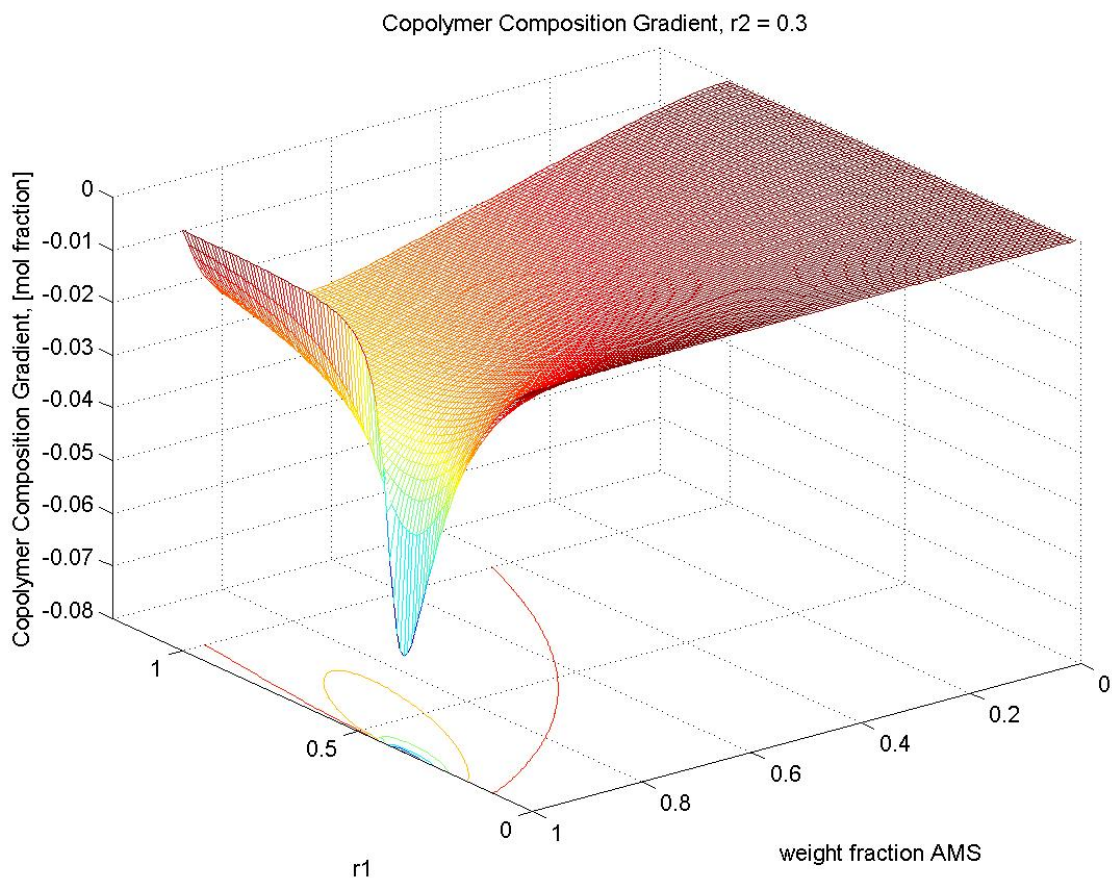


Figure 34: Copolymer Composition Gradient for r_{AMS} (r_1) @ $100^\circ C$, $r_2 = 0.3$

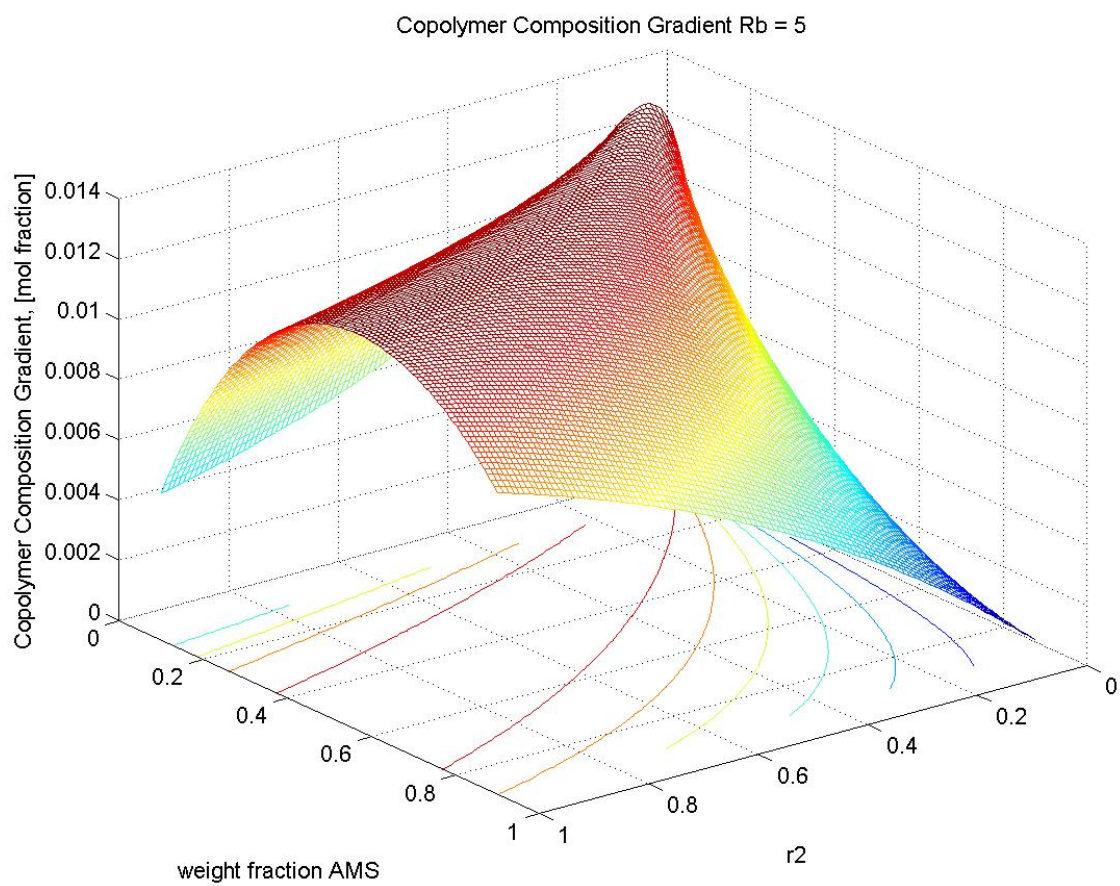


Figure 35: Copolymer Composition Gradient for r_2 @ 140°C , $R_b = 5$